Gas dynamics in disks:
Planet signatures and dynamical instabilities.

Wladimir (Wlad) Lyra

Tenure-track Professor

California State University Northridge

3rd DTA symposium. The origins of planetary systems: From the current view to new horizons.

Tokyo, June 1st, 2015

Outline

- Observational Evidence

- Dynamical Instabilities
    - Magnetorotational Instability
    - Effect of non-ideal MHD
        - Ohmic dead zone and instabilities
        - Ambipolar diffusion and Hall MHD
    - Dead zone instabilities
        - Vertical shear instability
        - Convective overstability

- Planet-disk interaction
- Vortex fitting
- Spiral fitting
- HL Tau

Observational evidence: Spirals

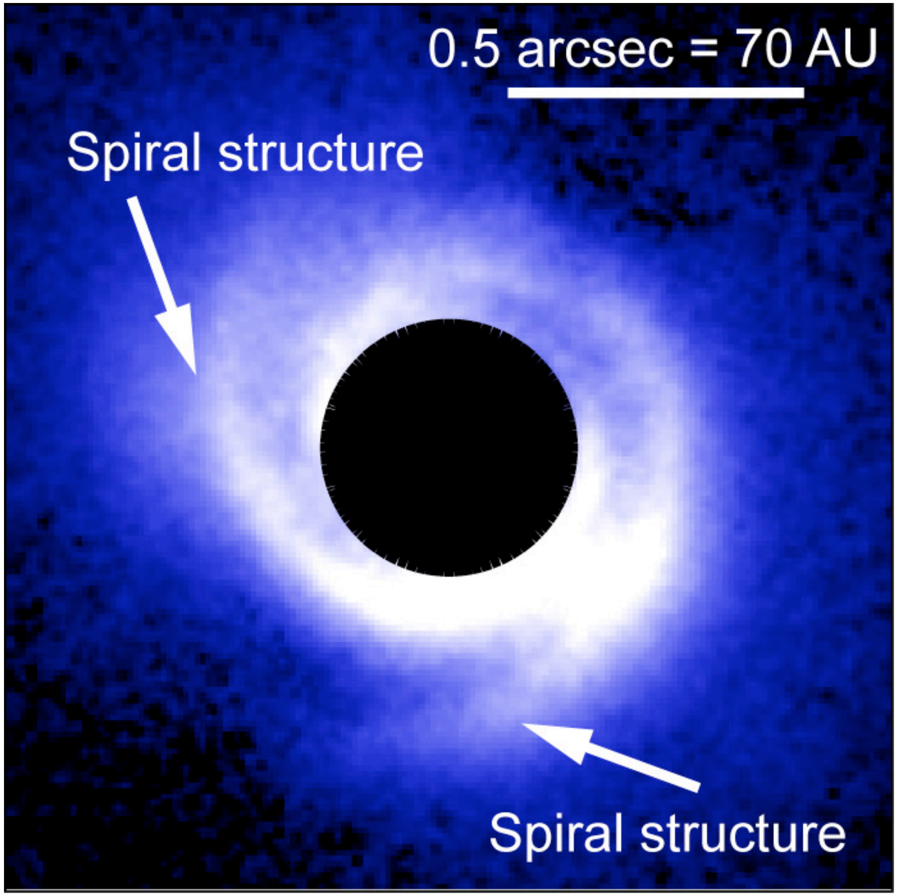

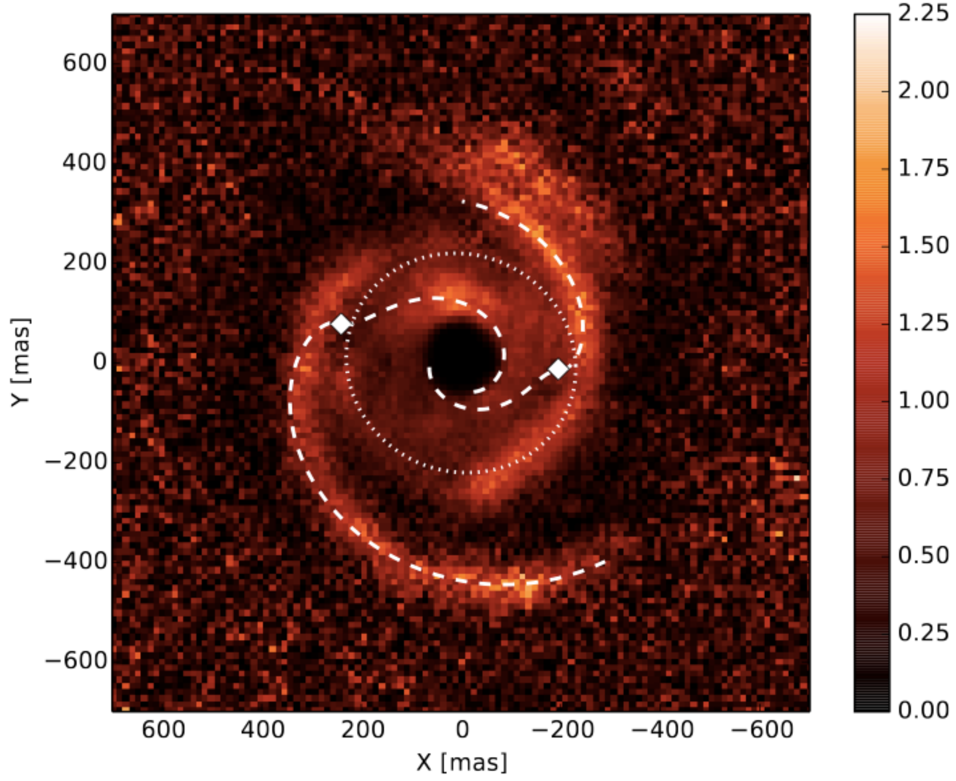

Observational evidence: Vortices(?)

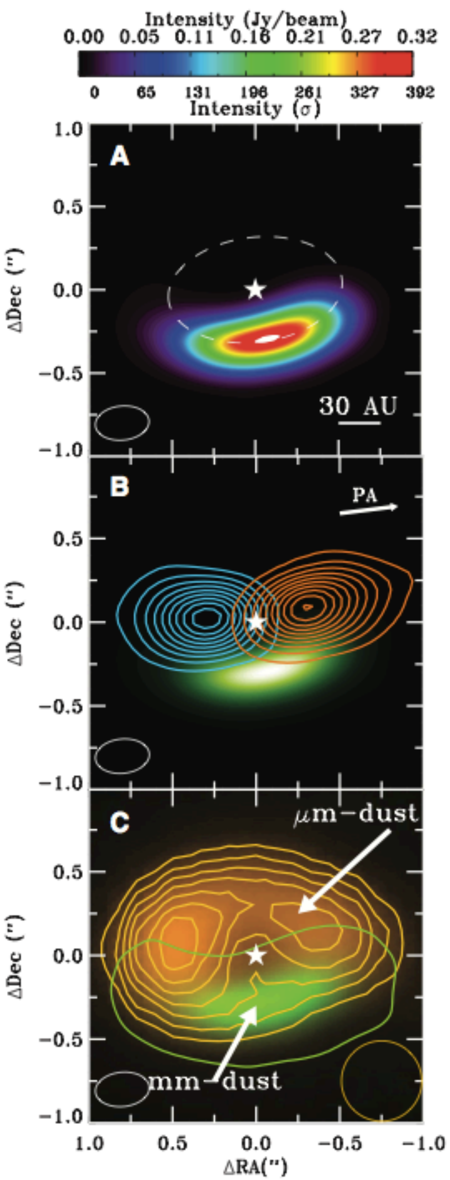

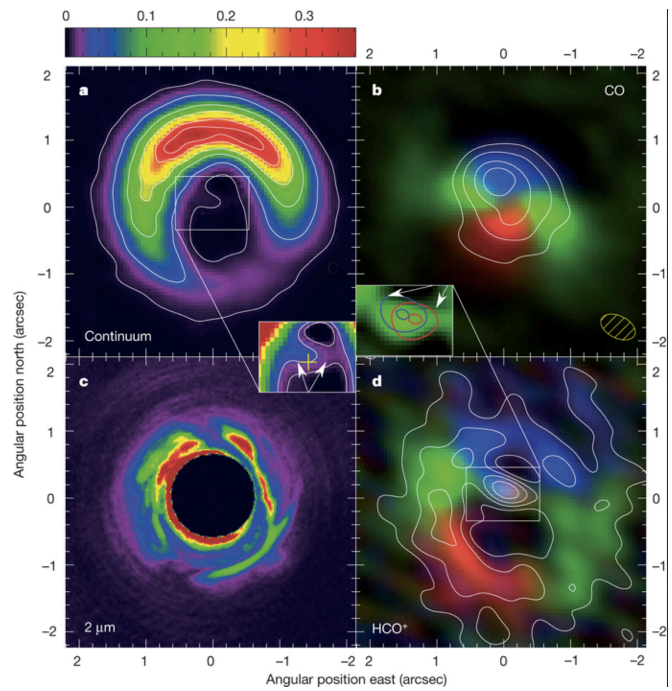

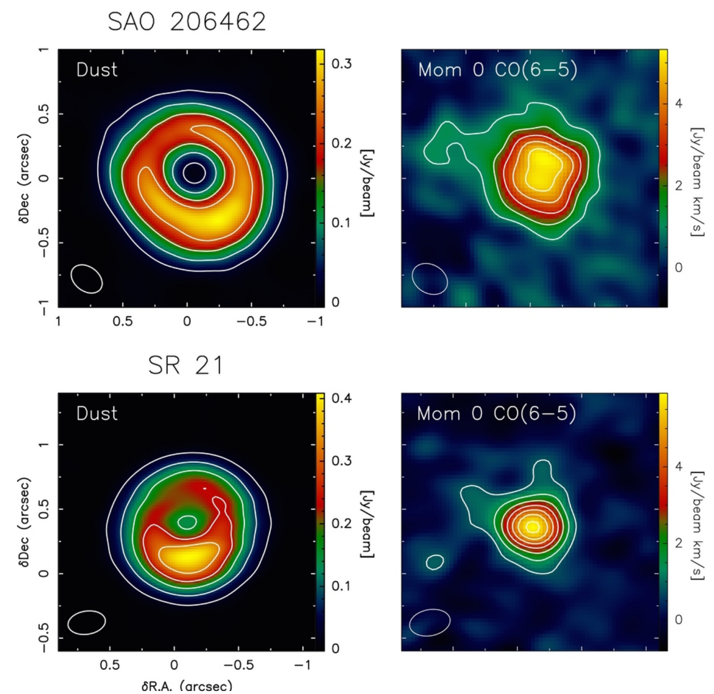

Observational evidence: Gaps

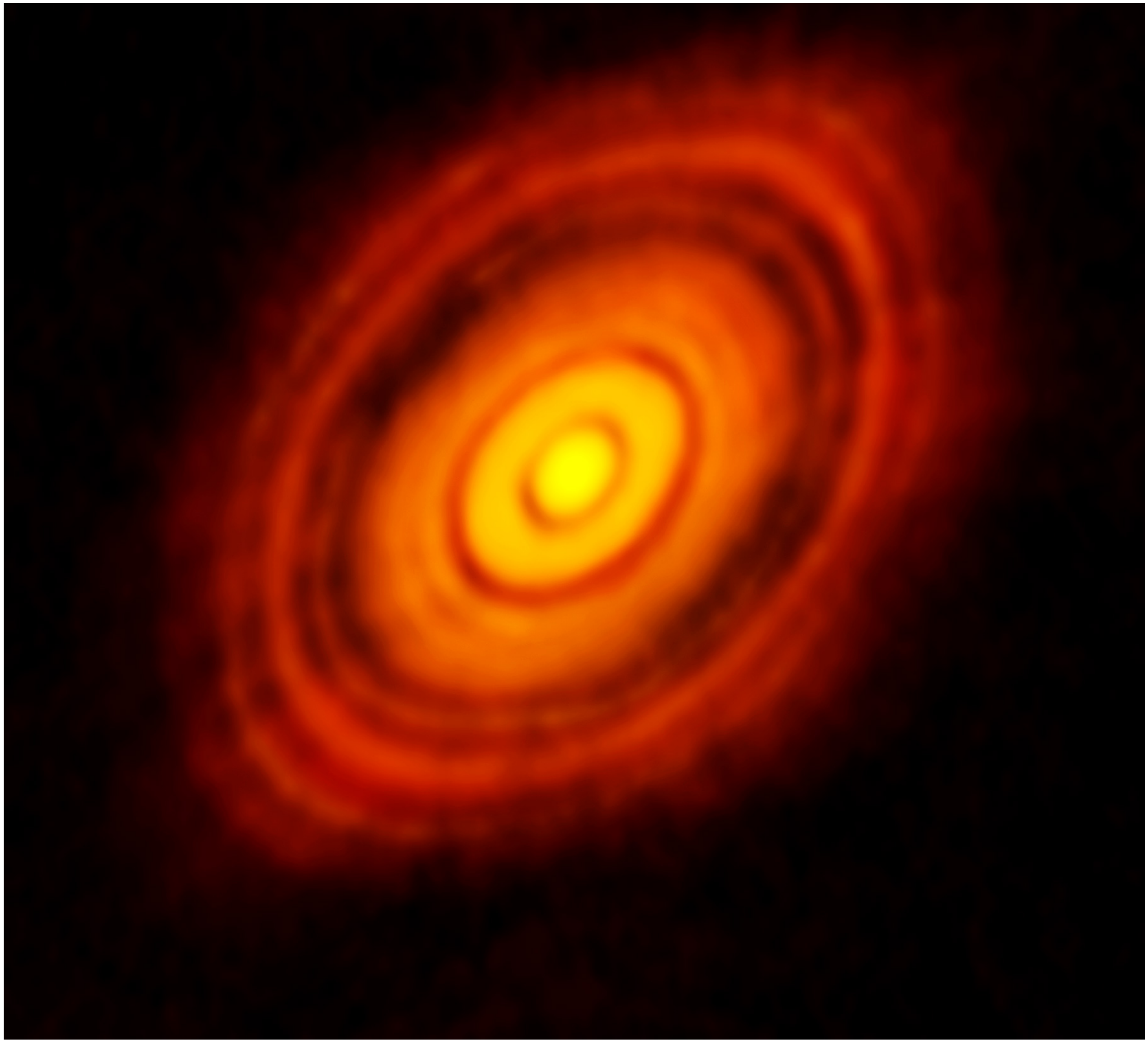

Protoplanetary Disks: Observational Perspective

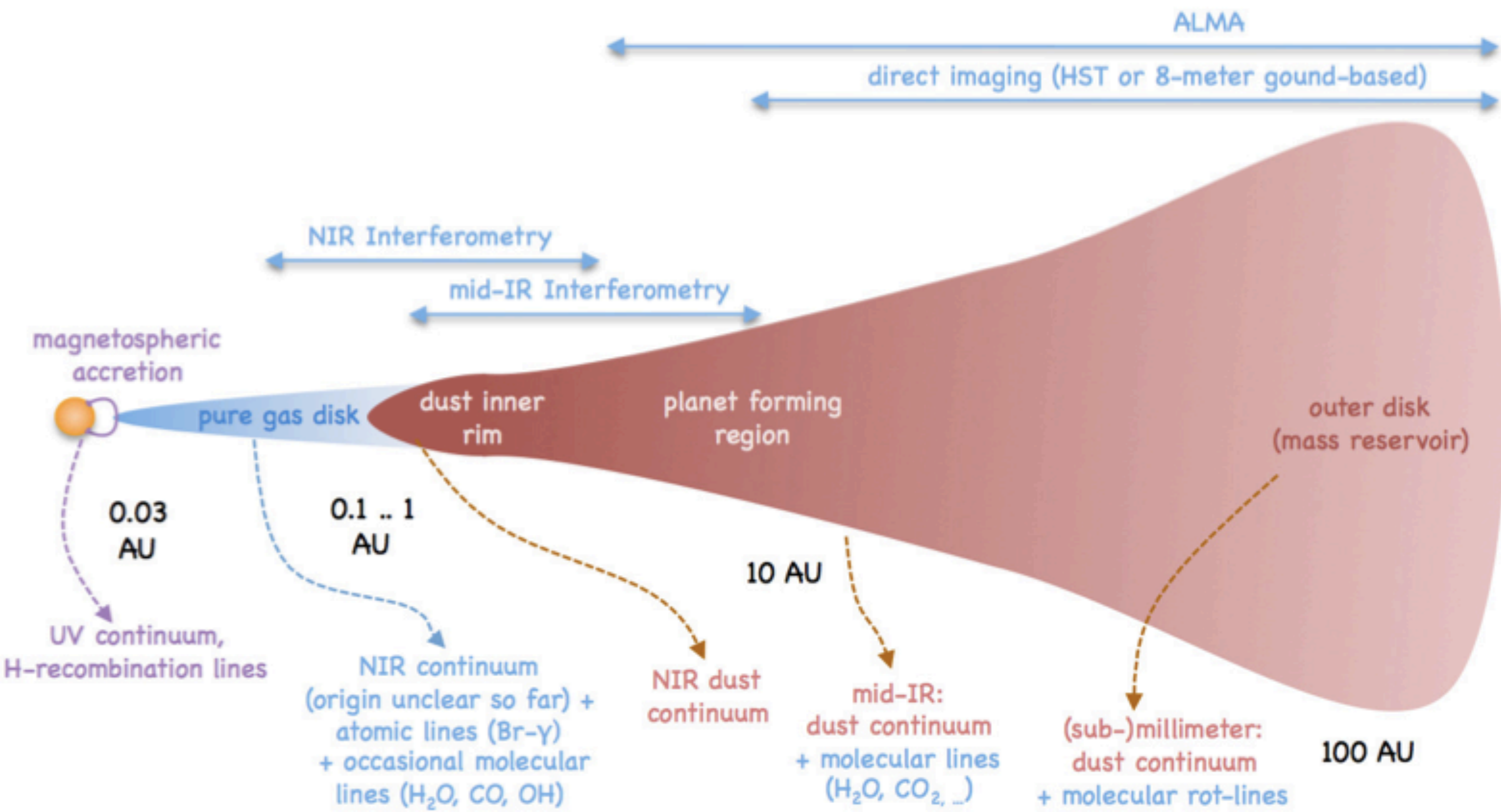

Protoplanetary Disks: Dynamical Perspective

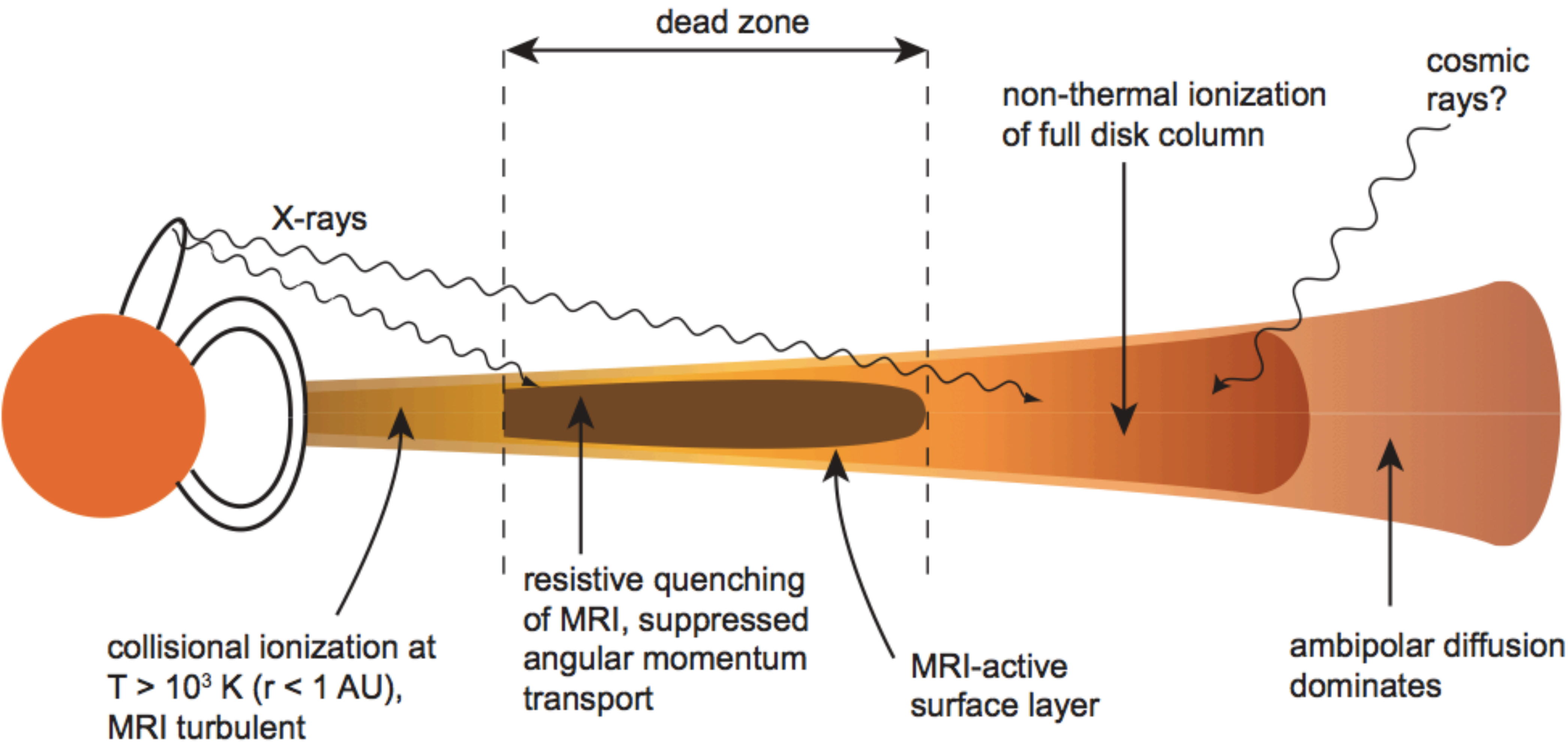

Magneto-Rotational Instability

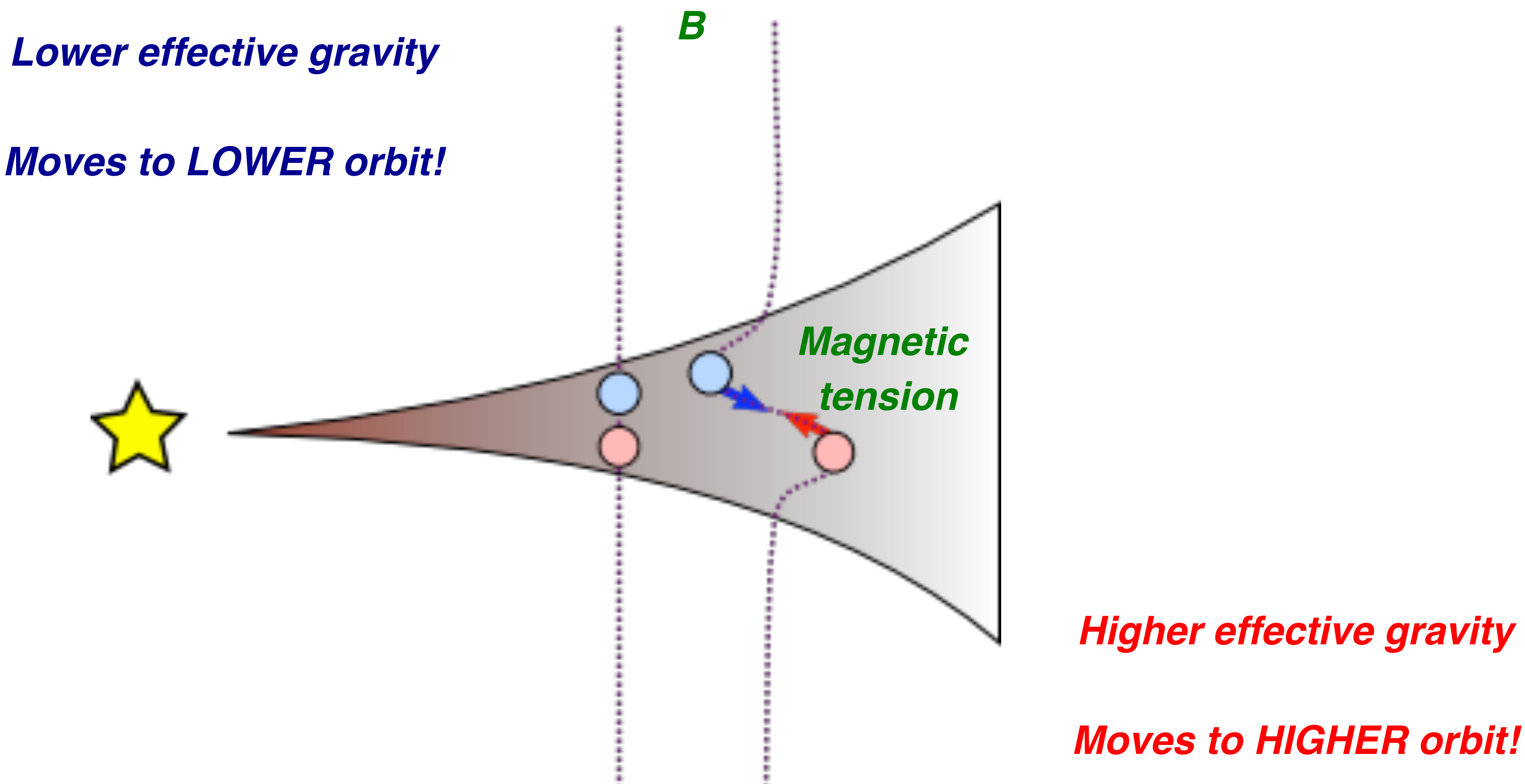

Turbulence and Accretion in 3D Global MHD Simulations of Stratified Protoplanetary Disk

Flock et al. (2011)

A simple dead zone model

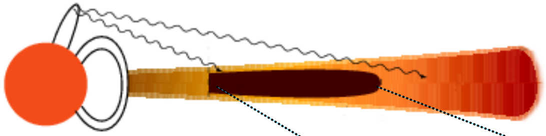

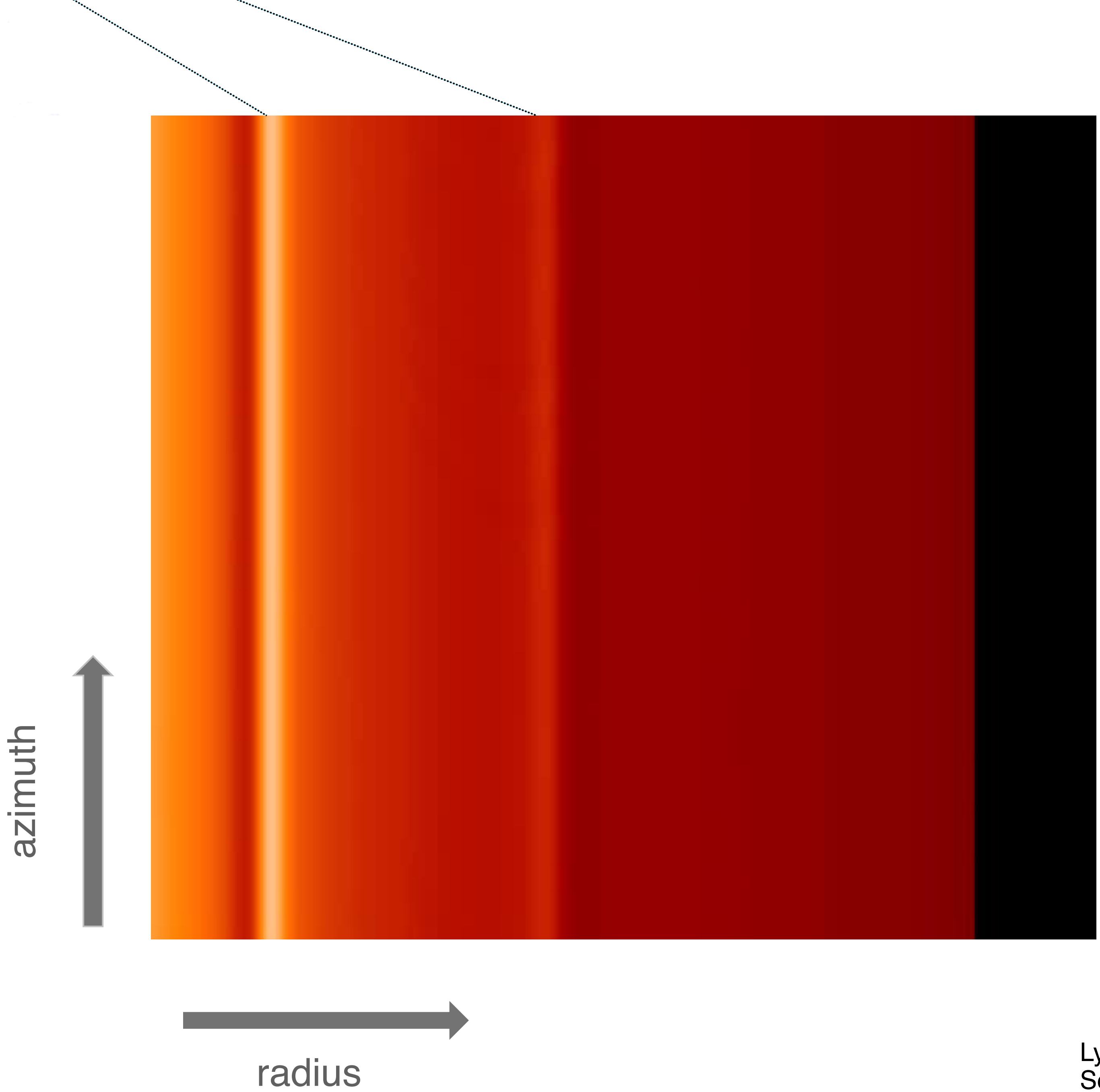

Lyra et al. (2008b);
See also Varniere & Tagger (2006)

Kelvin-Helmholtz Instability

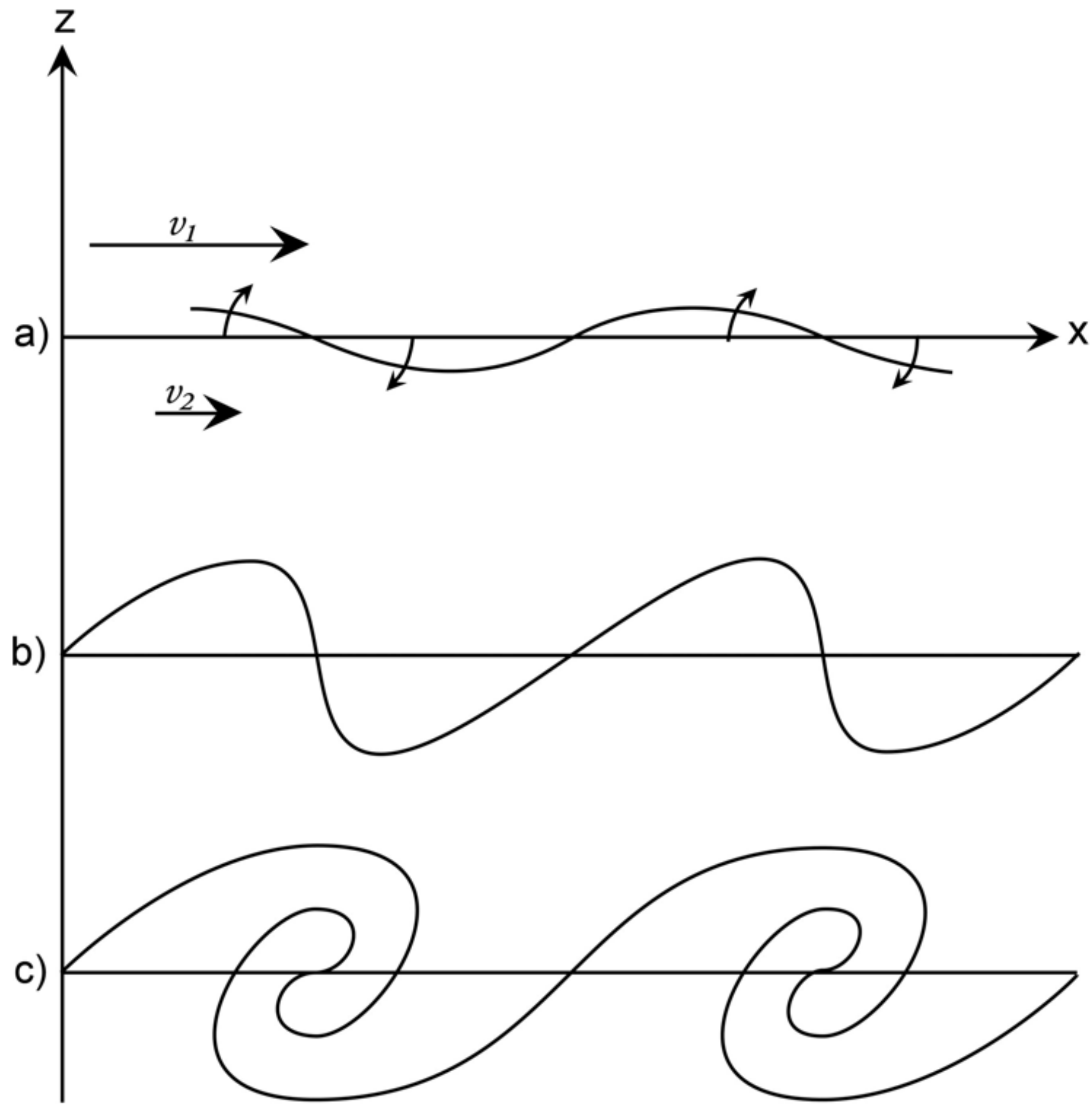

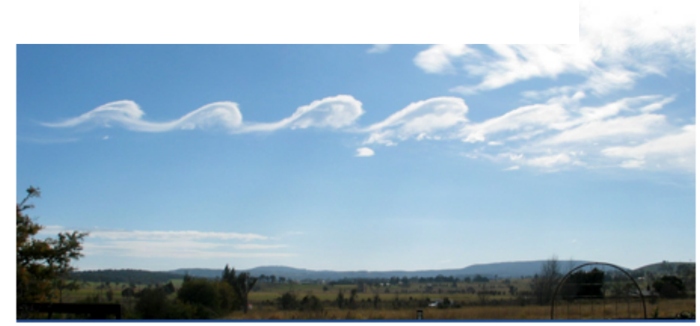

Rossby wave instability

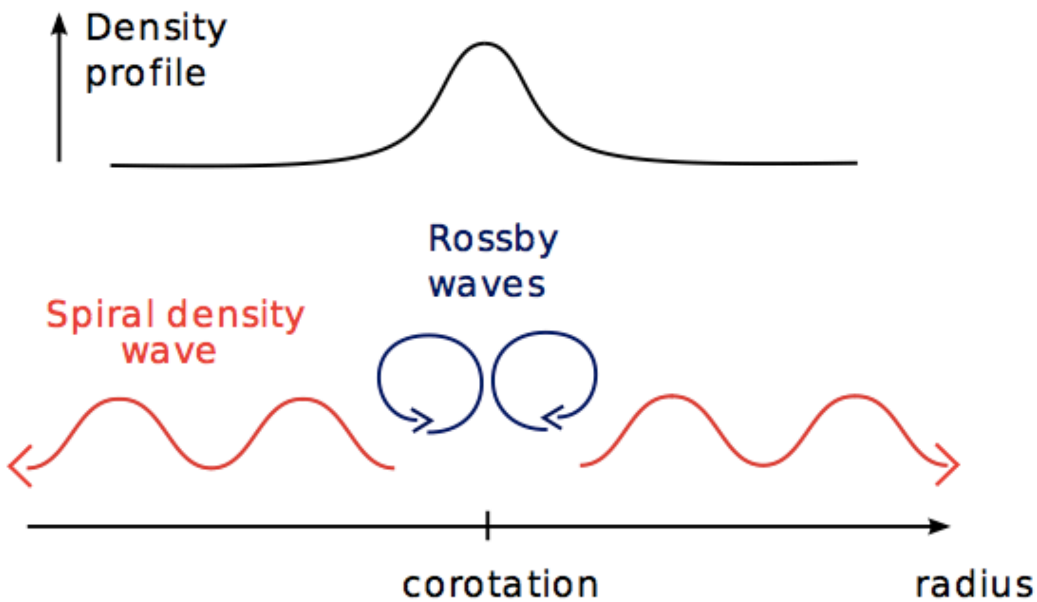

Meheut et al (2010)

Needs a pressure bump.

Rule of thumb:

Modest **~30% local increase** yet SHARP **sharper than 2H**.

Lovelace & Hohlfeld 1978
Toomre 1981
Papaloizou & Pringle 1984,1985
Hawley 1987
Lovelace 1999
Li et al. 2000, 2001
Tagger 2001
Varniere & Tagger 2006
de Val Borro et al. 2007
Lyra et al. 2008b, 2009ab
Meheut et al. 2010, 2012abc
Lin & Papaloizou 2011ab,2012
Lyra & Mac Low 2012
Lin 2012,2013

Peggy Varnière & Michel Tagger
Rossby Wave Instability at dead zone boundary

Reviving Dead Zones in Accretion Disks by Rossby Vortices at their Boundaries

P. Varnière[1,2] & M. Tagger[3]

[1] Department of Physics & Astronomy, Rochester University, Rochester NY 14627-0171
[2] LAOG, Université J. Fourier UMR 5571 France, e-mail: pvarni@pas.rochester.edu
[3] Service d'Astrophysique (UMR Astroparticules et cosmologie) CEA/Saclay F-91191 Gif sur Yvette e-mail: tagger@cea.fr

the date of receipt and acceptance should be inserted later

Abstract. Models of the accretion disks of Young Stellar Objects show that they should not be ionized at a few AU from the star, and thus not subject to the MHD turbulence believed to cause accretion. This has been suggested to create a 'Dead Zone' where accretion remains unexplained. Here we show that the existence of the Dead Zone self-consistently creates a density profile favorable to the Rossby Wave Instability of Lovelace et al. (1999). This instability will create and sustain Rossby vortices in the disk which could lead to enhanced planet formation.

Key words. accretion disks; Instabilities; planetary systems: formation

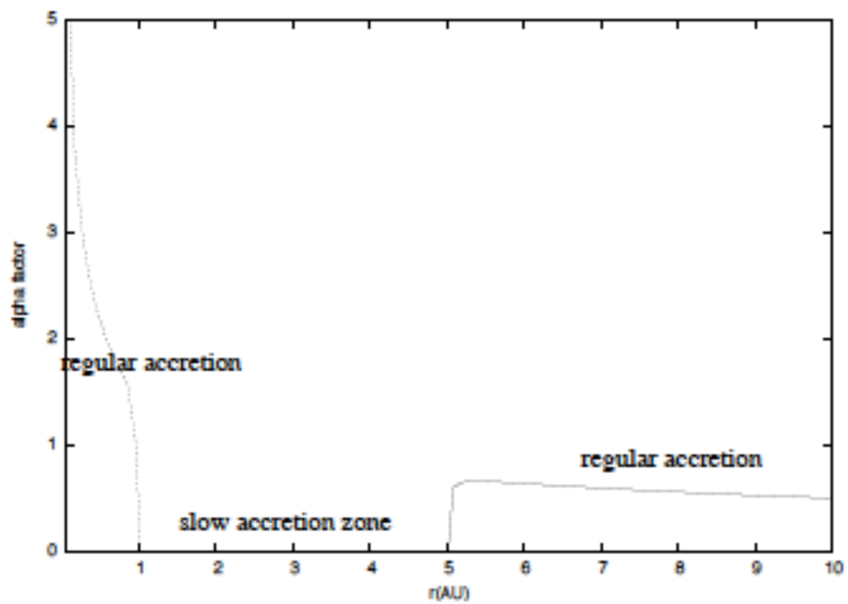

Fig. 1. Profile of the α-viscosity implemented to represent a Dead Zone between 1 and 5 AU with $(\epsilon, \delta_r) = (10^{-5}, 50)$.

Varnière & Tagger (2006)

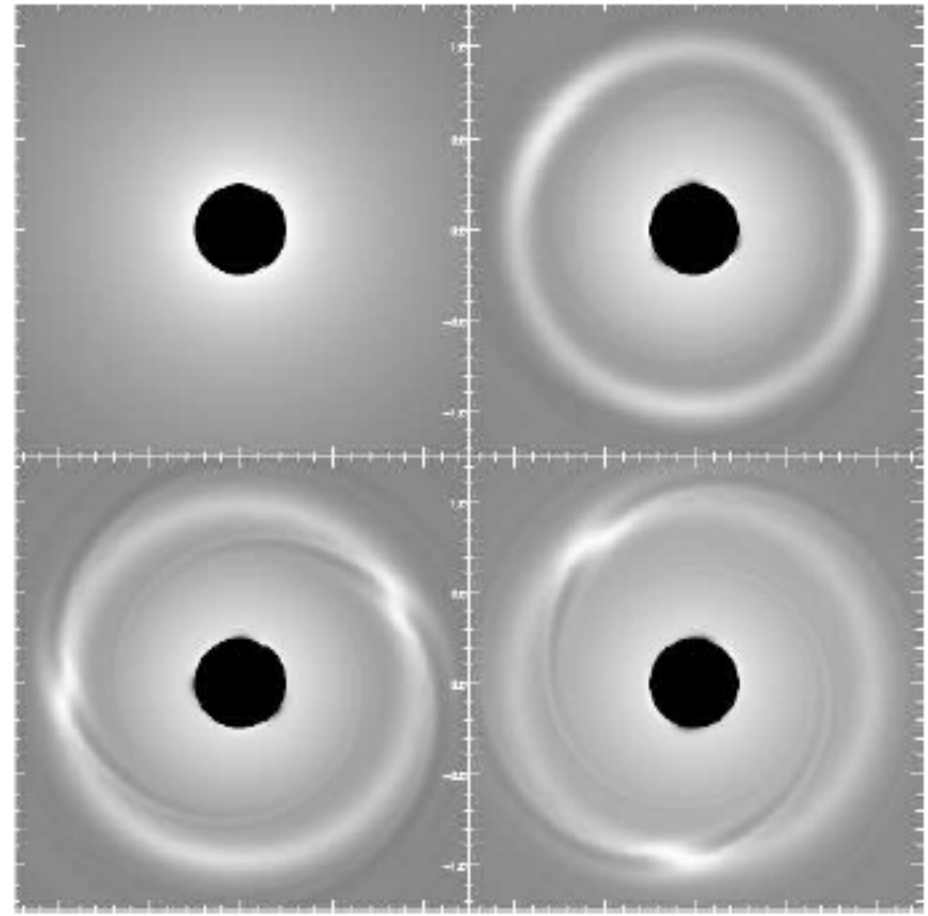

Fig. 3. Zoom of the first 2 inner AU of the simulation at $t = 0, 100, 200, 300$ years, showing the density. One sees three vortices forming, later evolving to two vortices, near the outer edge of the Dead Zone.

3D strat RWI

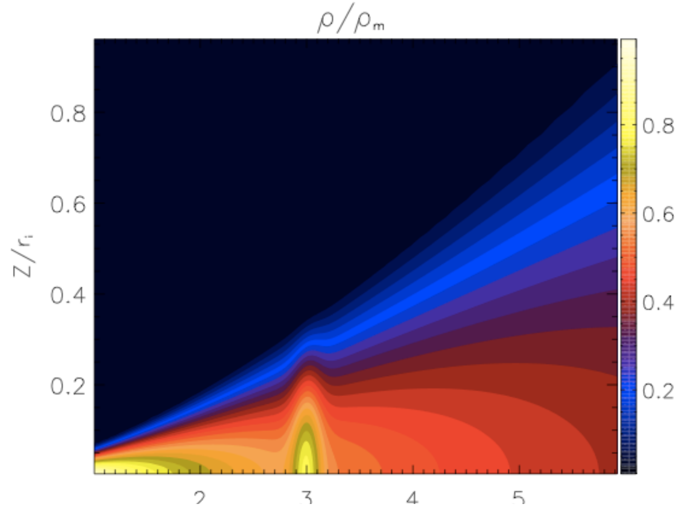

Meheut et al. (2010, 2012abc, 2013)

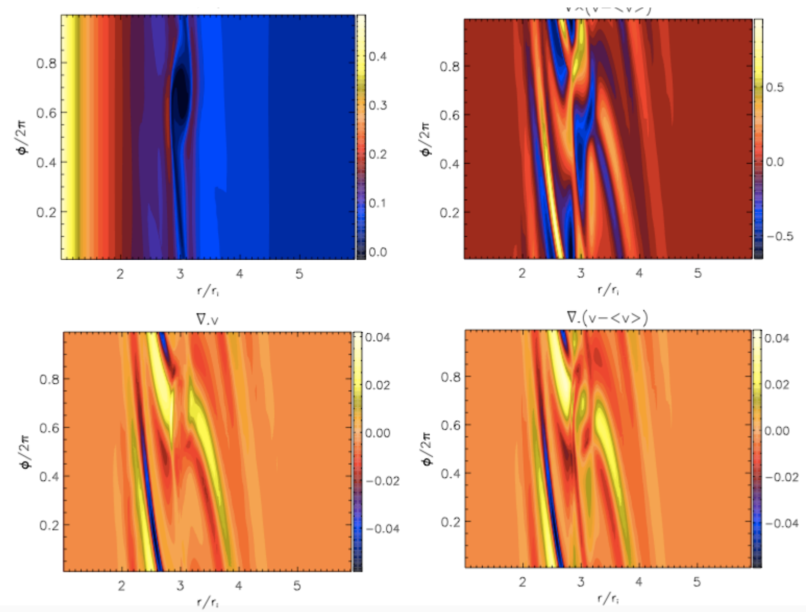

3D strat RWI self-gravity

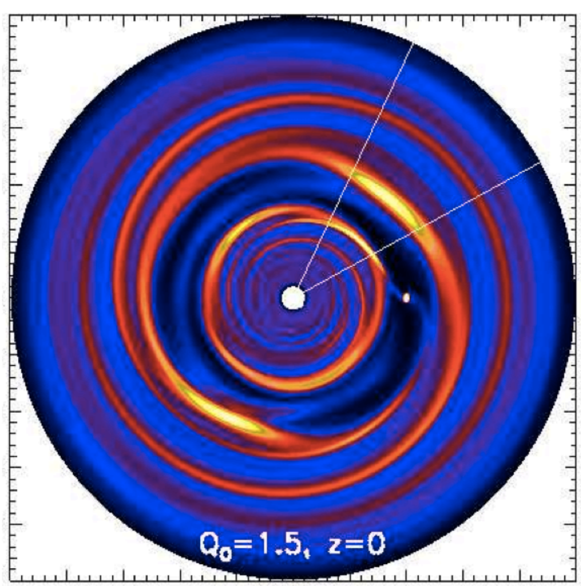

3D strat RWI polytropic

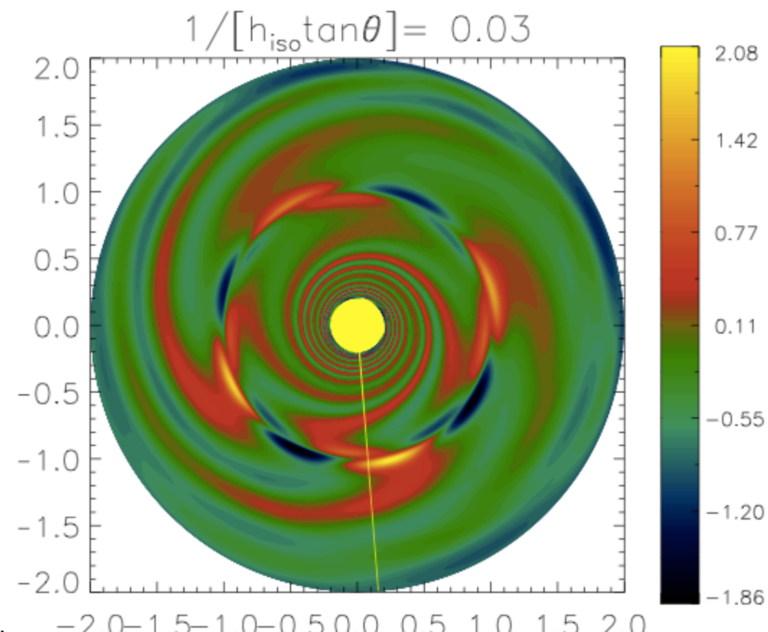

Lin (2012ab, 2013, 2014)

Inner Active/Dead zone boundary

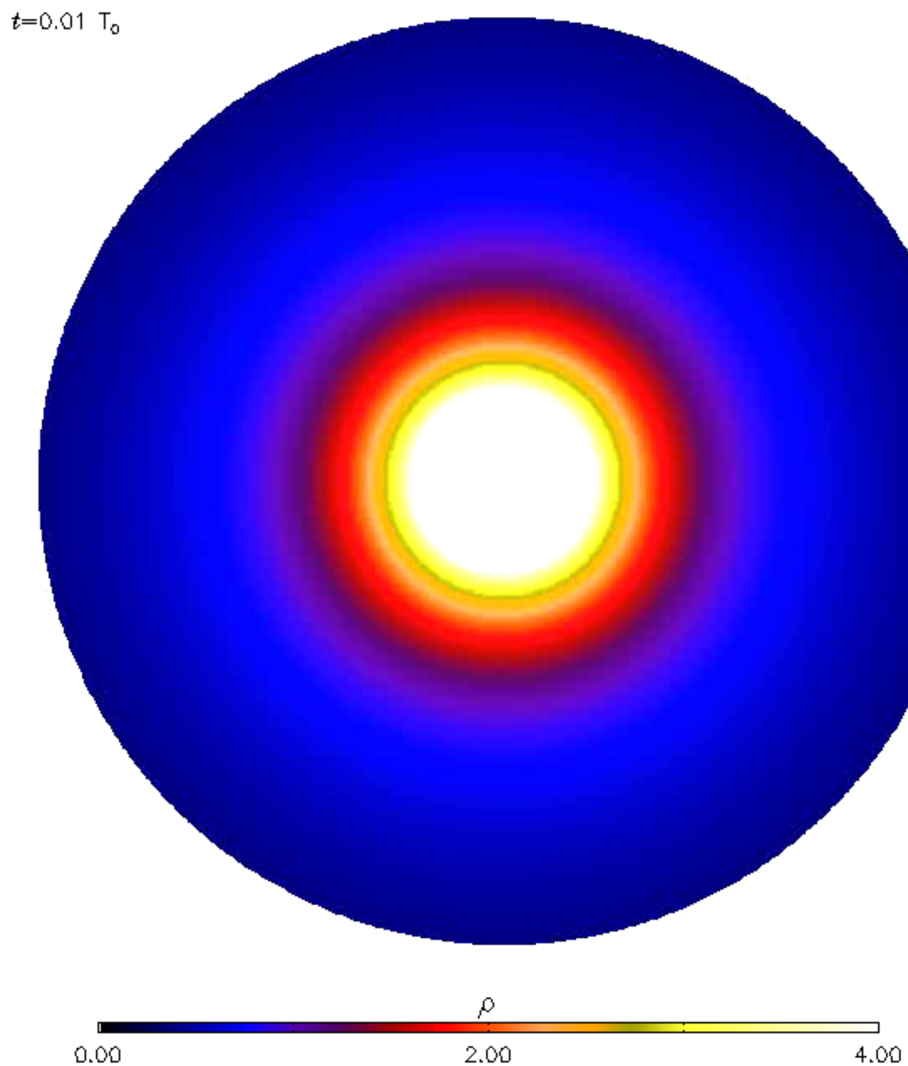

Unstratified isothermal MHD
with static Ohmic resistivity jumps.

$$
\begin{aligned}
\frac{\partial \rho}{\partial t} &= -\left(\boldsymbol{u}\cdot\boldsymbol{\nabla}\right)\rho - \rho\boldsymbol{\nabla}\cdot\boldsymbol{u}, \\
\frac{\partial \boldsymbol{u}}{\partial t} &= -\left(\boldsymbol{u}\cdot\boldsymbol{\nabla}\right)\boldsymbol{u} - \frac{1}{\rho}\boldsymbol{\nabla}p - \boldsymbol{\nabla}\Phi + \frac{\boldsymbol{J}\times\boldsymbol{B}}{\rho}, \\
\frac{\partial \boldsymbol{A}}{\partial t} &= \boldsymbol{u}\times\boldsymbol{B} - \eta\mu_0\boldsymbol{J} \\
p &= \rho c_s^2.
\end{aligned}
$$

$$
\eta(r) = \eta_0 - \frac{\eta_0}{2}\left[\tanh\left(\frac{r-r_1}{h_1}\right) - \tanh\left(\frac{r-r_2}{h_2}\right)\right]
$$

Magnetized inner disk + resistive outer disk

Lyra & Mac Low (2012);
see also Faure et al. (2015)

Active/dead zone boundary

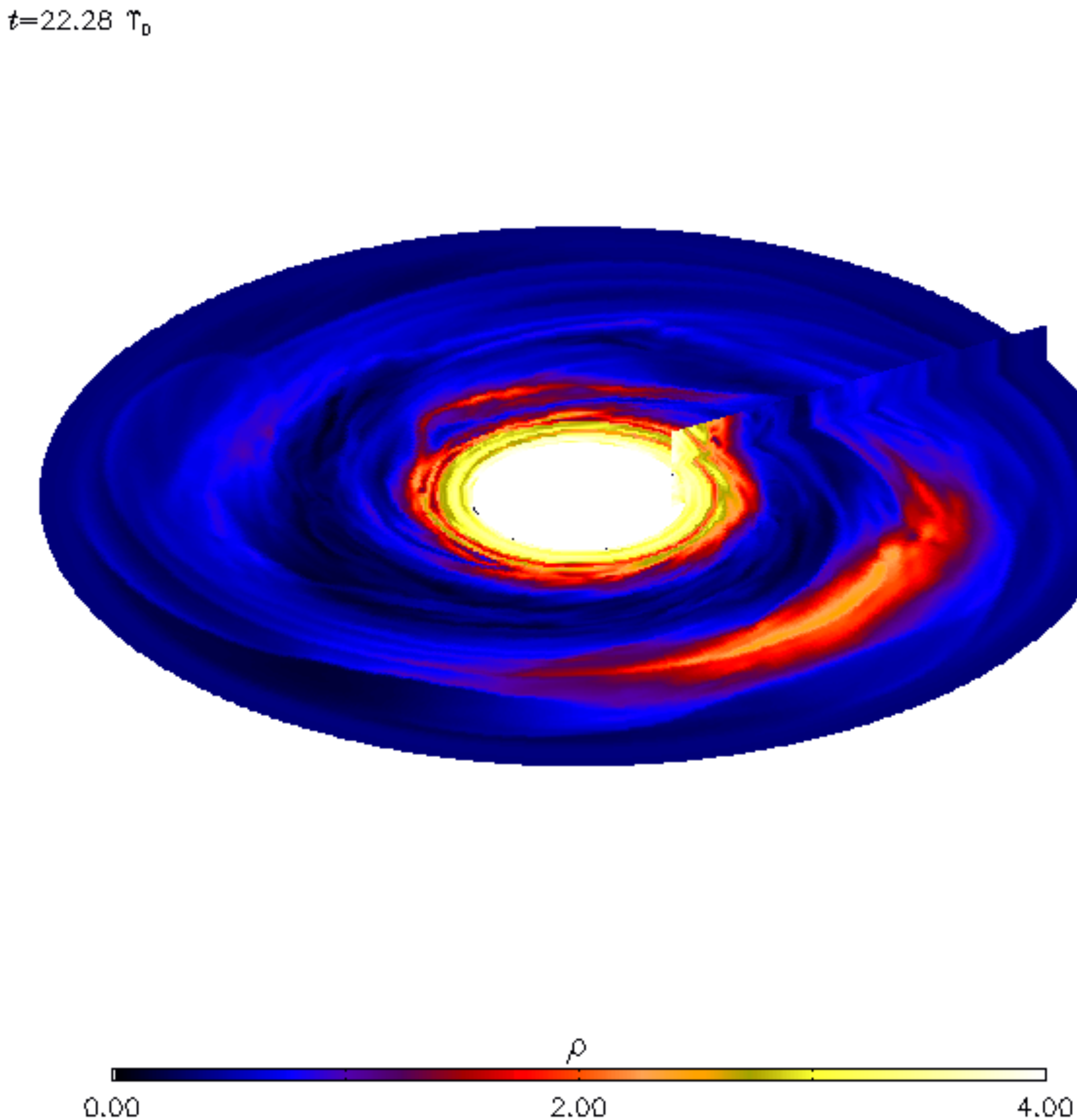

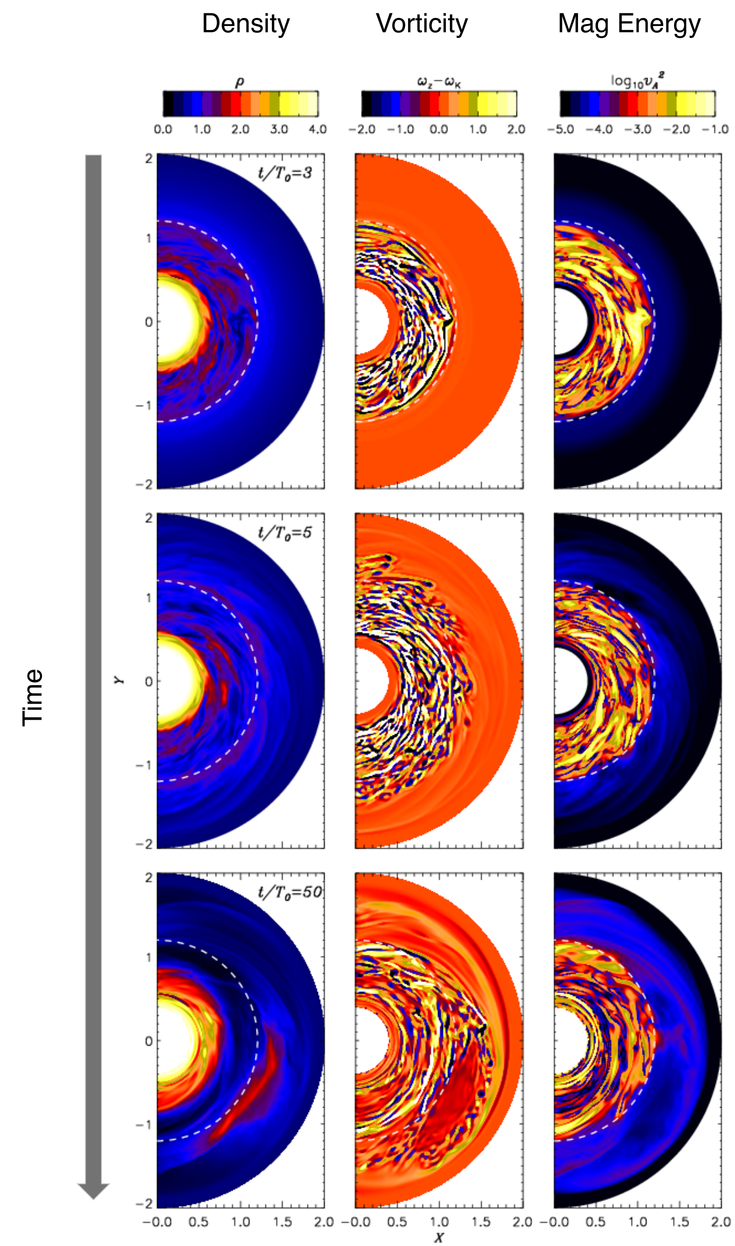

Magnetized inner disk + resistive outer disk

Lyra & Mac Low (2012)

Significant angular momentum transport

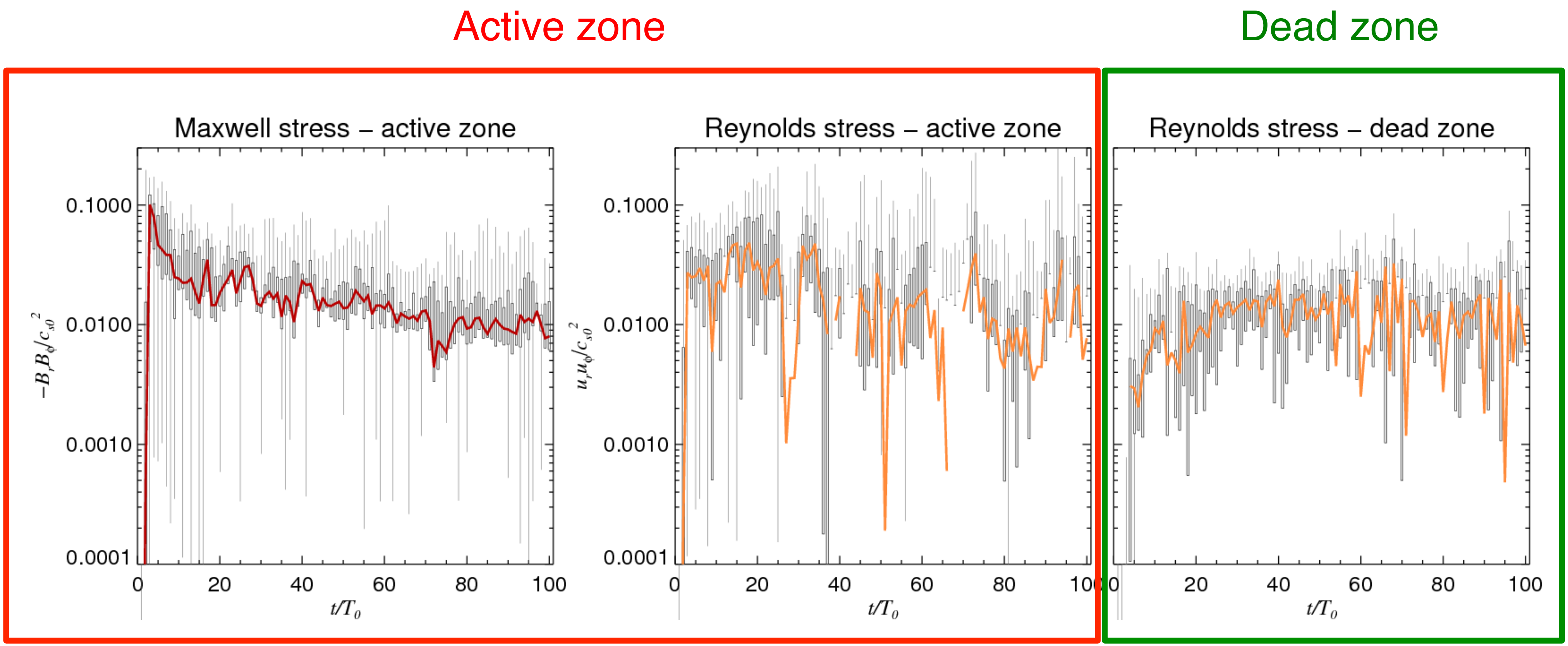

Large mass accretion rates in the dead zone,

comparable to the MRI in the active zone

Lyra & Mac Low (2012)

(Pre-)History of Rossby Wave Instability

WHAT AMPLIFIES THE SPIRALS?

Alar Toomre

Massachusetts Institute of Technology

Toomre (1981)

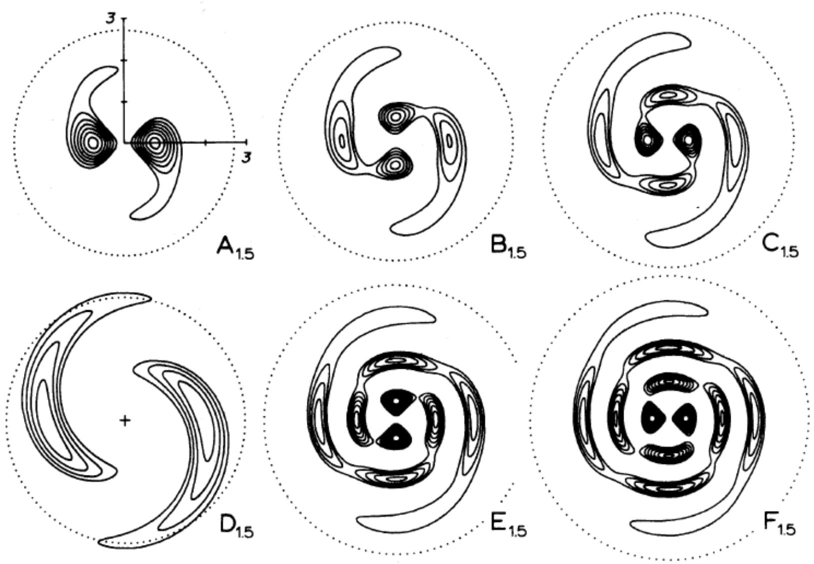

Fig. 12 Comparison of modes A-F for that Gaussian disk in which only 2/3 of the density remains "active". Their eigenfrequencies were reported at location 1.5 in Fig. 11. The corotation circles are again shown dotted; they have expanded markedly from Fig. 10.

One black sheep still needs to be dealt with. I am referring, of course, to the mode marked D in Figs. 10-12. As luck has it, the pattern speed (and even the growth rate) of this mode lands it smack amidst the swing-amplified modes in the full-mass Fig. 10. And it is there somewhat contaminated by the latter — as if only to confuse us! **That mode D is a wolf in sheep's clothing becomes clear,** however, once we weaken those rival modes in Figs. 11-12 by reducing the active disk mass. Its shape and hefty growth rate then point firmly to a different kind of animal.

What is mode D? It seems genuinely to be an edge mode which (a) arises only if the disk density drops off abruptly enough with radius, and yet (b) does not require any wave transport into or through the central regions. Kalnajs and I can support claim (a) with some experimental findings that any analogue of mode D occurs at most very weakly in the yet more soft-edged exponential disk — and it is altogether absent from Zang's $V = \text{const}$ disk — whereas it can be aroused to fresh fury by artificially truncating either of those disks in a smooth but sudden enough manner. We can also vouch for claim (b) with the little discovery that any "freezing" of our Gaussian disk inward of (say) $r = 1$ hardly alters the eigen-

Planetary gap RWI

(de Val-Borro et al. 2006, 2007)

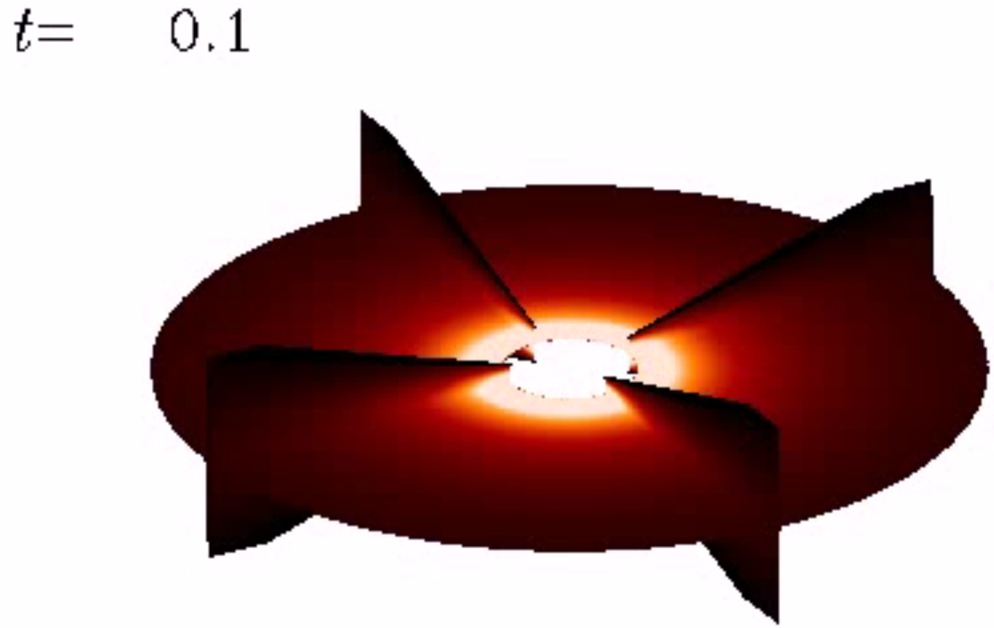

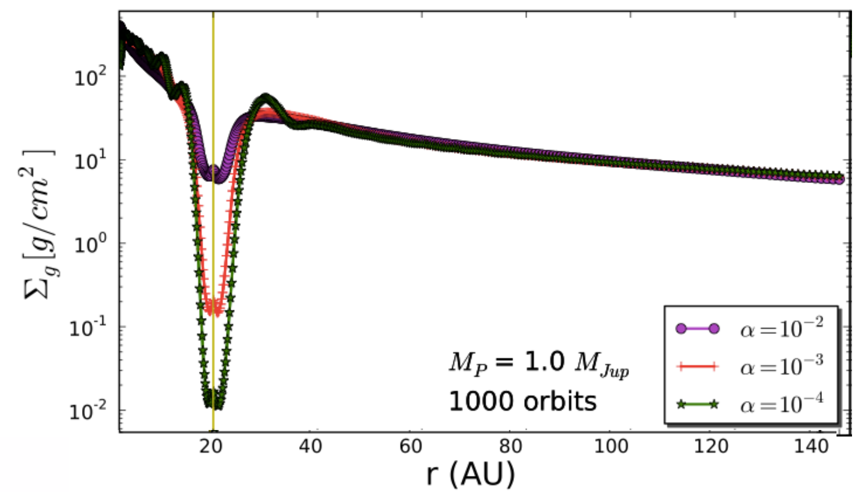

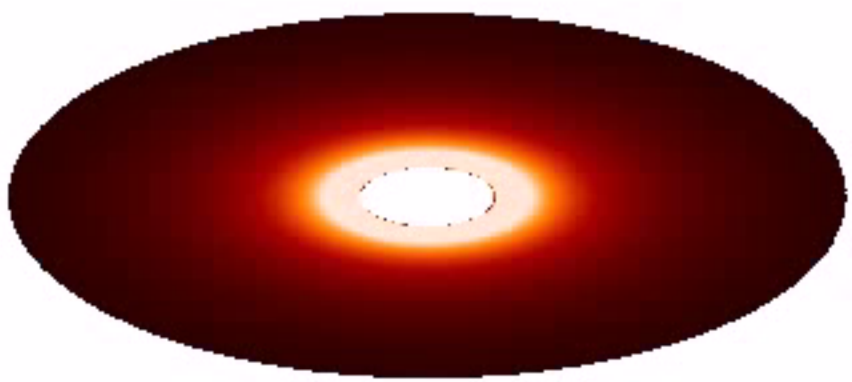

Lyra (2009)

Planet tides carve gap

Gap walls are unstable to Kelvin-Helmholtz instability

Koller et al. (2003)
RWI at planetary gap

THE ASTROPHYSICAL JOURNAL, 596:L91–L94, 2003 October 10

VORTICES IN THE CO-ORBITAL REGION OF AN EMBEDDED PROTOPLANET

JOSEF KOLLER,[1,2] HUI LI,[1] AND DOUGLAS N. C. LIN[3]
Received 2003 June 26; accepted 2003 August 13; published 2003 September 15

ABSTRACT

We present global two-dimensional inviscid disk simulations with an embedded planet, emphasizing the nonlinear dynamics in its co-orbital region. We find that the potential vorticity of the flow in this region is not conserved because of the presence of two spiral shocks produced by the planet. As the system evolves, the potential vorticity profile develops extrema (inflection points) that eventually render the flow unstable. Vortices are produced in association with the potential vorticity minima. Born in the separatrix region, these vortices experience close encounters with the planet, consequently exerting strong torques on the planet. The existence of these vortices have important implications for understanding the migration rates of low-mass planets.

Subject headings: accretion, accretion disks — hydrodynamics — planetary systems: protoplanetary disks

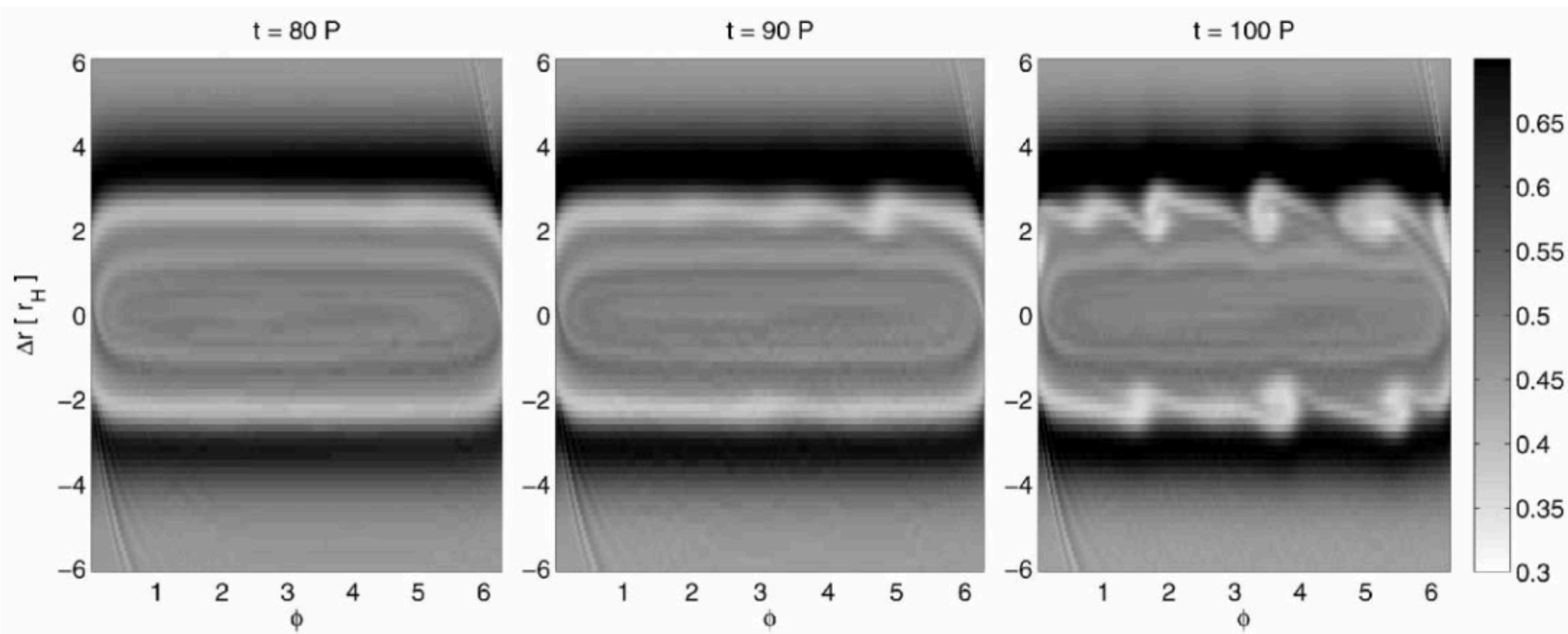

The code comparison project of 2006 (de Val-Borro et al. 2006)

Problem of choice:
2D 'vanilla' planet-disk interaction.

Several codes showed gap-edge vortices.

Follow-up work
(de Val-Borro et al. 2007)
showed that to be
the result of RWI

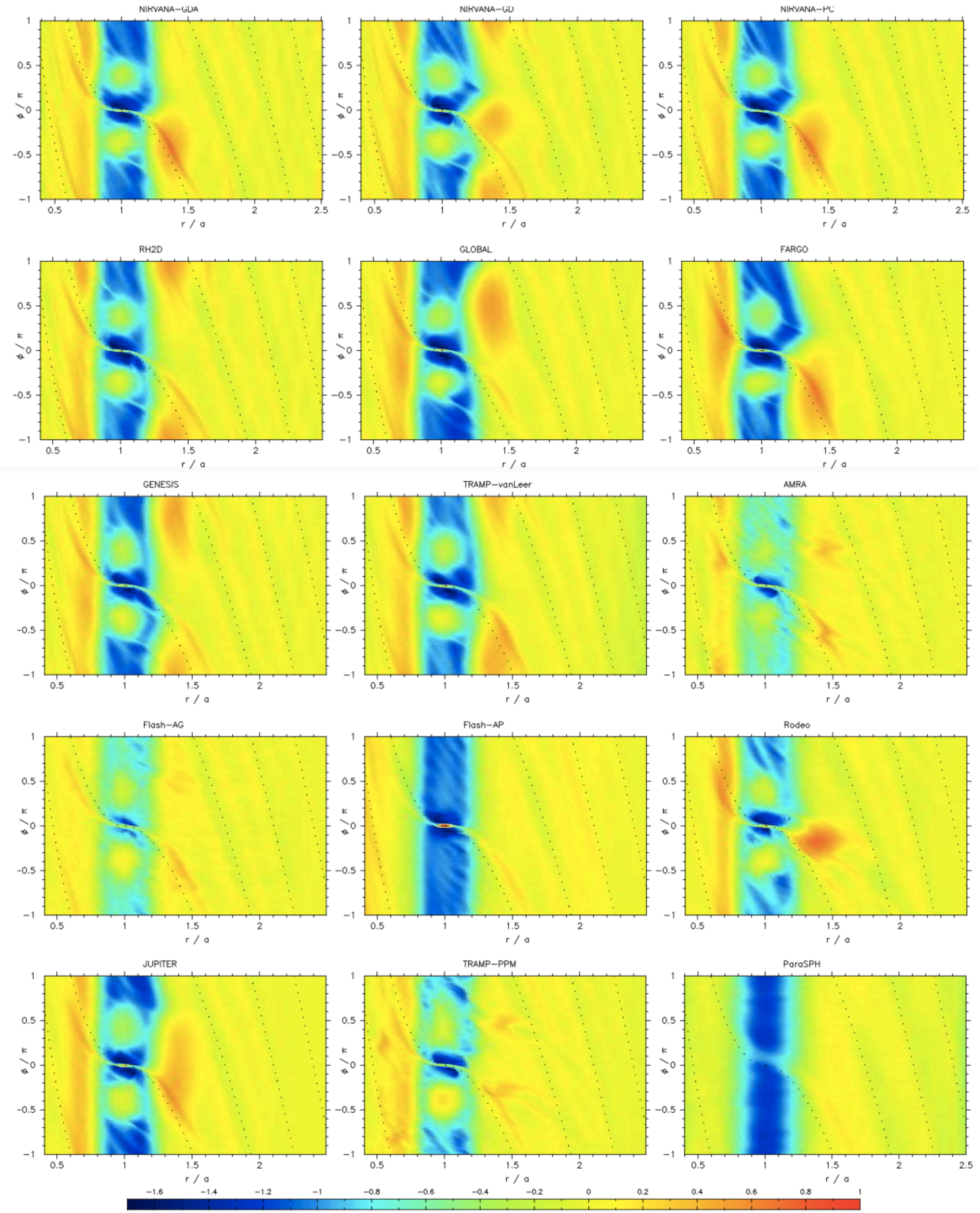

Inner Active/Dead zone boundary

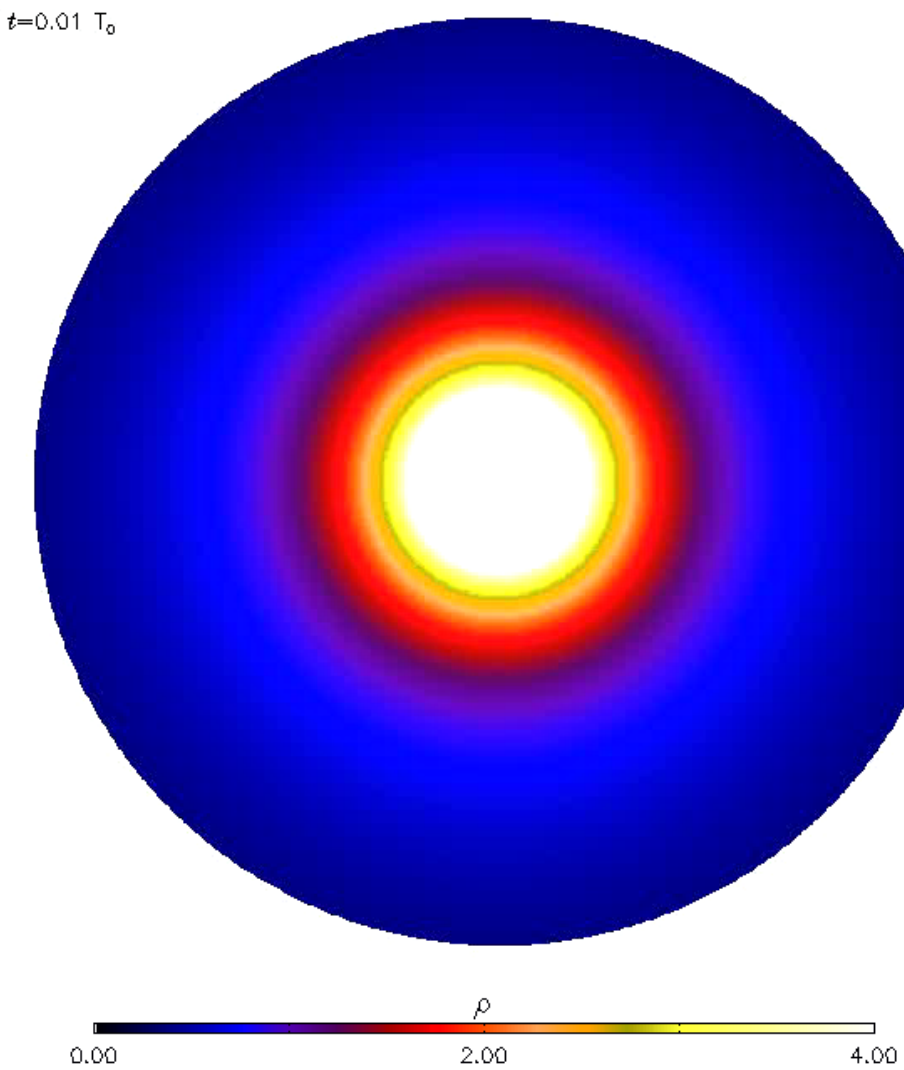

Unstratified isothermal MHD
with static Ohmic resistivity jumps.

$$\frac{\partial \rho}{\partial t} = -(\boldsymbol{u}\cdot\boldsymbol{\nabla})\,\rho - \rho\boldsymbol{\nabla}\cdot\boldsymbol{u},$$

$$\frac{\partial \boldsymbol{u}}{\partial t} = -(\boldsymbol{u}\cdot\boldsymbol{\nabla})\,\boldsymbol{u} - \frac{1}{\rho}\boldsymbol{\nabla}p - \boldsymbol{\nabla}\Phi + \frac{\boldsymbol{J}\times\boldsymbol{B}}{\rho},$$

$$\frac{\partial \boldsymbol{A}}{\partial t} = \boldsymbol{u}\times\boldsymbol{B} - \eta\mu_0\boldsymbol{J}$$

$$p = \rho c_s^2.$$

$$\eta(r) = \eta_0 - \frac{\eta_0}{2}\left[\tanh\left(\frac{r-r_1}{h_1}\right) - \tanh\left(\frac{r-r_2}{h_2}\right)\right]$$

Magnetized inner disk + resistive outer disk

Lyra & Mac Low (2012);
see also Faure et al. (2015)

Non-ideal MHD: Ohmic, Hall, Ambipolar terms

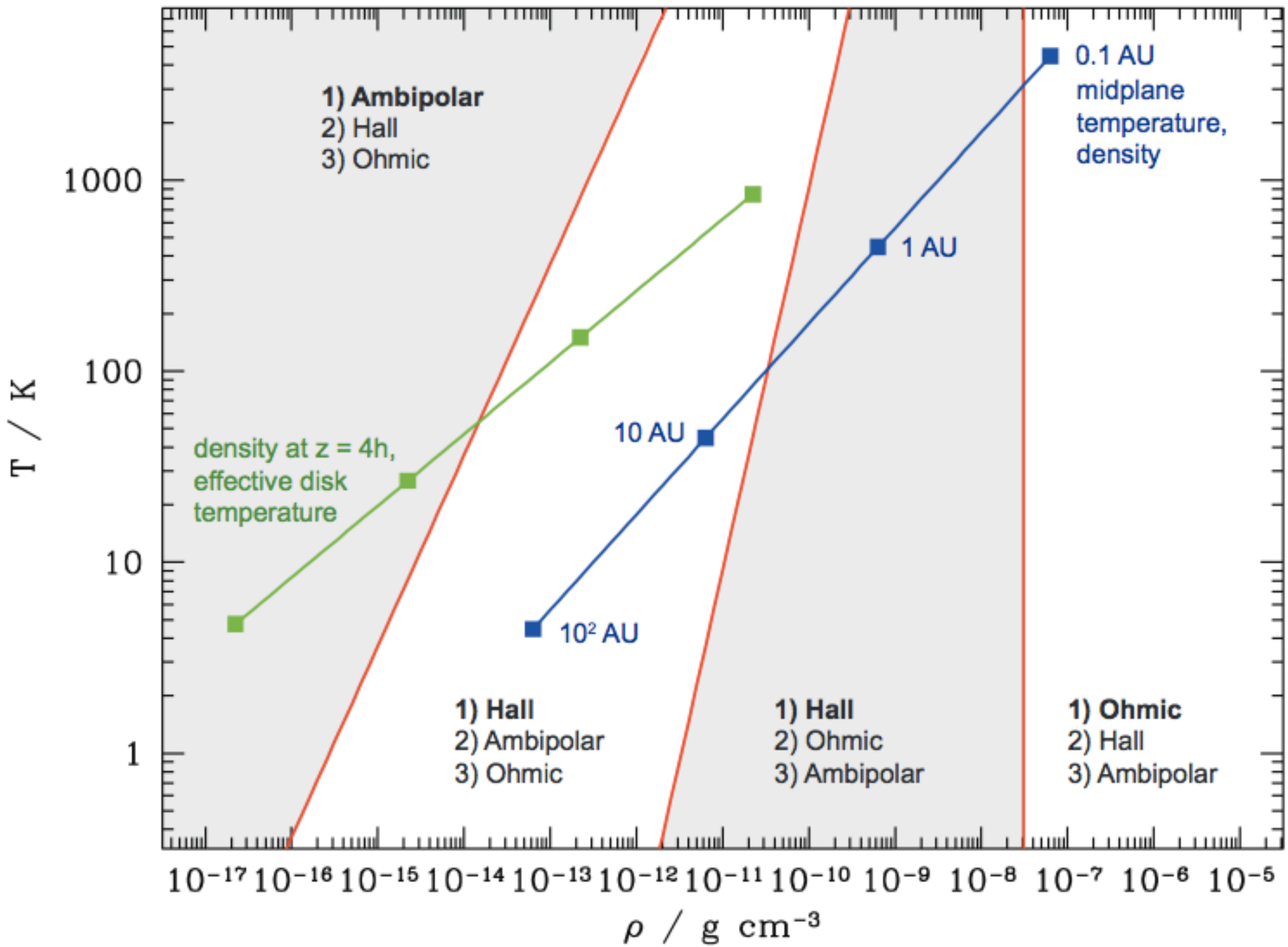

Ambipolar diffusion

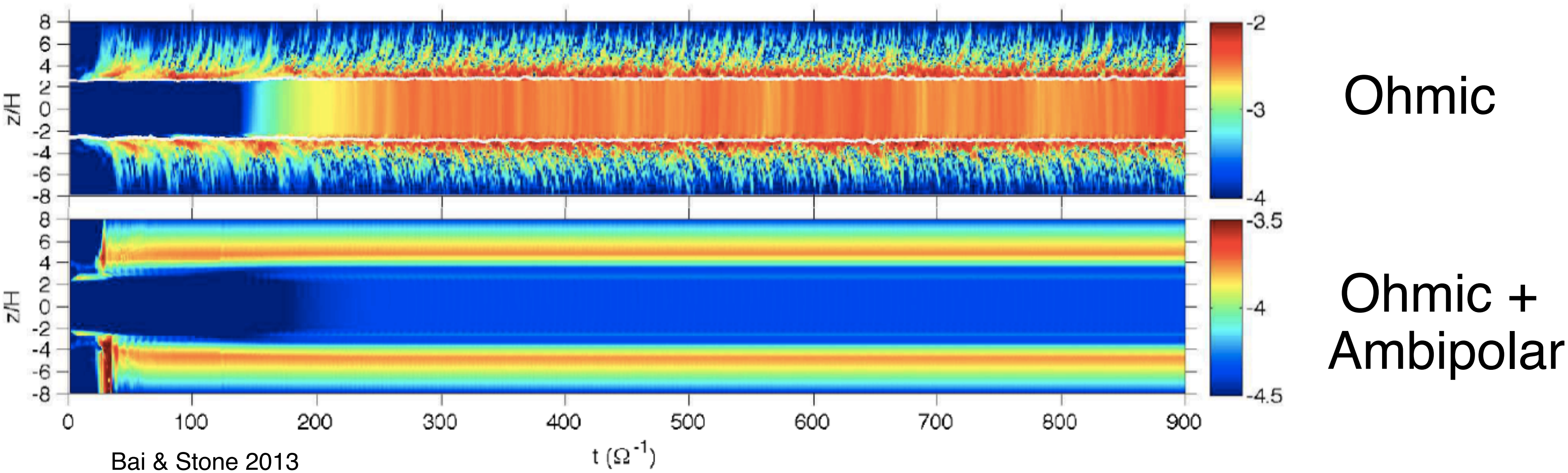

Bai & Stone 2013

Ambipolar diffusion

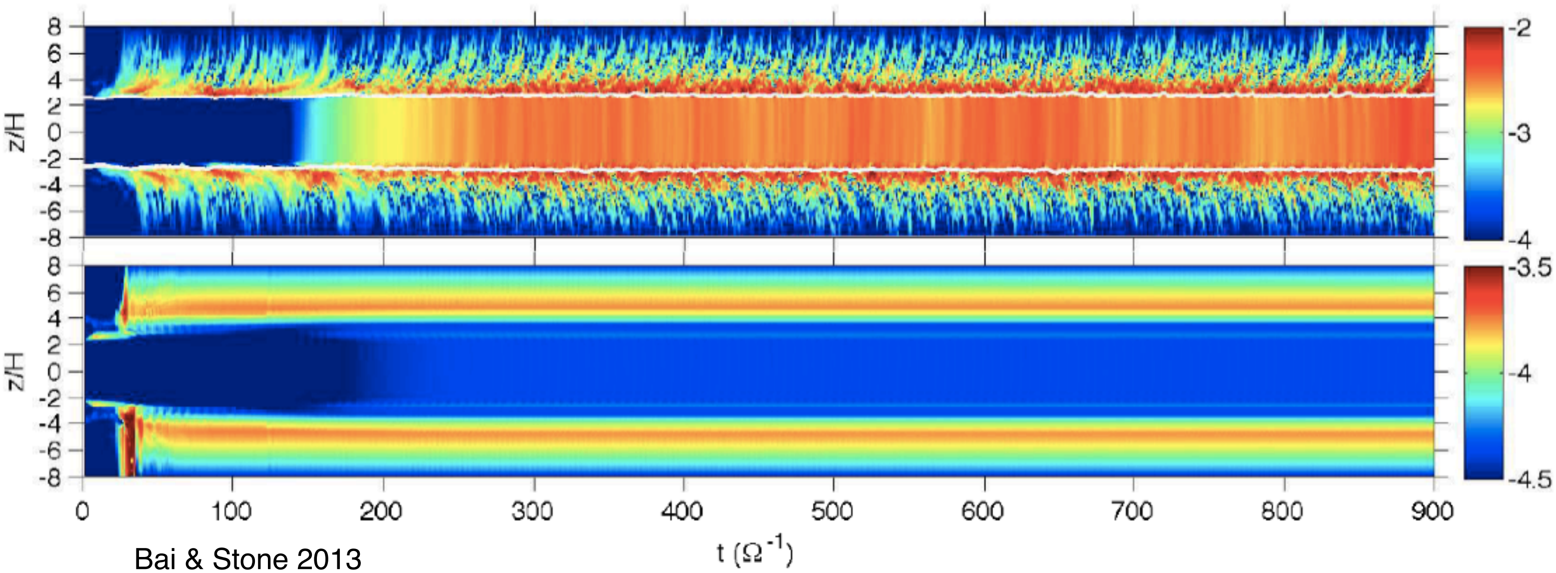

Ohmic

Ohmic + Ambipolar

Bai & Stone 2013

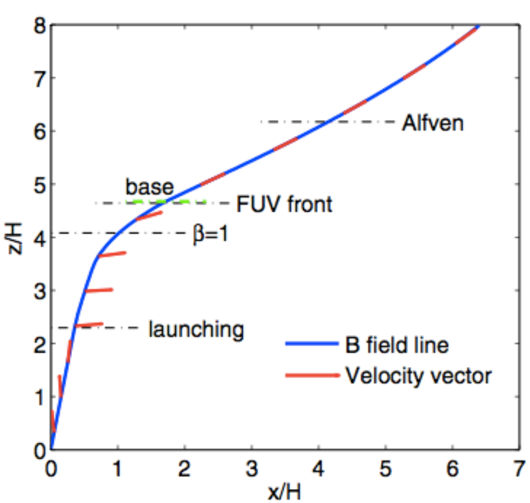

Figure 6. Poloidal field line geometry in our fiducial run OA-b5 (blue solid line). Overplotted are the unit vectors of the poloidal gas velocity (red arrows). The location of the wind launching point, the plasma $\beta = 1$ point, the FUV ionization front, and the Alfvén point are indicated (black dash-dotted). Also marked is the location at the base of the wind (green dashed).

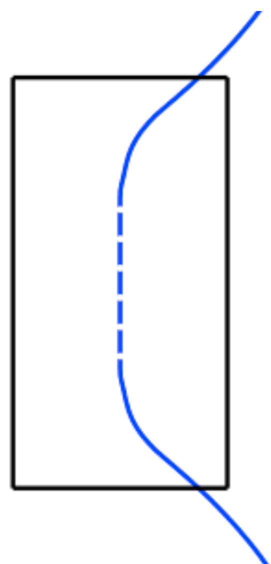

Ambipolar diffusion

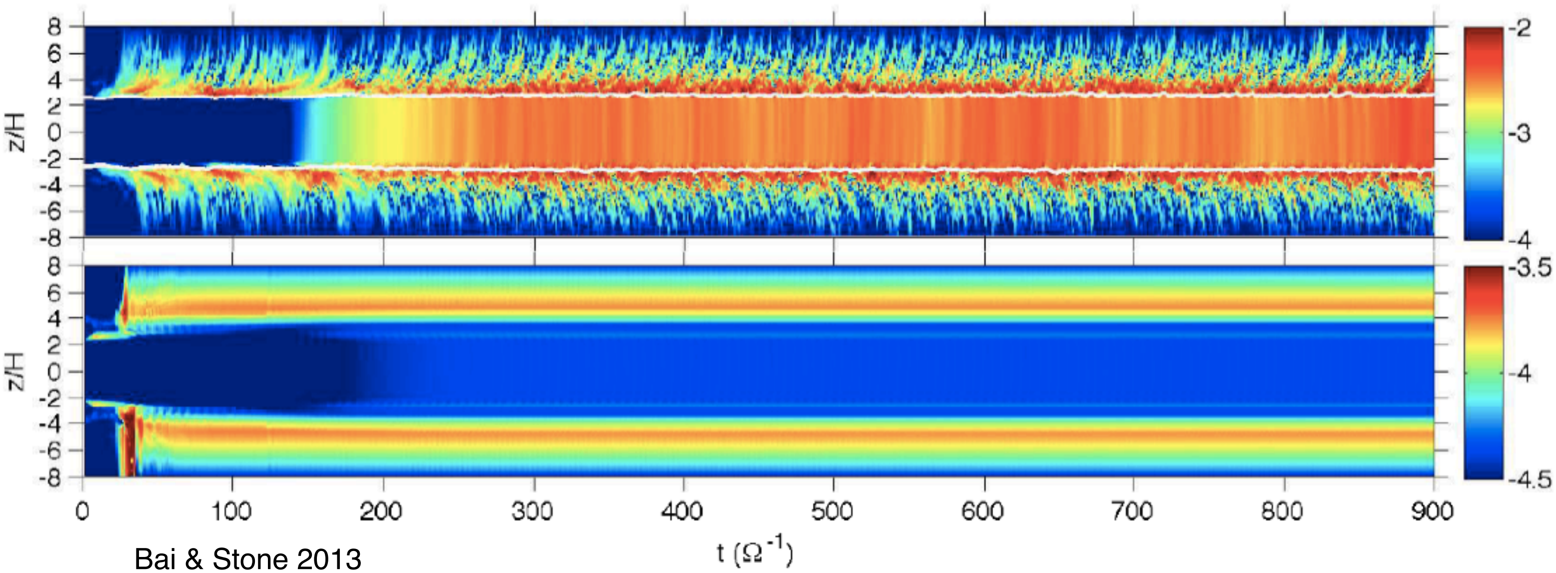

Ohmic

Ohmic + Ambipolar

Bai & Stone 2013

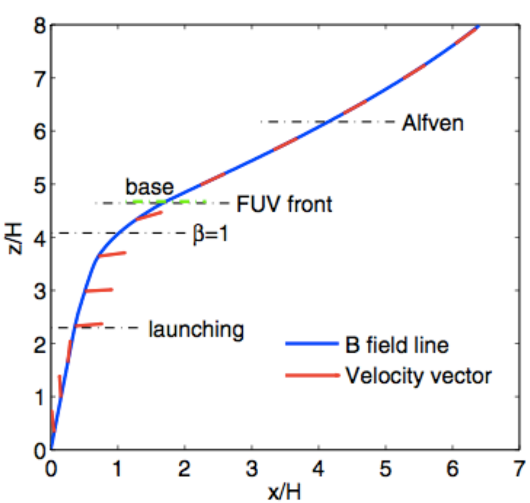

Figure 6. Poloidal field line geometry in our fiducial run OA-b5 (blue solid line). Overplotted are the unit vectors of the poloidal gas velocity (red arrows). The location of the wind launching point, the plasma $\beta = 1$ point, the FUV ionization front, and the Alfvén point are indicated (black dash-dotted). Also marked is the location at the base of the wind (green dashed).

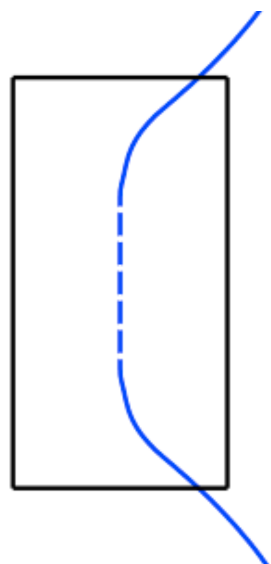

Ambipolar diffusion

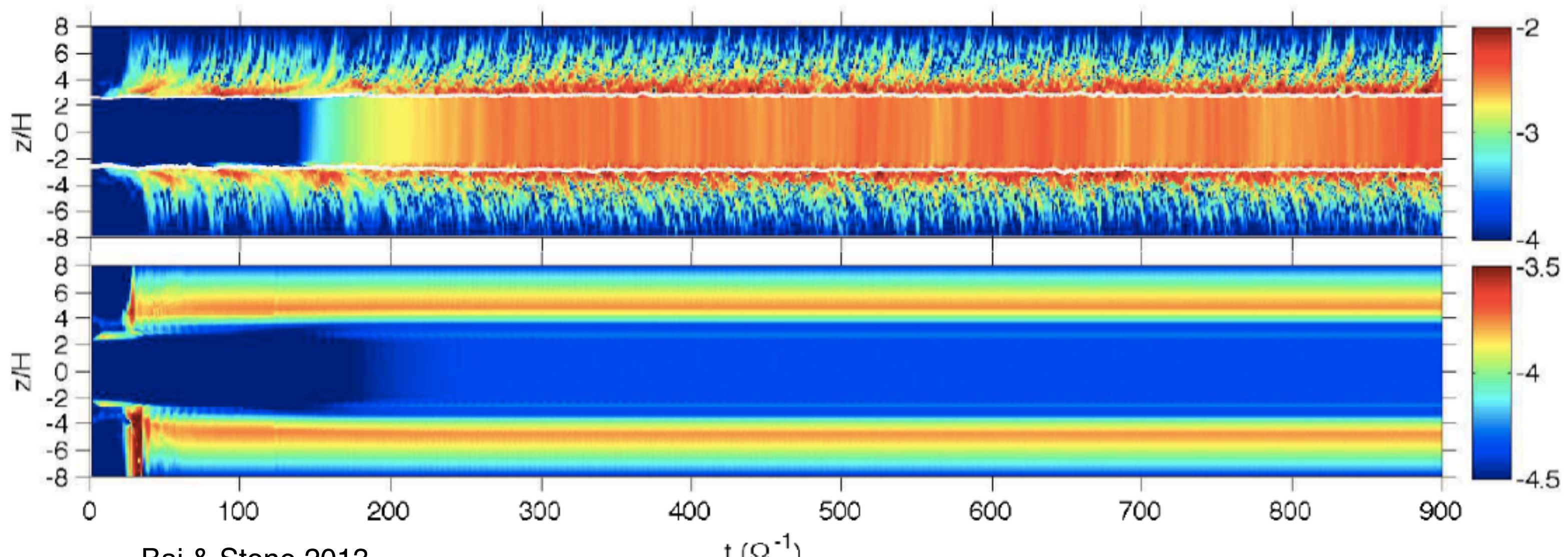

Ohmic

Ohmic + Ambipolar

Bai & Stone 2013

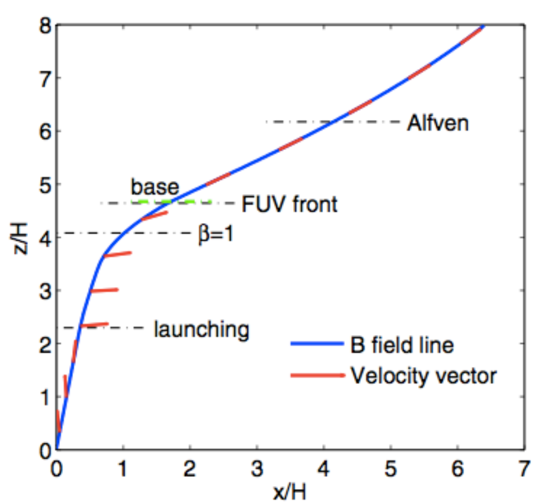

Figure 6. Poloidal field line geometry in our fiducial run OA-b5 (blue solid line). Overplotted are the unit vectors of the poloidal gas velocity (red arrows). The location of the wind launching point, the plasma $\beta = 1$ point, the FUV ionization front, and the Alfvén point are indicated (black dash-dotted). Also marked is the location at the base of the wind (green dashed).

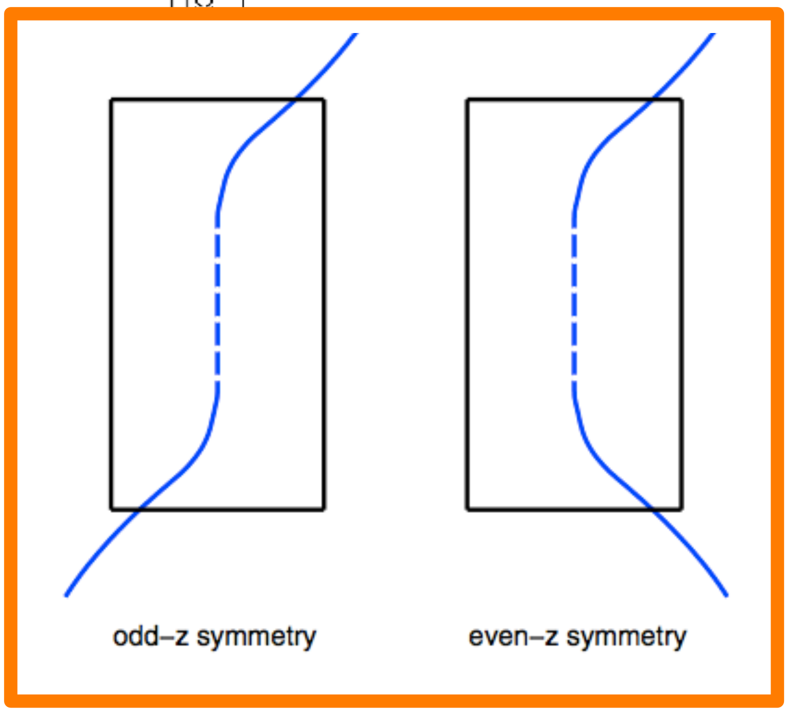

Global Ambipolar + Ohmic

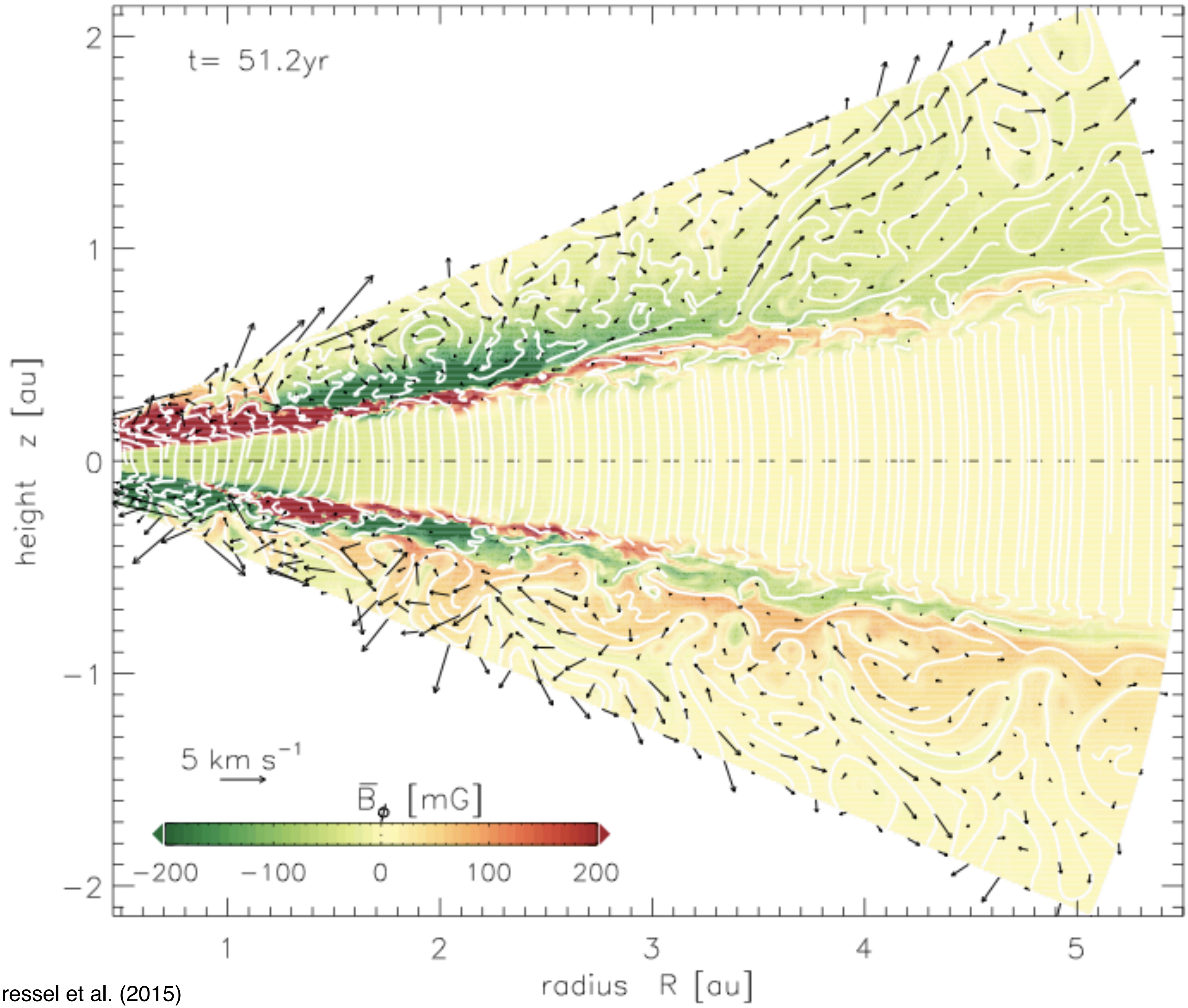

Gressel et al. (2015)

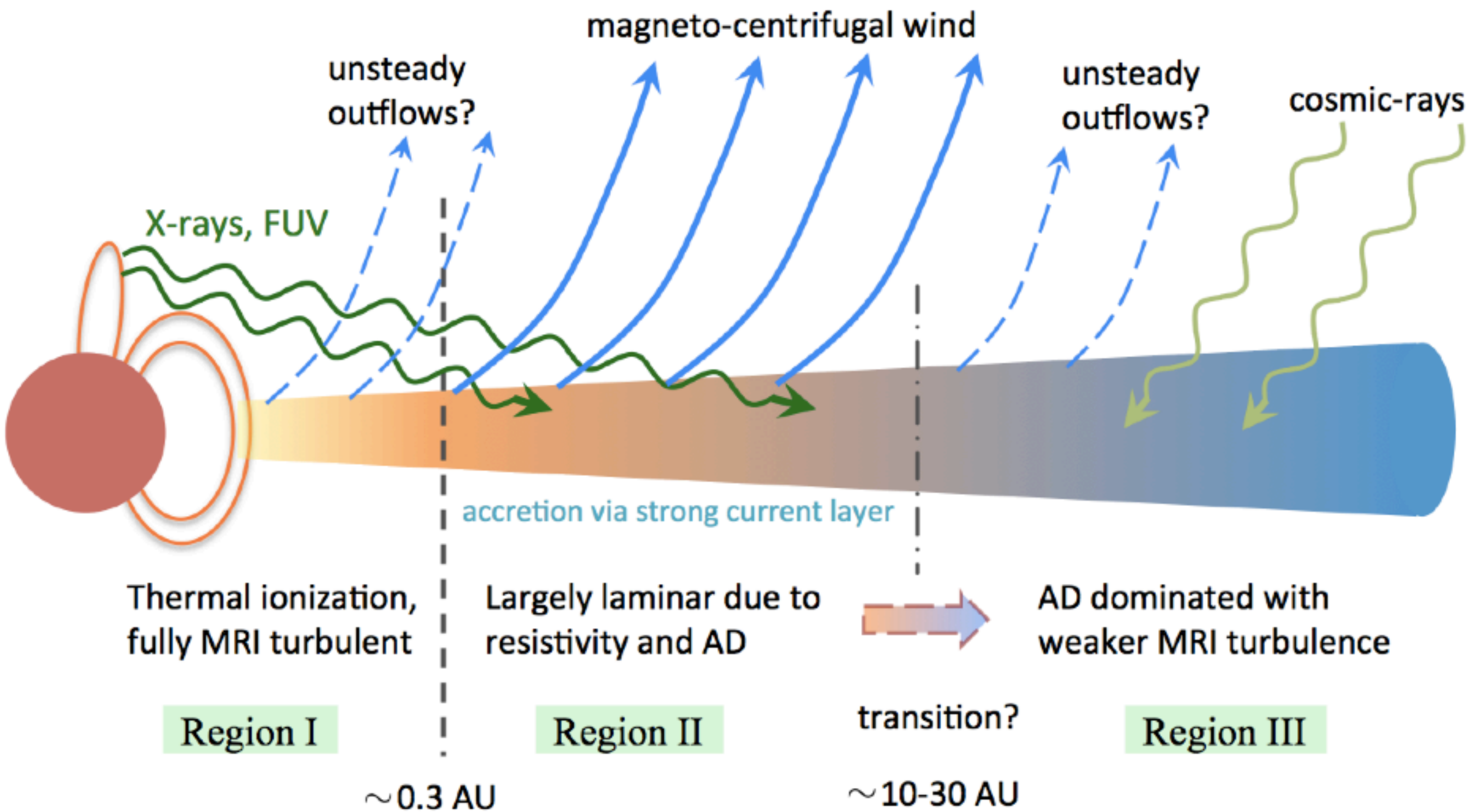
magneto-centrifugal wind
unsteady outflows?
unsteady outflows?
cosmic-rays
X-rays, FUV
accretion via strong current layer
Thermal ionization, fully MRI turbulent
Largely laminar due to resistivity and AD
AD dominated with weaker MRI turbulence
transition?
Region I
Region II
Region III
~0.3 AU
~10-30 AU

Hall term

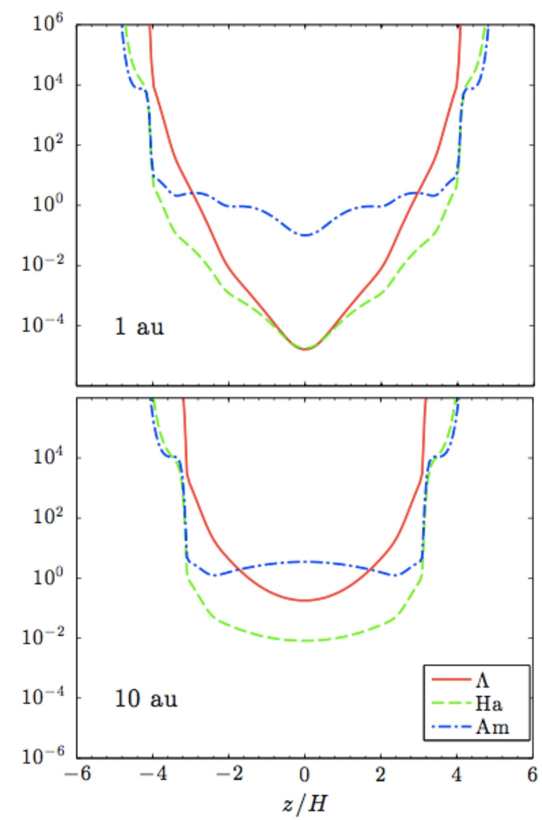

Thanatology in Protoplanetary Discs

The combined influence of Ohmic, Hall, and ambipolar diffusion on dead zones

Geoffroy Lesur[1,2], Matthew W. Kunz[3⋆], and Sébastien Fromang[4]

Large-scale azimuthal field generated. Couples to radial field fluctuations to generate large stress.

The flow stays laminar

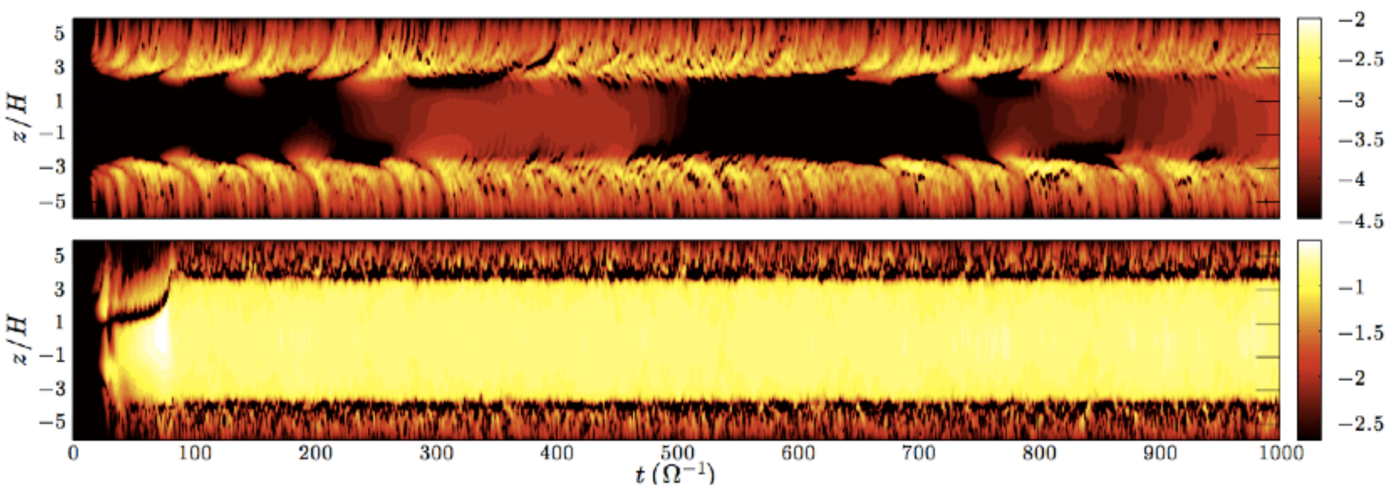

Ohmic

Ohmic + Hall

Fig. 6. Space-time diagram of the logarithm of the horizontally averaged Maxwell stress, $\log\langle -B_x B_y\rangle$, in the Ohmic (1-O-5; top) and Ohmic-Hall (I-OH-5; bottom) runs.

The full monty

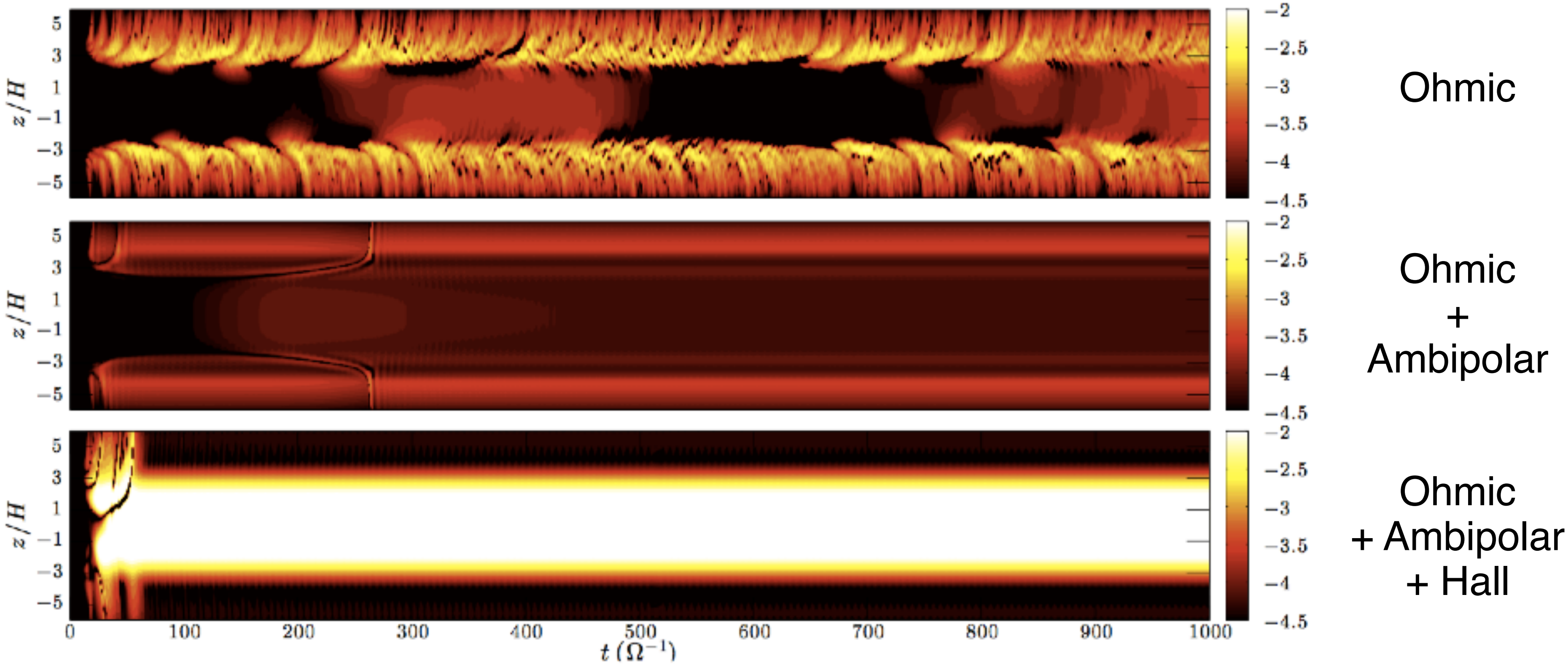

Fig. 9. Space-time evolution of the logarithm of the horizontally-averaged magnetic stress, $\log\langle M_{xy}\rangle$, in the Ohmic (1-O-5; top), Ohmic-ambipolar (1-OA-5; middle), and Ohmic-ambipolar-Hall (1-OHA-5; bottom) runs.

Ambipolar “kills” accretion.
Hall “ressurects” it.

Large scale B_ϕ couples to δB_r, leading to laminar stress.
Wind is also amplified.

Lesur et al. (2014)

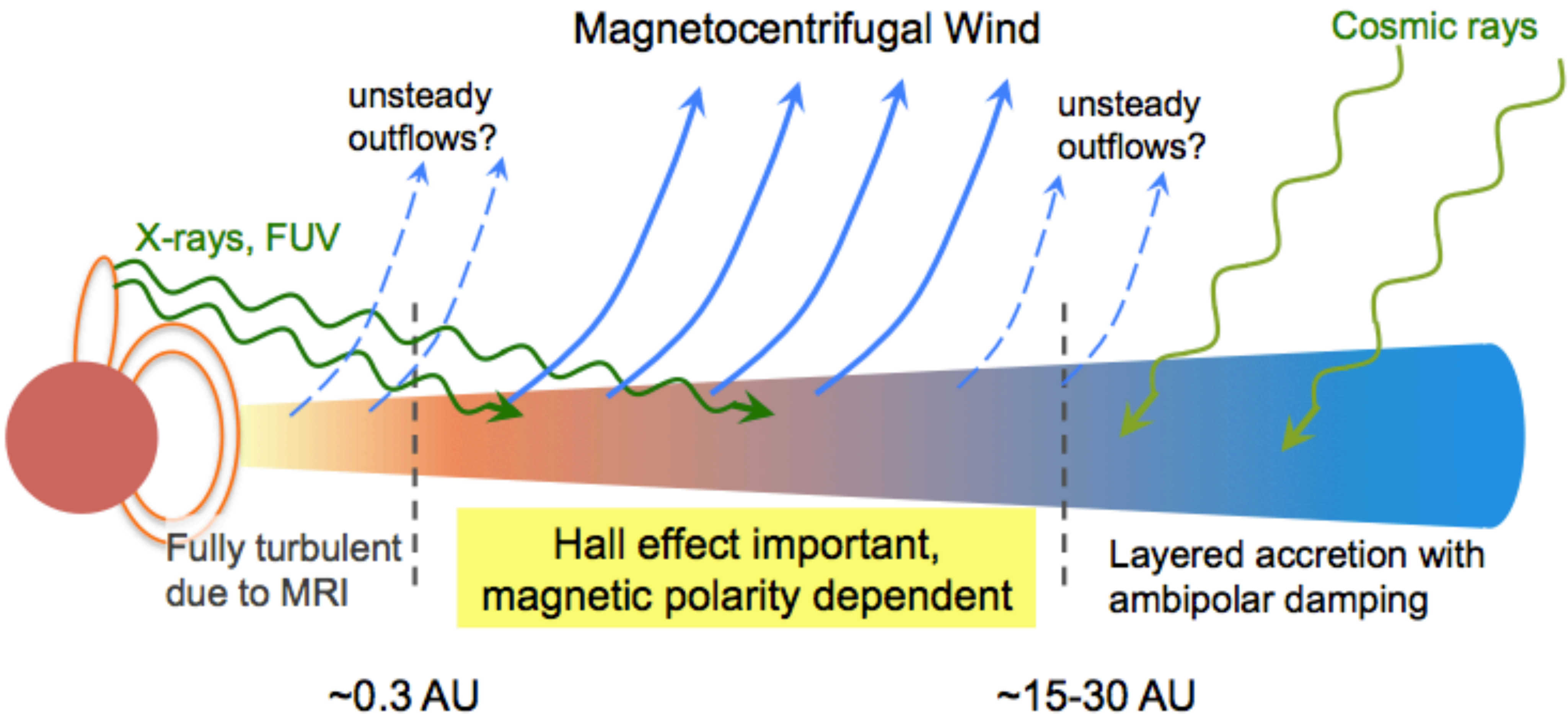
Magnetocentrifugal Wind
Cosmic rays
unsteady outflows?
unsteady outflows?
X-rays, FUV
Fully turbulent due to MRI
Hall effect important, magnetic polarity dependent
Layered accretion with ambipolar damping
~0.3 AU
~15-30 AU

Dead zone – Vertical Shear Instability

Stress

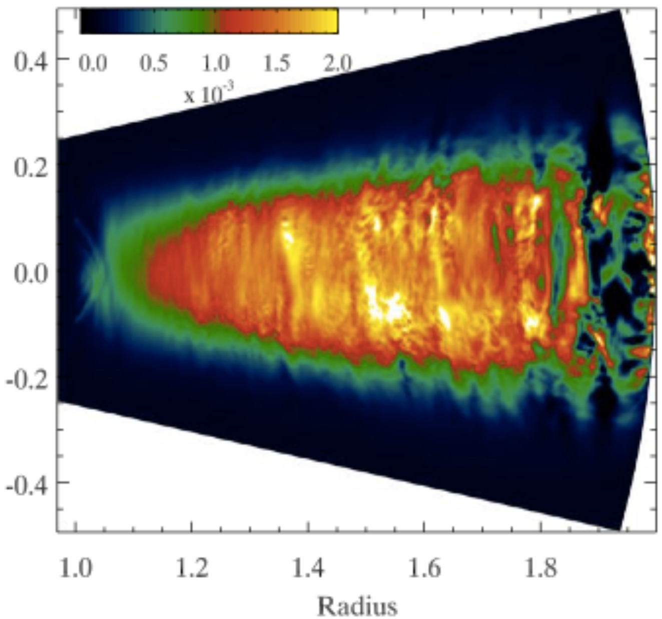

Vertical velocities

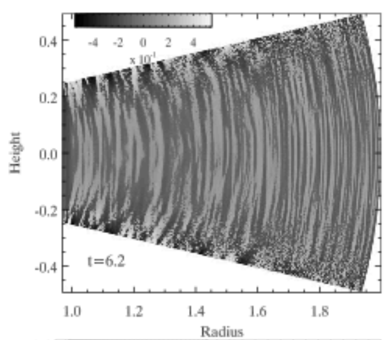

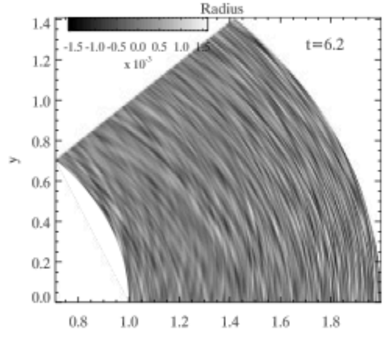

Taylor-Proudman theorem:
should rotate in cylinders.

For baroclinic disks, that is *not* the case.

Non-zero baroclinic term.

Dependecy on
cooling times.

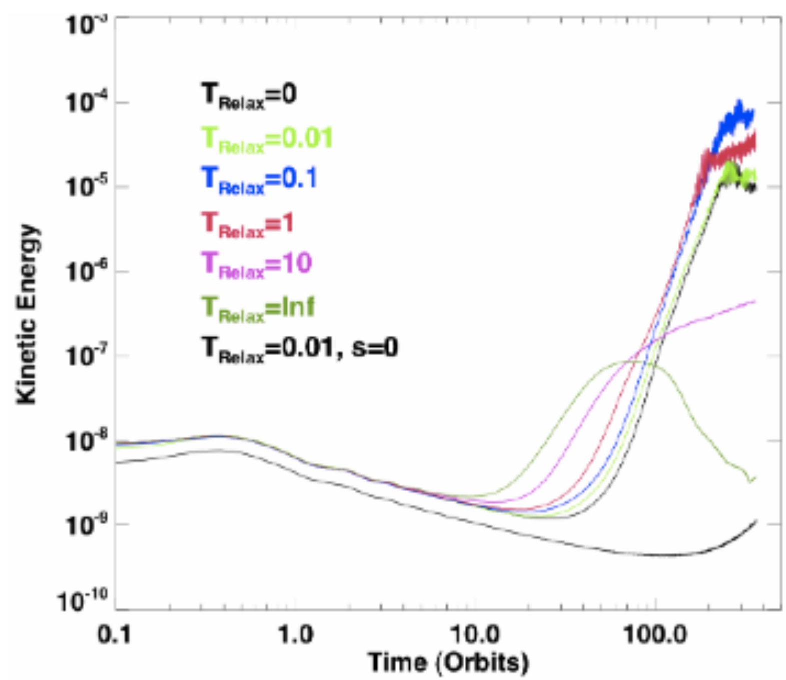

Dead zone - Convective Overstability

Klahr & Hubbard (2014), Lyra (2014)

$$\boxed{\begin{aligned}
&\frac{\partial\rho}{\partial t} + (\boldsymbol{u}\cdot\boldsymbol{\nabla})\,\rho = -\rho\boldsymbol{\nabla}\cdot\boldsymbol{u},\\
&\frac{\partial\boldsymbol{u}}{\partial t} + (\boldsymbol{u}\cdot\boldsymbol{\nabla})\,\boldsymbol{u} = -\frac{1}{\rho}\boldsymbol{\nabla}p + \boldsymbol{g},\\
&\frac{\partial p}{\partial t} + (\boldsymbol{u}\cdot\boldsymbol{\nabla})\,p = -\gamma p\boldsymbol{\nabla}\cdot\boldsymbol{u} - \frac{p}{T}\frac{(T-T_0)}{\tau},
\end{aligned}}$$

$$\bar{\omega}^3 + i\varsigma\bar{\omega}^2 - \bar{\omega}\mu^2(\kappa^2+N^2) - i\varsigma\kappa^2\mu^2 = 0,$$

$$\varsigma = 1/\gamma\tau \qquad \mu^2 = \quad k_z^2/k^2.$$

$$\boxed{\tau_{\max} = \frac{1}{\gamma}\left|\frac{k}{k_z}\right|\frac{1}{\sqrt{\kappa^2+N^2}} \qquad \sigma_{\max} = -\frac{1}{4}\left|\frac{k_z}{k}\right|\frac{N^2}{\sqrt{\kappa^2+N^2}}}$$

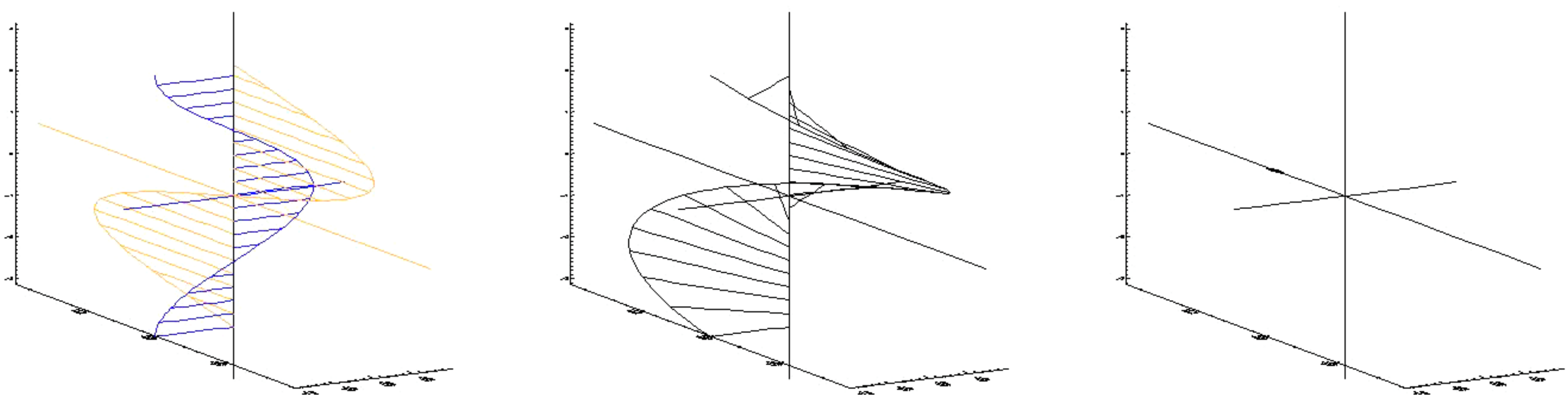

Lyra (2014)

Dead zone - Convective Overstability

Klahr & Hubbard (2014), Lyra (2014)

$$\boxed{\begin{aligned}
&\frac{\partial \rho}{\partial t} + (\boldsymbol{u}\cdot\boldsymbol{\nabla})\,\rho = -\rho\boldsymbol{\nabla}\cdot\boldsymbol{u},\\
&\frac{\partial \boldsymbol{u}}{\partial t} + (\boldsymbol{u}\cdot\boldsymbol{\nabla})\,\boldsymbol{u} = -\frac{1}{\rho}\boldsymbol{\nabla} p + \boldsymbol{g},\\
&\frac{\partial p}{\partial t} + (\boldsymbol{u}\cdot\boldsymbol{\nabla})\,p = -\gamma p\boldsymbol{\nabla}\cdot\boldsymbol{u} - \frac{p}{T}\frac{(T-T_0)}{\tau},
\end{aligned}}$$

$$\bar{\omega}^3 + i\varsigma\bar{\omega}^2 - \bar{\omega}\mu^2(\kappa^2+N^2) - i\varsigma\kappa^2\mu^2 = 0,$$

$$\varsigma = 1/\gamma\tau \qquad \mu^2 = \quad k_z^2/k^2.$$

$$\boxed{\tau_{\max} = \frac{1}{\gamma}\left|\frac{k}{k_z}\right|\frac{1}{\sqrt{\kappa^2+N^2}} \qquad \sigma_{\max} = -\frac{1}{4}\left|\frac{k_z}{k}\right|\frac{N^2}{\sqrt{\kappa^2+N^2}}}$$

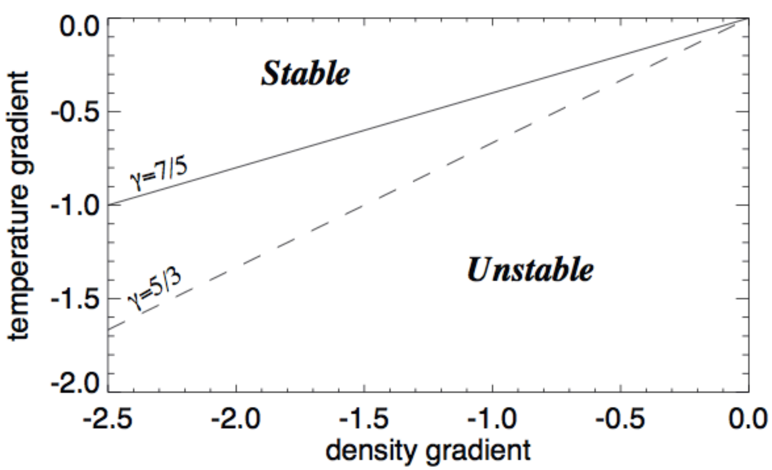

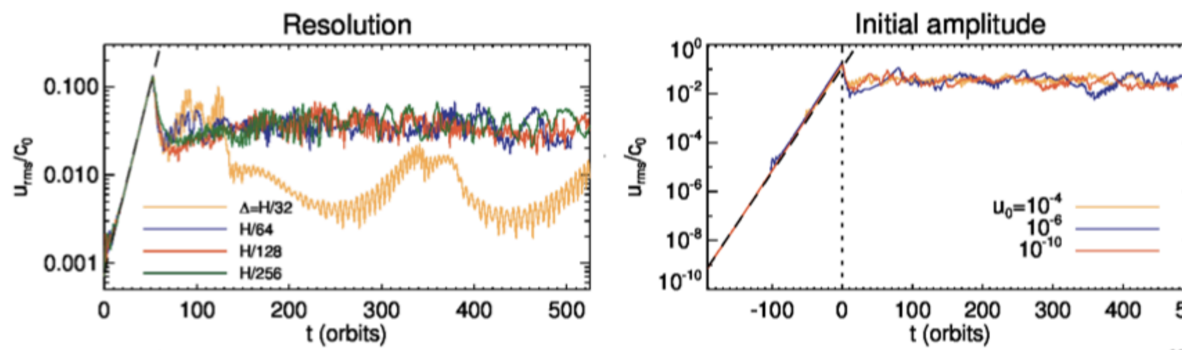

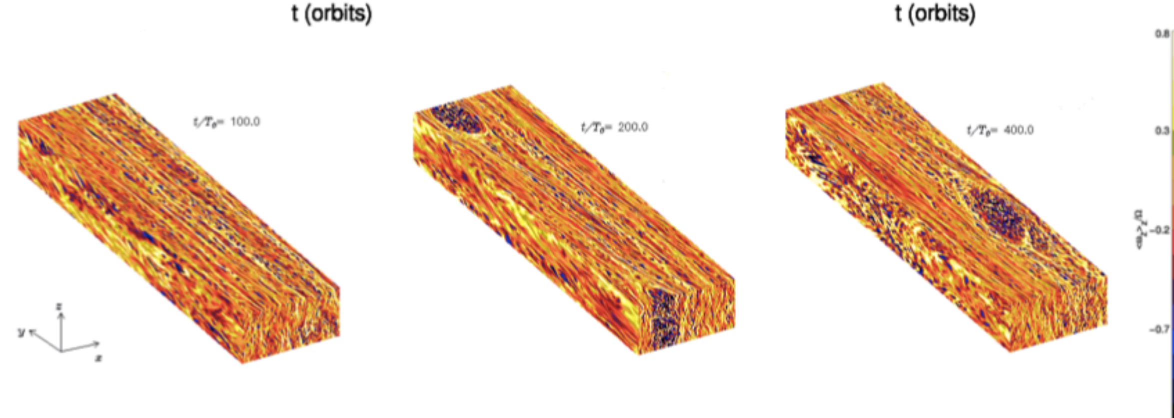

Lyra (2014)

Saturated state – self-sustenance of vortices

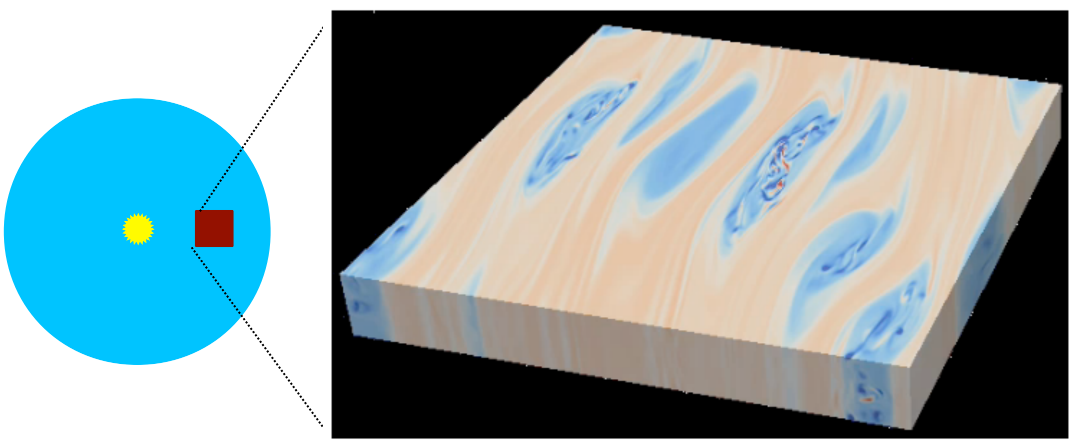

Lesur & Papaloizou (2010)

Sketch of the
Baroclinic Instability

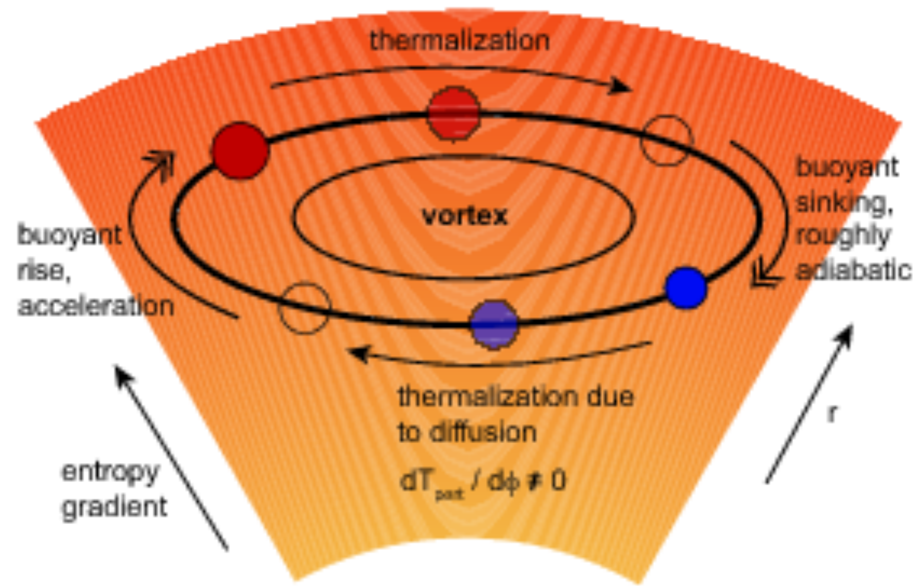

Armitage (2010)

$$\frac{\partial \omega}{\partial t} = \underbrace{-(\boldsymbol{u}\cdot\nabla)\omega}_{\text{advection}} \underbrace{-\,\omega(\nabla\cdot\boldsymbol{u})}_{\text{compression}} + \underbrace{(\omega\cdot\nabla)\boldsymbol{u}}_{\text{stretching}} + \underbrace{\frac{1}{\rho^2}\nabla\rho\times\nabla p}_{\text{baroclinicity}} + \underbrace{\nu\nabla^2\omega}_{\text{dissipation}}$$

Saturated state – self-sustenance of vortices

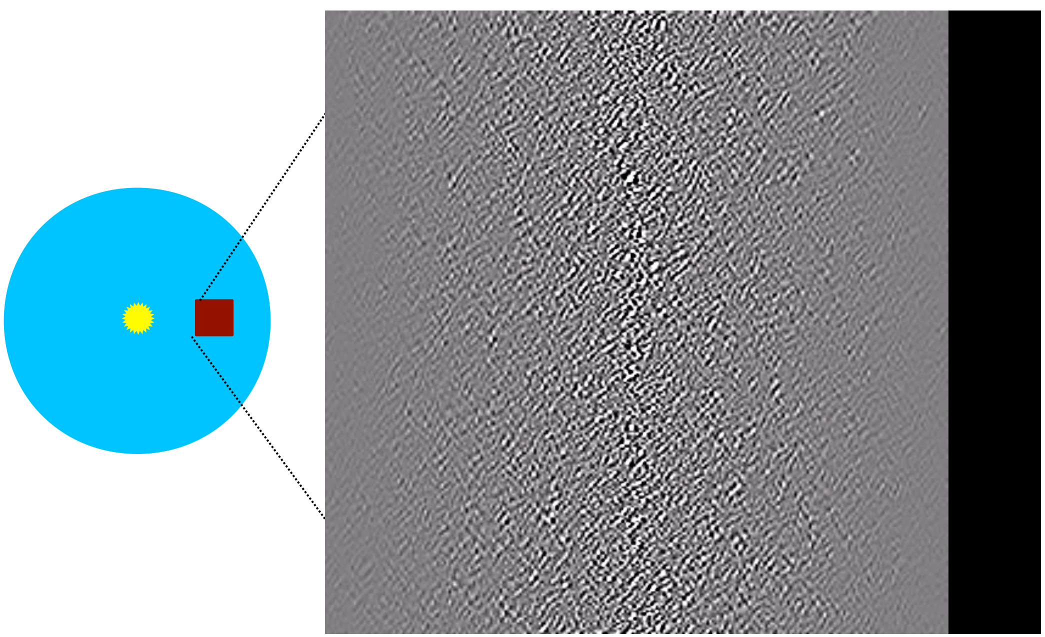

Lyra & Klahr (2011)

Sketch of the Baroclinic Instability

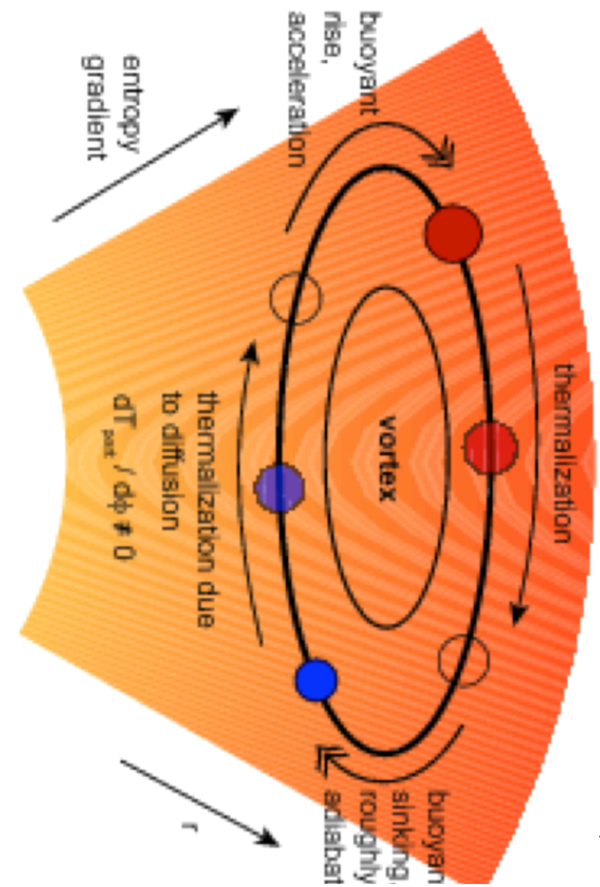

Armitage (2010

$$\frac{\partial \omega}{\partial t} = \underbrace{-(\boldsymbol{u}\cdot\nabla)\omega}_{\text{advection}} \underbrace{-\omega(\nabla\cdot\boldsymbol{u})}_{\text{compression}} + \underbrace{(\omega\cdot\nabla)\boldsymbol{u}}_{\text{stretching}} + \underbrace{\frac{1}{\rho^2}\nabla\rho\times\nabla p}_{\text{baroclinicity}} + \underbrace{\nu\nabla^2\omega}_{\text{dissipation}}$$

Vortices and layered accretion

What happens when the vortex is magnetized?

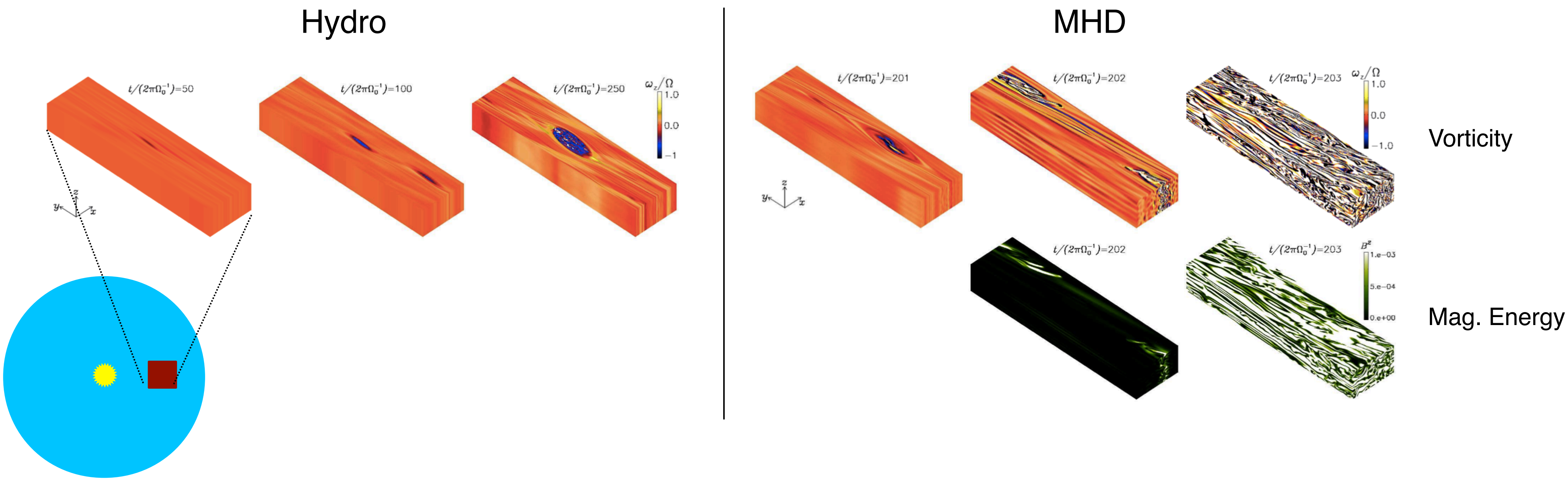

Lyra & Klahr (2011)

Vortices and layered accretion

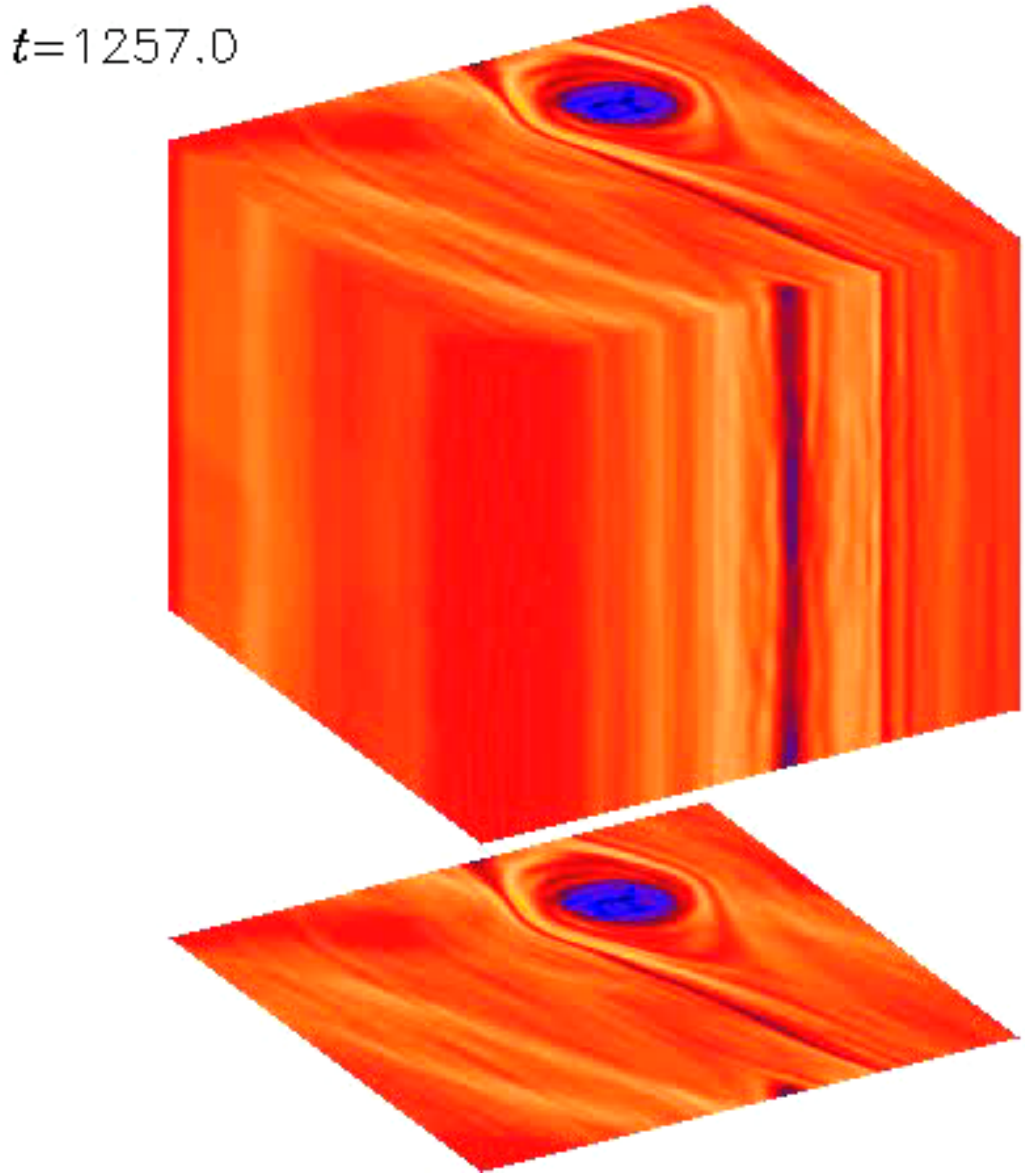

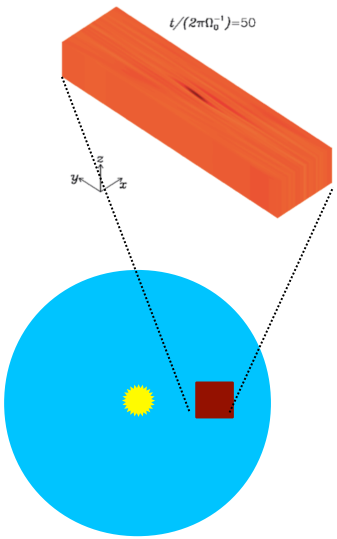

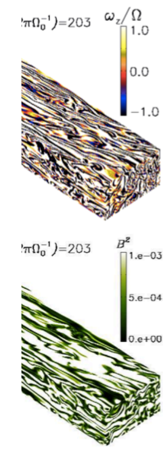

Vorticity

Mag. Energy

Vortices and layered accretion

What happens when the vortex is magnetized?

Hydro

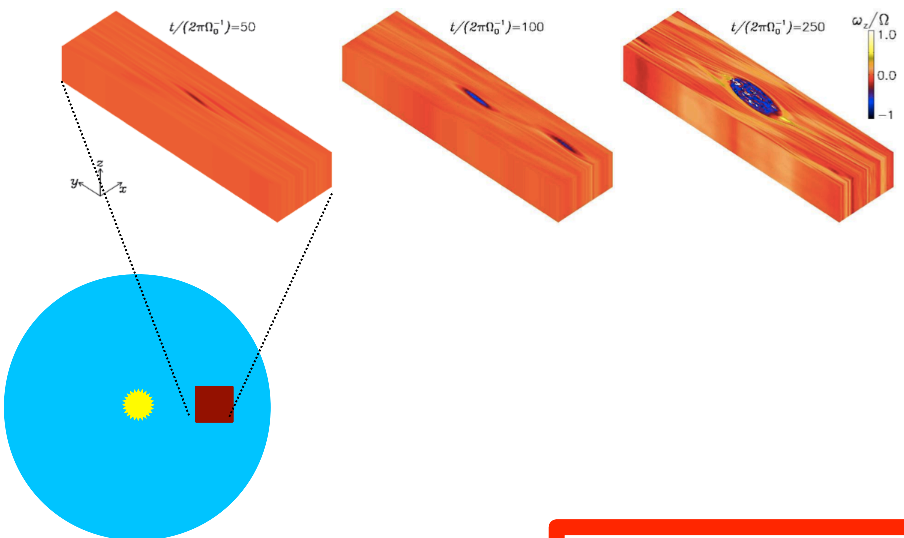

MHD

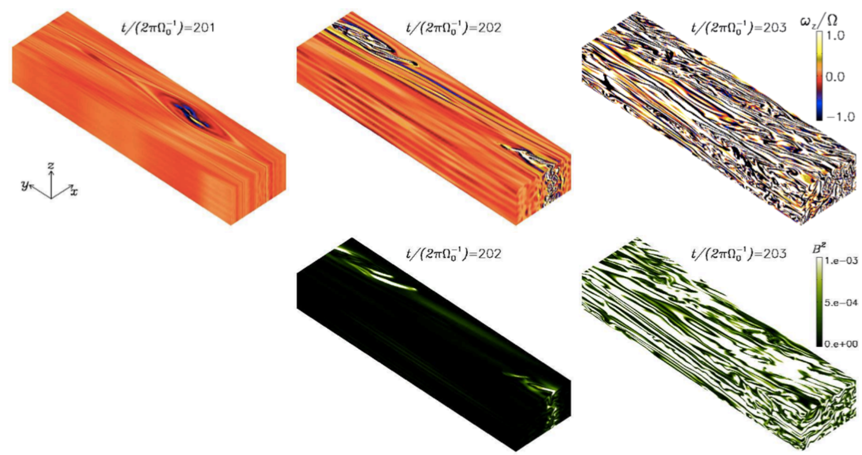

Vorticity

Mag. Energy

Vortices
do not survive magnetization

Lyra & Klahr (2011)

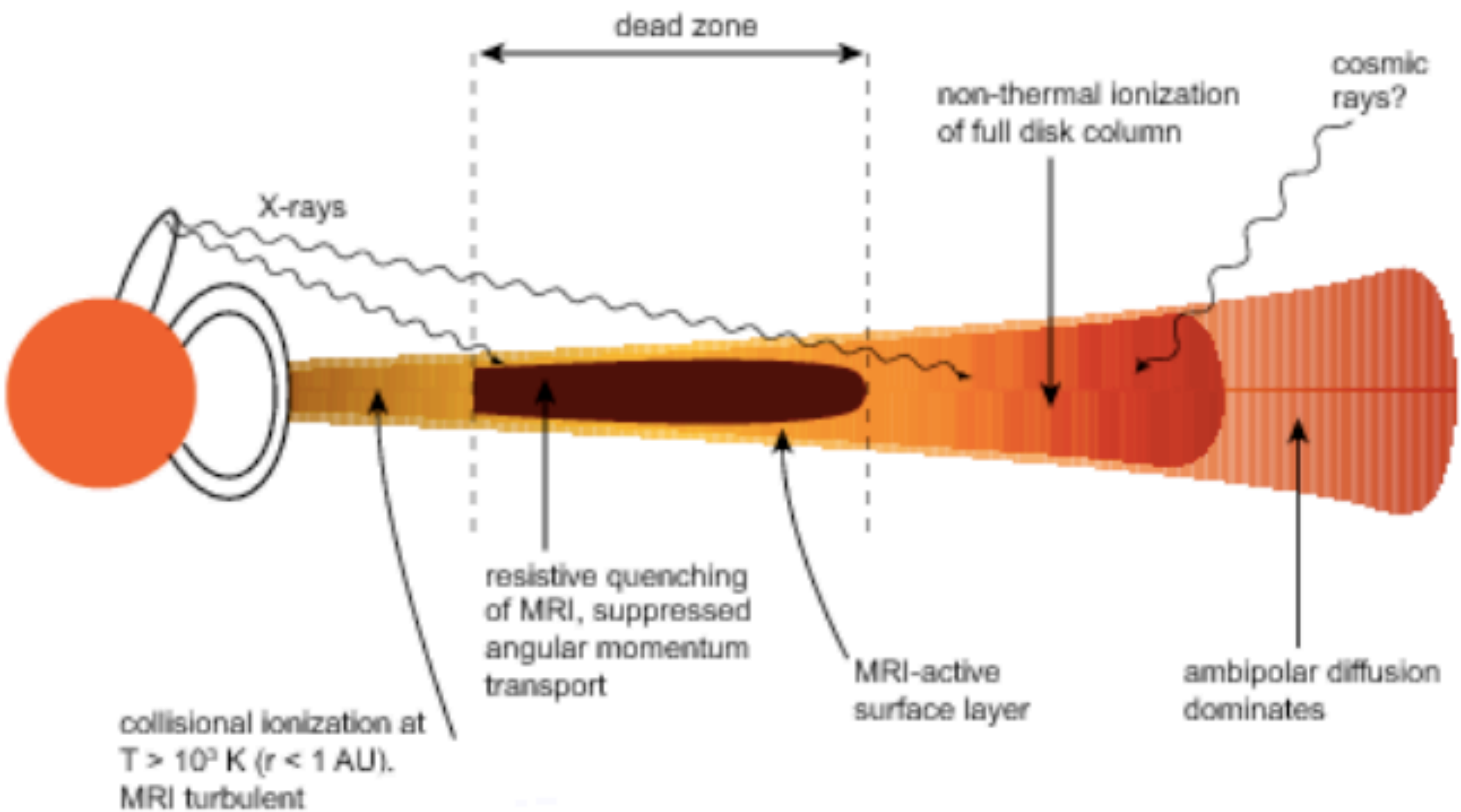
dead zone
cosmic rays?
non-thermal ionization of full disk column
X-rays
resistive quenching of MRI, suppressed angular momentum transport
MRI-active surface layer
ambipolar diffusion dominates
collisional ionization at T > 10³ K (r < 1 AU). MRI turbulent

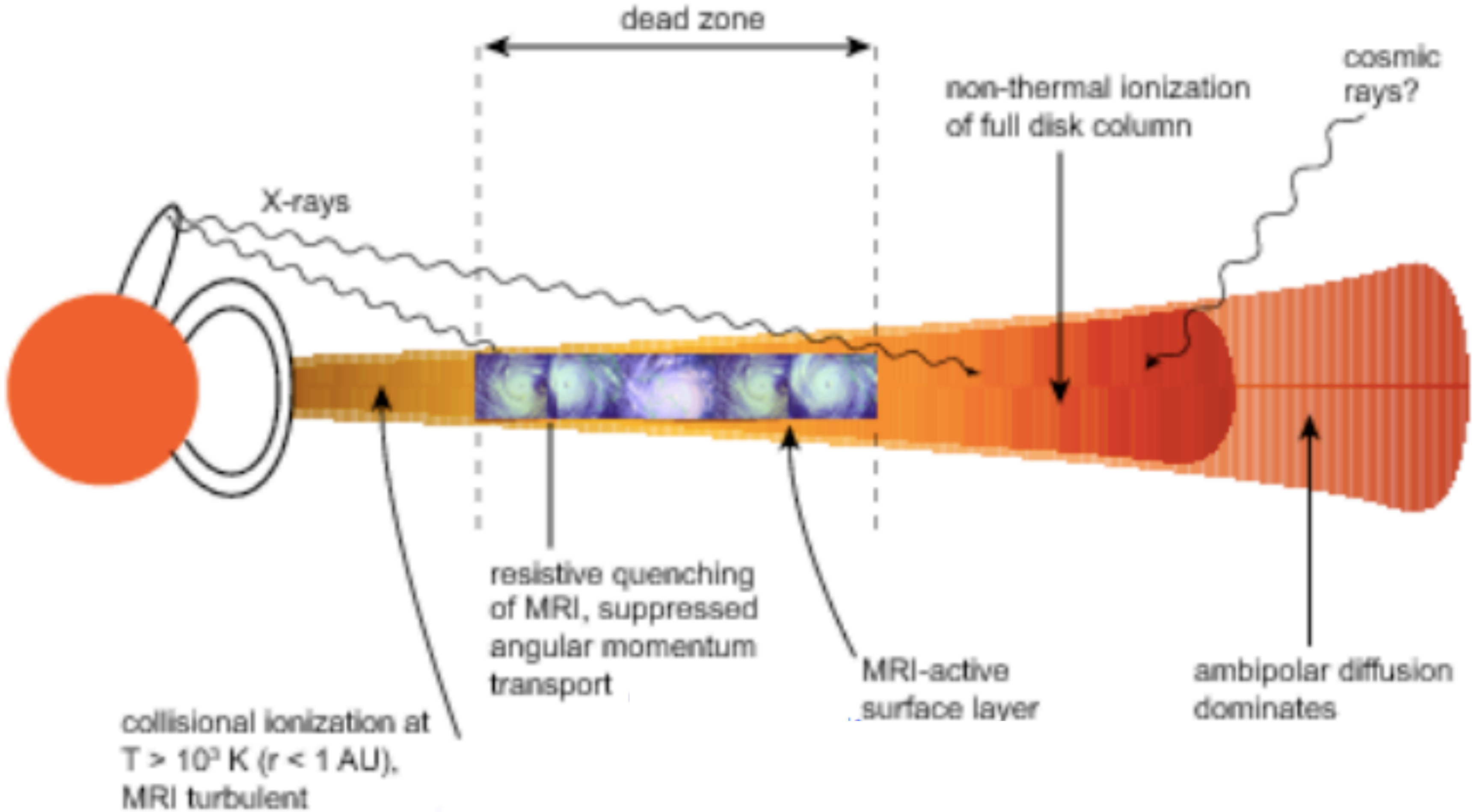
dead zone
cosmic rays?
non-thermal ionization of full disk column
X-rays
resistive quenching of MRI, suppressed angular momentum transport
MRI-active surface layer
ambipolar diffusion dominates
collisional ionization at T > 10³ K (r < 1 AU), MRI turbulent

Observational evidence: gaps, spirals, and vortices

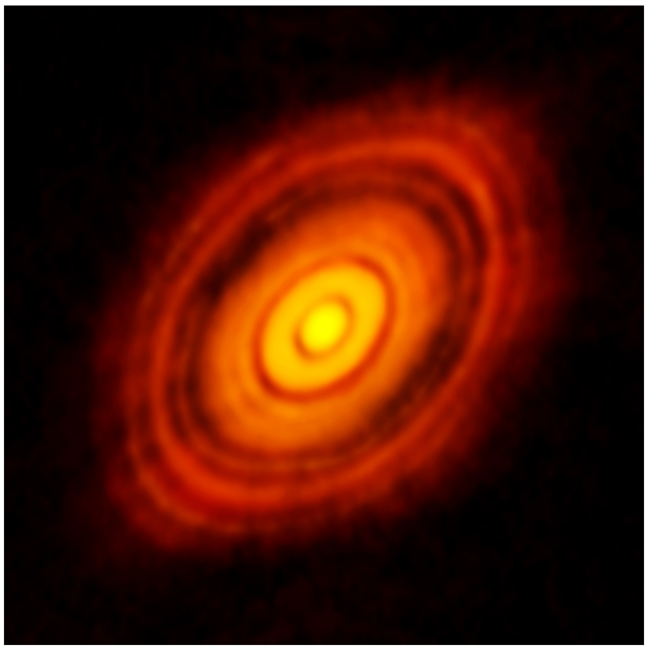

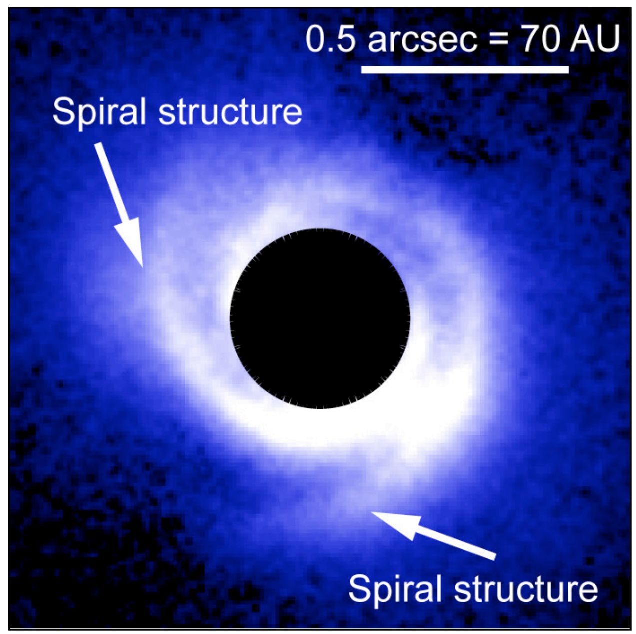

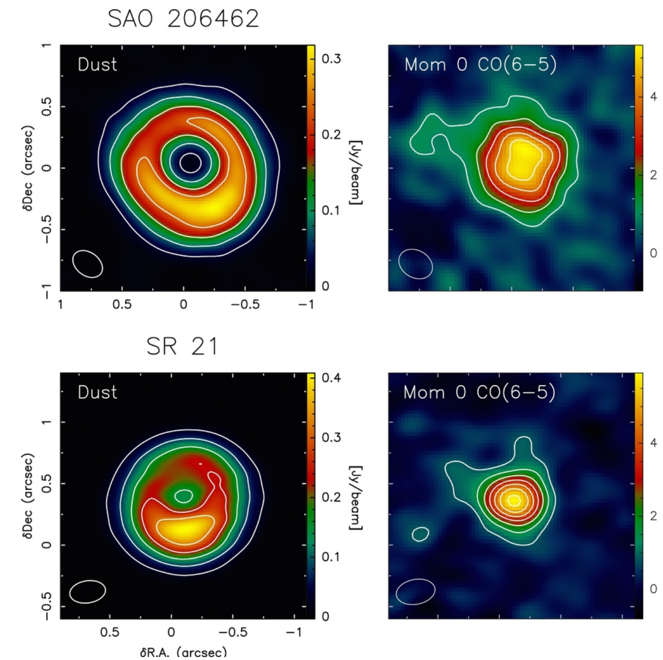

Planet-disk interaction: gaps, spirals, and vortices.

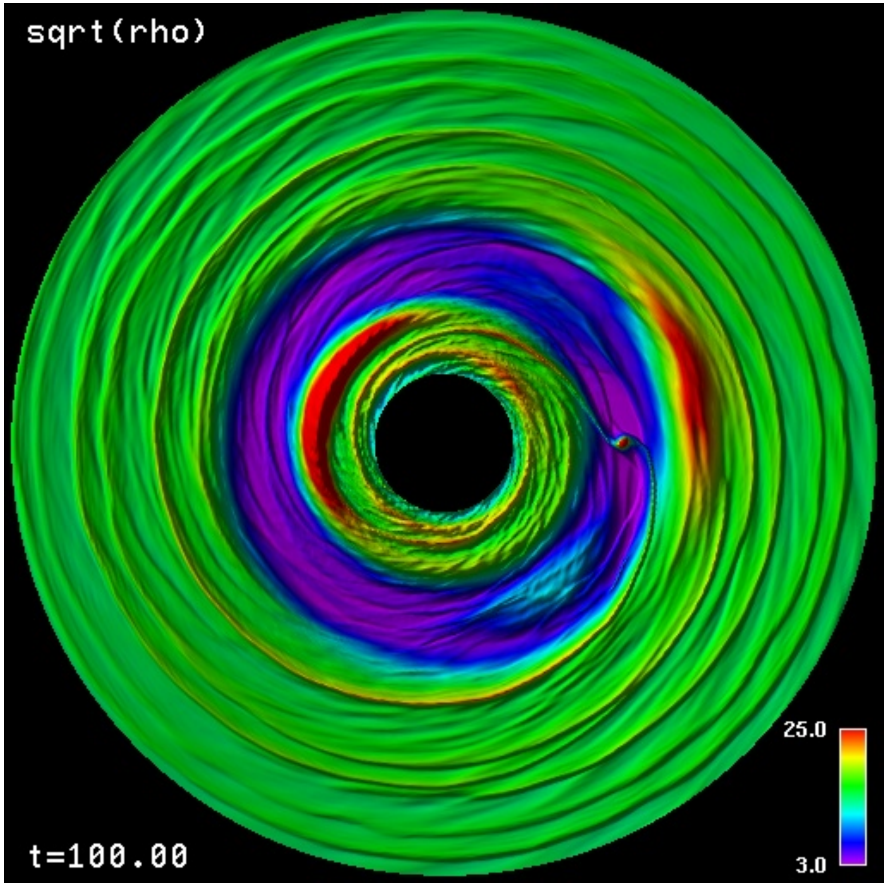

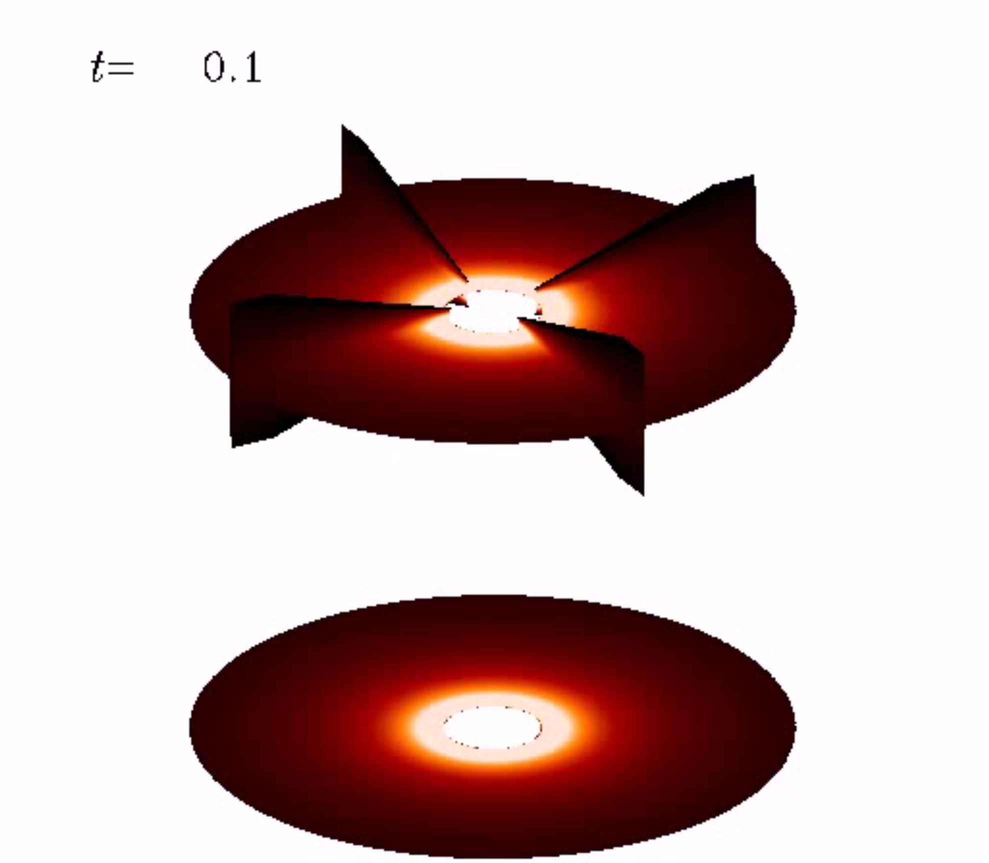

Drag-Diffusion Equilibrium

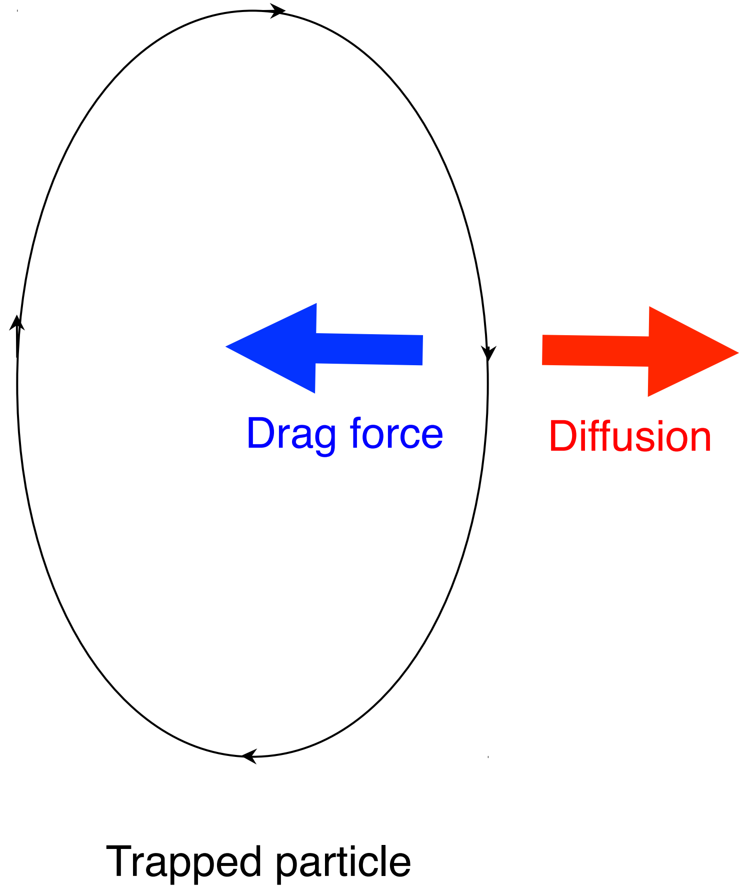

Drag-Diffusion Equilibrium

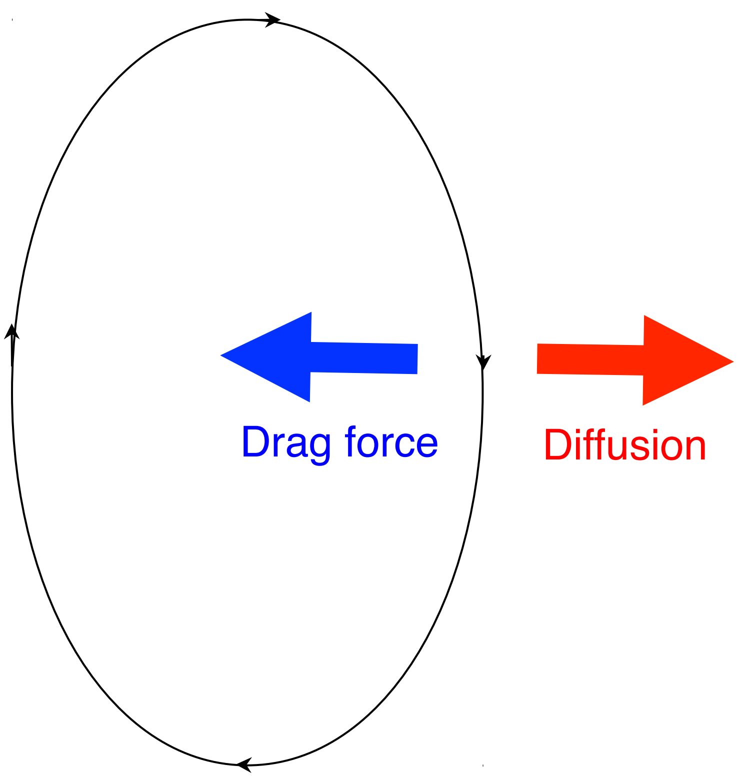

Trapped particle

Dust continuity equation

$$\frac{\partial \rho_d}{\partial t} = -\underbrace{(\boldsymbol{v}\cdot\boldsymbol{\nabla})\rho_d}_{\text{advection}} - \underbrace{\rho_d \boldsymbol{\nabla}\cdot\boldsymbol{v}}_{\text{compression}} + \underbrace{D\nabla^2\rho_d}_{\text{diffusion}},$$

Drag-Diffusion Equilibrium

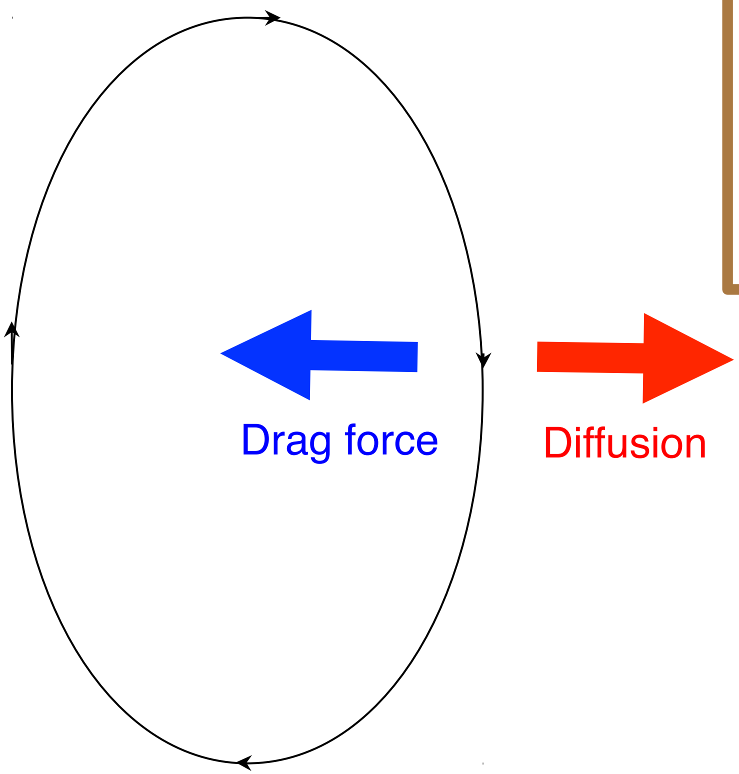

Trapped particle

Steady-state solution

$$\rho_d(a,z) = \varepsilon\rho_0\,(S+1)^{3/2}\,\exp\left\{-\frac{[a^2 f^2(\chi)+z^2]}{2H^2}(S+1)\right\}$$

Lyra & Lin (2013)

$$S = \frac{St}{\delta}$$

$$\delta = v_{\rm rms}^2/c_s^2,$$

a = vortex semi-minor axis
H = disk scale height (temperature)
χ = vortex aspect ratio
δ = diffusion parameter
St = Stokes number (particle size)
f(χ) = model-dependent scale function

Analytical solution for dust trapping

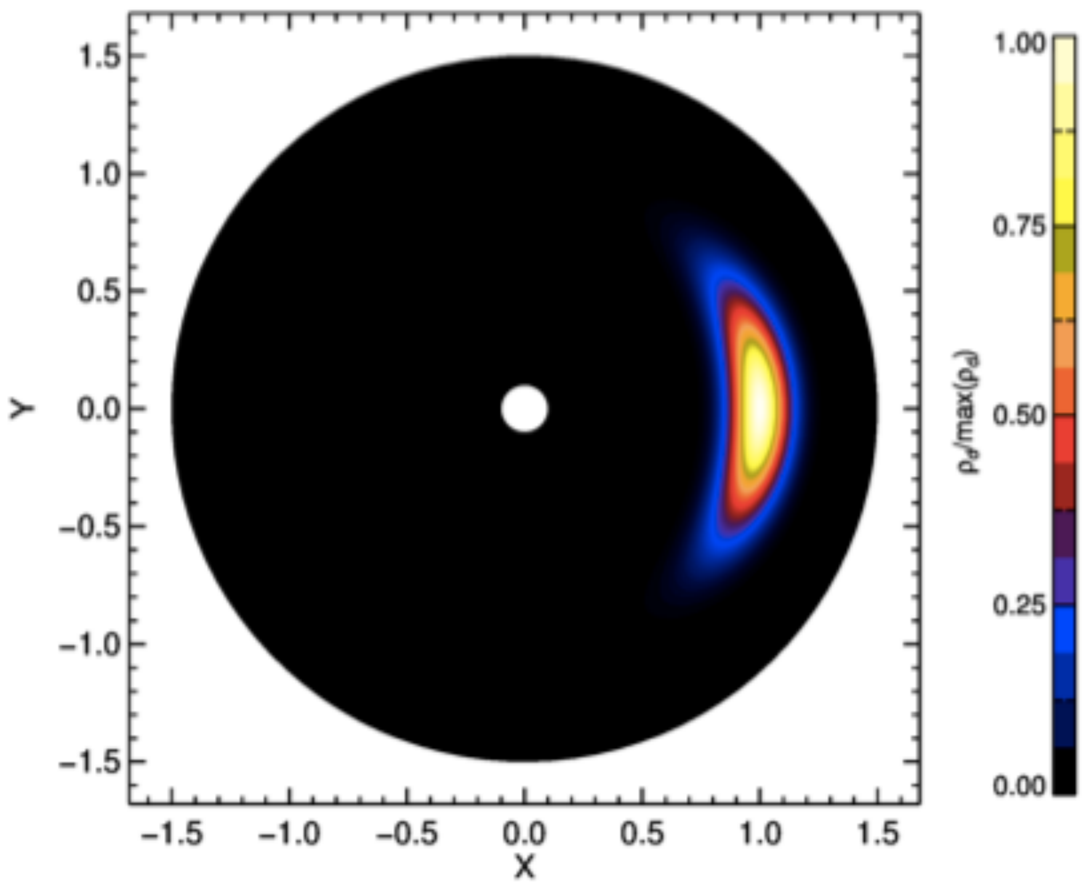

Solution

$$\rho_d(a) = \rho_{d\,\max} \exp\left(-\frac{a^2}{2H_V^2}\right),$$

$$H_V = \frac{H}{f(\chi)}\sqrt{\frac{1}{S+1}}$$

$$S = \frac{St}{\delta}$$

$$\delta = v_{\rm rms}^2/c_s^2,$$

Solution for

$H/r=0.1$ $\chi=4$ $S=1$

a = vortex semi-minor axis
H = disk scale height (temperature)
χ = vortex aspect ratio
δ = diffusion parameter
St = Stokes number (particle size)
$f(\chi)$ = model-dependent scale function

Lyra & Lin (2013)

Analytical vs Numerical

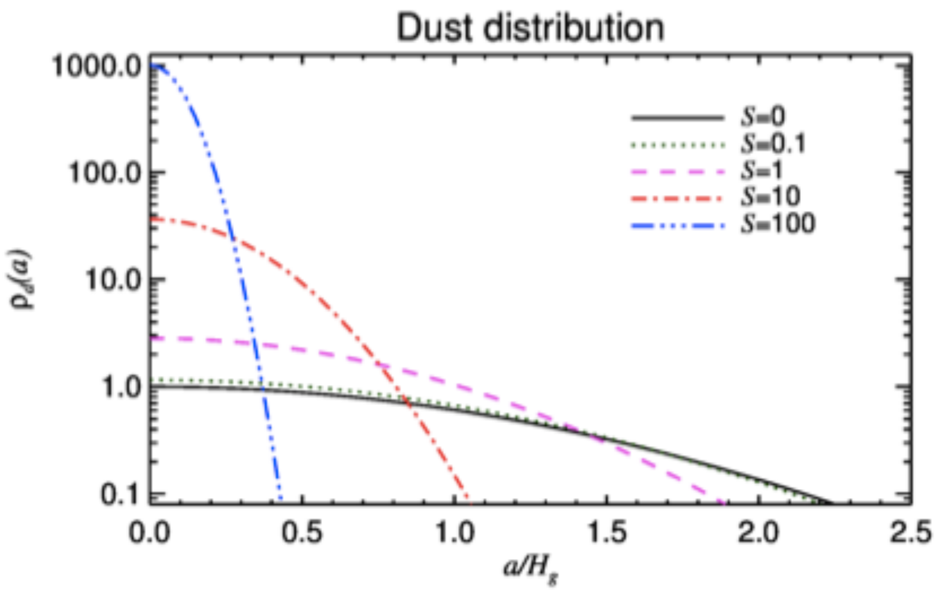

$$S = \frac{St}{\delta} \qquad \delta = v_{\rm rms}^2 / c_s^2,$$

Lyra & Lin (2013)

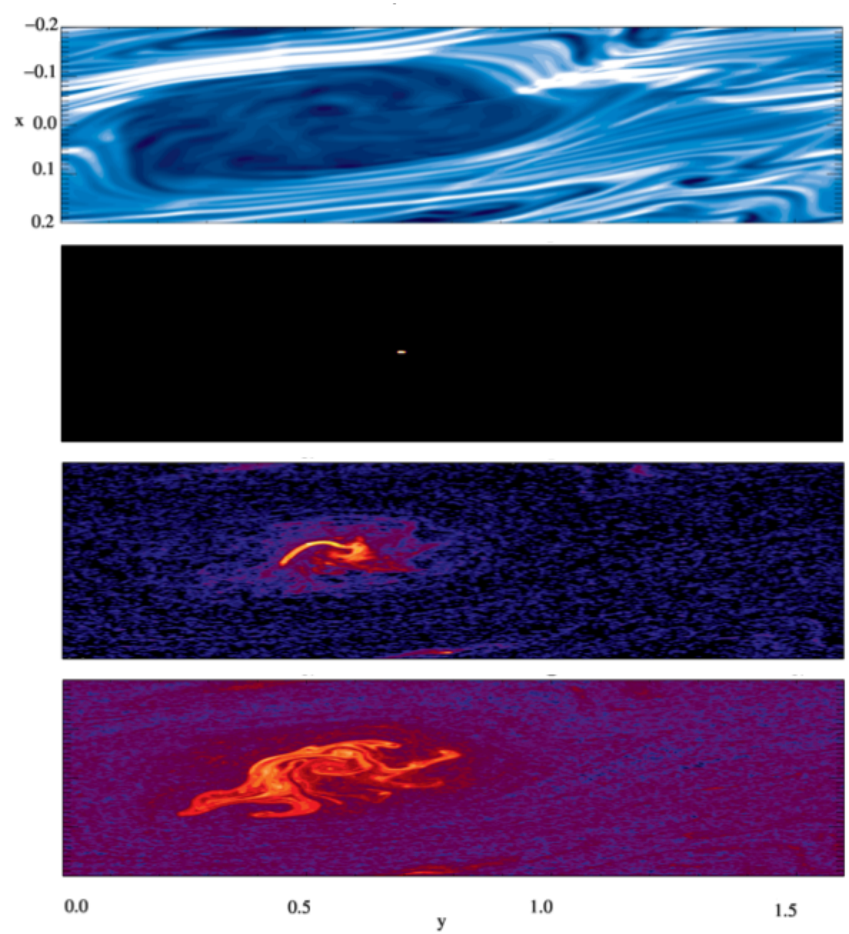

Gas

St=1

St=0.05

St=0.01

Raettig et al (2015)

Derived quantities

$$\rho_d(a,z) = \varepsilon\rho_0\,(S+1)^{3/2}\,\exp\left\{-\frac{[a^2 f^2(\chi)+z^2]}{2H^2}(S+1)\right\}$$

Lyra & Lin (2013)

Gas distribution

$$\rho_g(a) = \rho_{g\max}\,\exp\left(-\frac{a^2}{2H_g^2}\right),$$

Maximum dust density

$$\rho_{d\max} = \varepsilon\,\rho_0\,(S+1)^{3/2}$$

Gas contrast

$$\frac{\rho_{g\max}}{\rho_{g\min}} = \exp\left[\frac{f^2(\chi)}{2\chi^2\omega_V^2}\right],$$

Dust contrast

$$\frac{\rho_{d\max}}{\rho_{d\min}} = \frac{\rho_{g\max}}{\rho_{g\min}}\exp(S),$$

Total trapped mass

$$\int \rho_d(a,z)dV = (2\pi)^{3/2}\,\varepsilon\rho_0\,\chi H H_g^2$$

Vortex size

$$a_s = H(\chi\omega_V)^{-1}$$

H = disk scale height (temperature)
χ = vortex aspect ratio
δ = diffusion parameter
St = Stokes number (particle size)
$f(\chi)$ = model-dependent scale function
ε = dust-to-gas ratio

Applying the model to Oph IRS 48

Observed parameters

Aspect ratio: 3.1

Dust contrast: 130

Temperature: 60K

Trapped mass: 9 M_{Earth}

Derived parameters

S=4.8

Stokes number, St=0.008

$\delta = 0.005$, $v_{rms} = 4\%\ c_s$

Trapped mass: 11 M_{Earth}

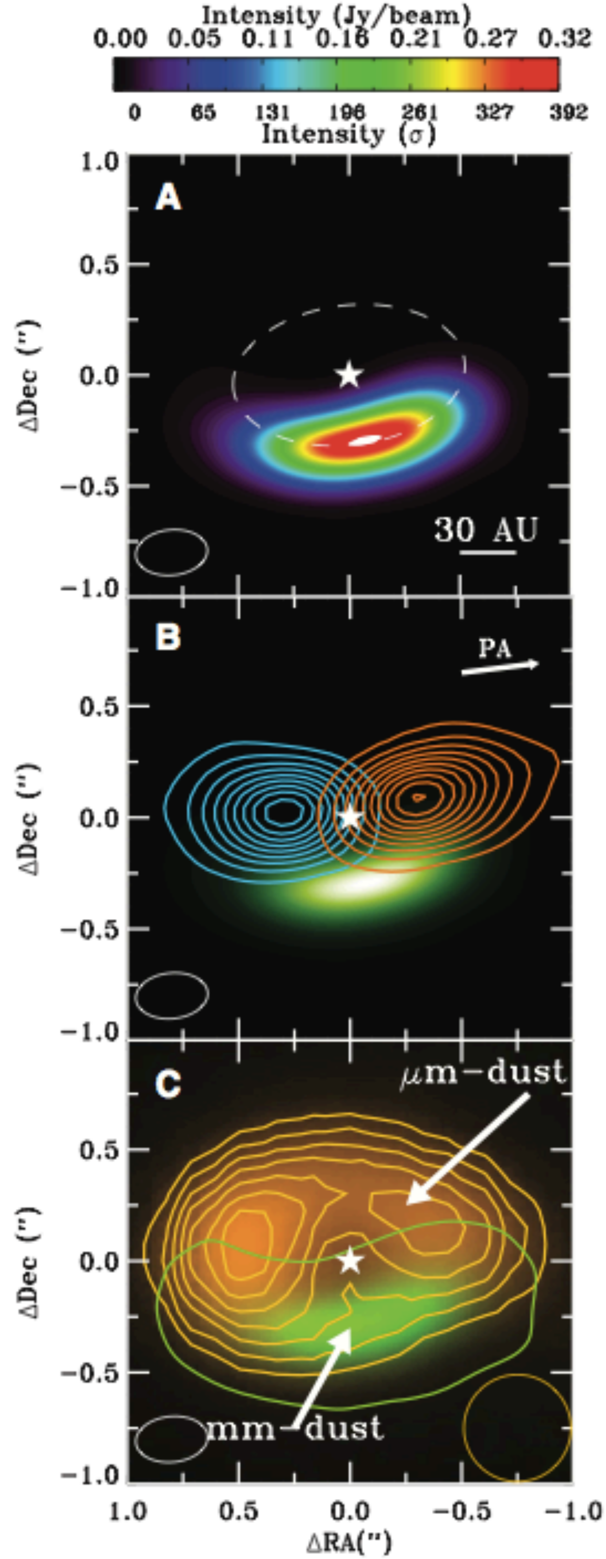

asymmetric mm dust at 63 AU

Gas detection: Keplerian rotation

Micron-sized dust follows gas

Lyra & Lin (2013)

Turbulence in vortex cores

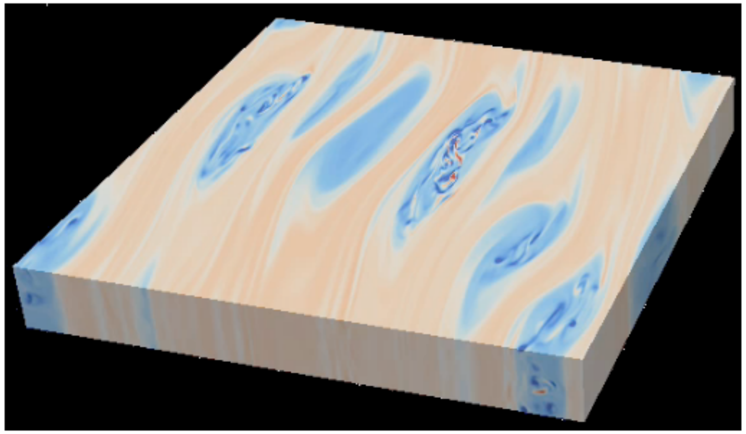

Lesur & Papaloizou (2010)

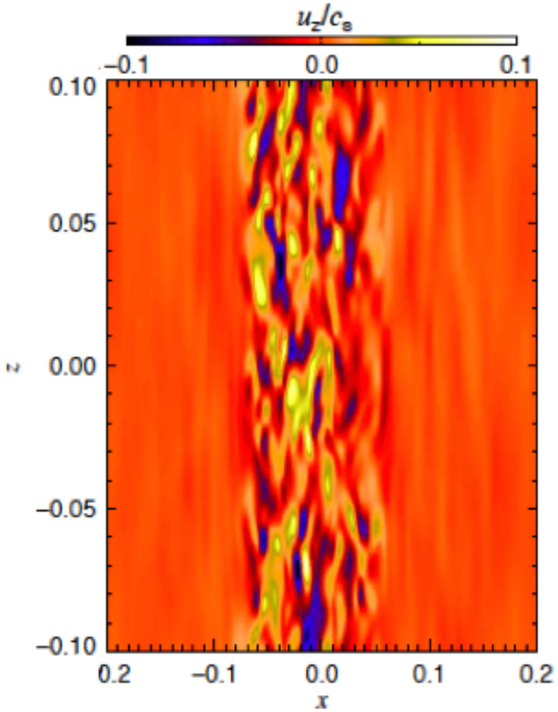

Lyra & Klahr (2011)

Turbulence in vortex cores:

max at ~10% of sound speed
rms at ~3% of sound speed

Outer Dead/Active zone transition RWI

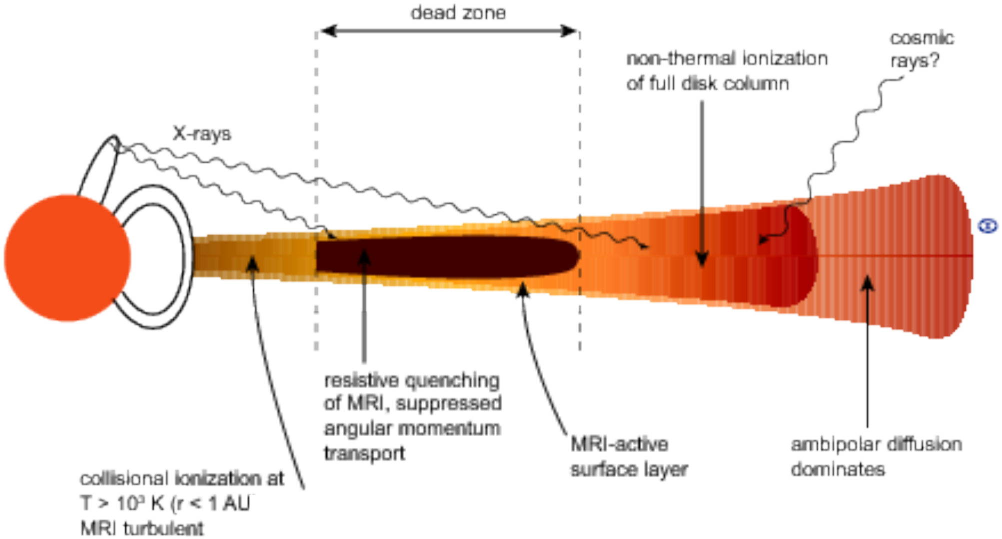

Armitage (2010)

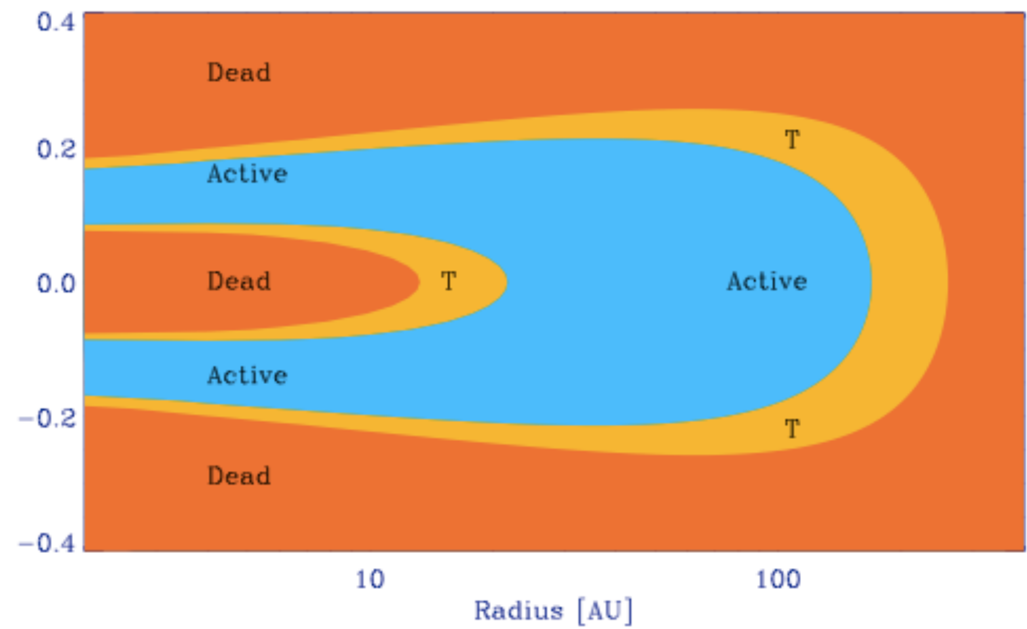

Dzyurkevitch et al (2013)

The **outer** dead zone transition in ionization supposed

TOO SMOOTH

to generate an RWI-unstable bump.

Outer Dead/Active zone transition: 3D MHD

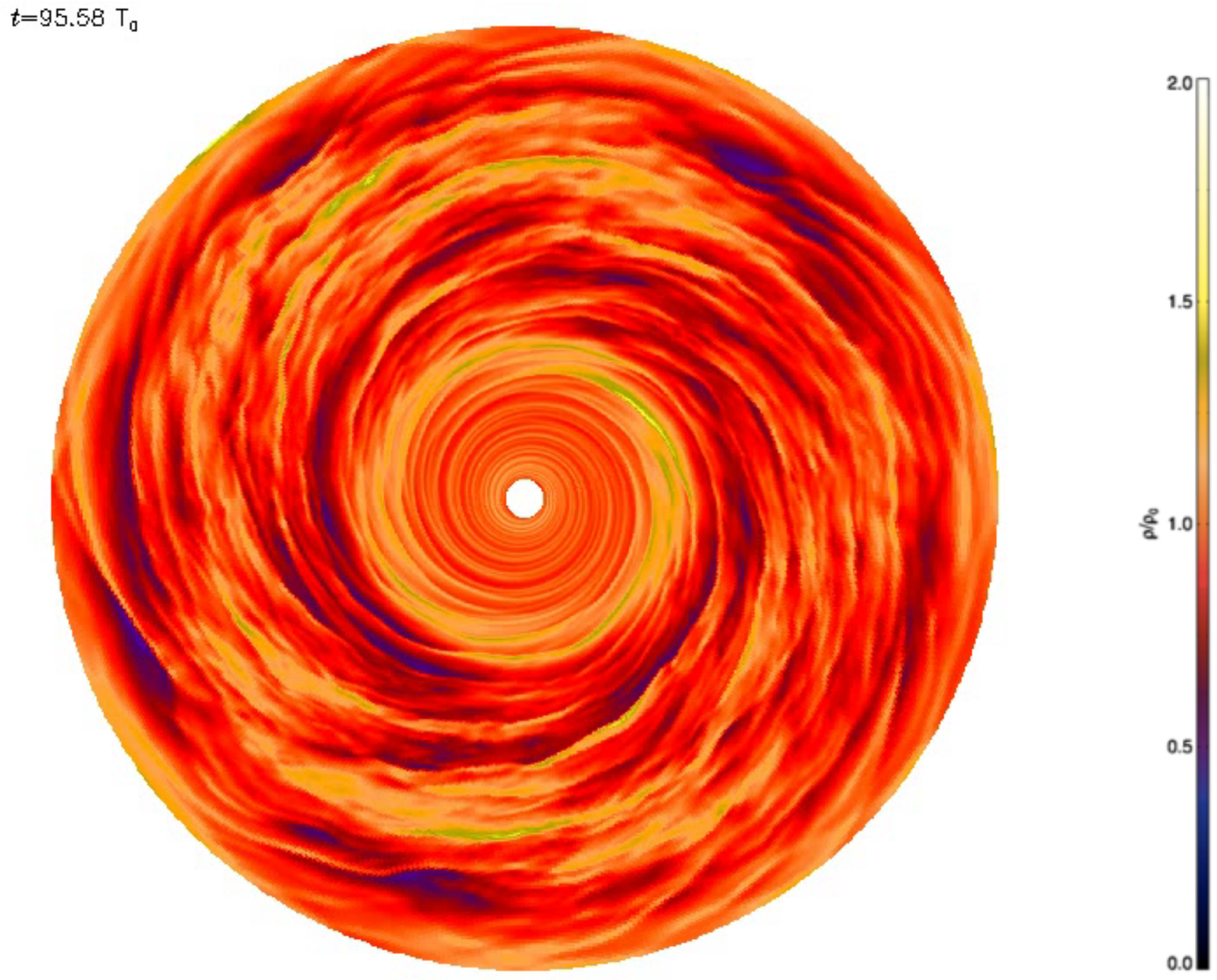

Resistive inner disk + magnetized outer disk

Lyra et al (2015)

Outer Dead/Active zone transition RWI

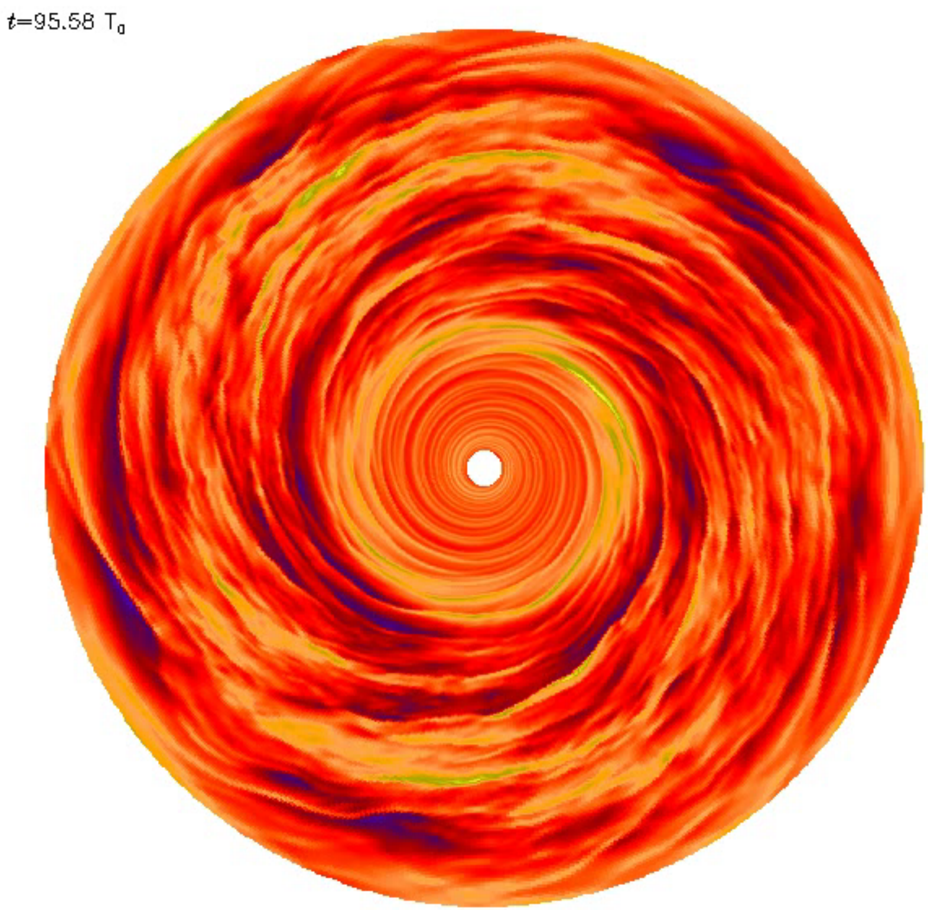

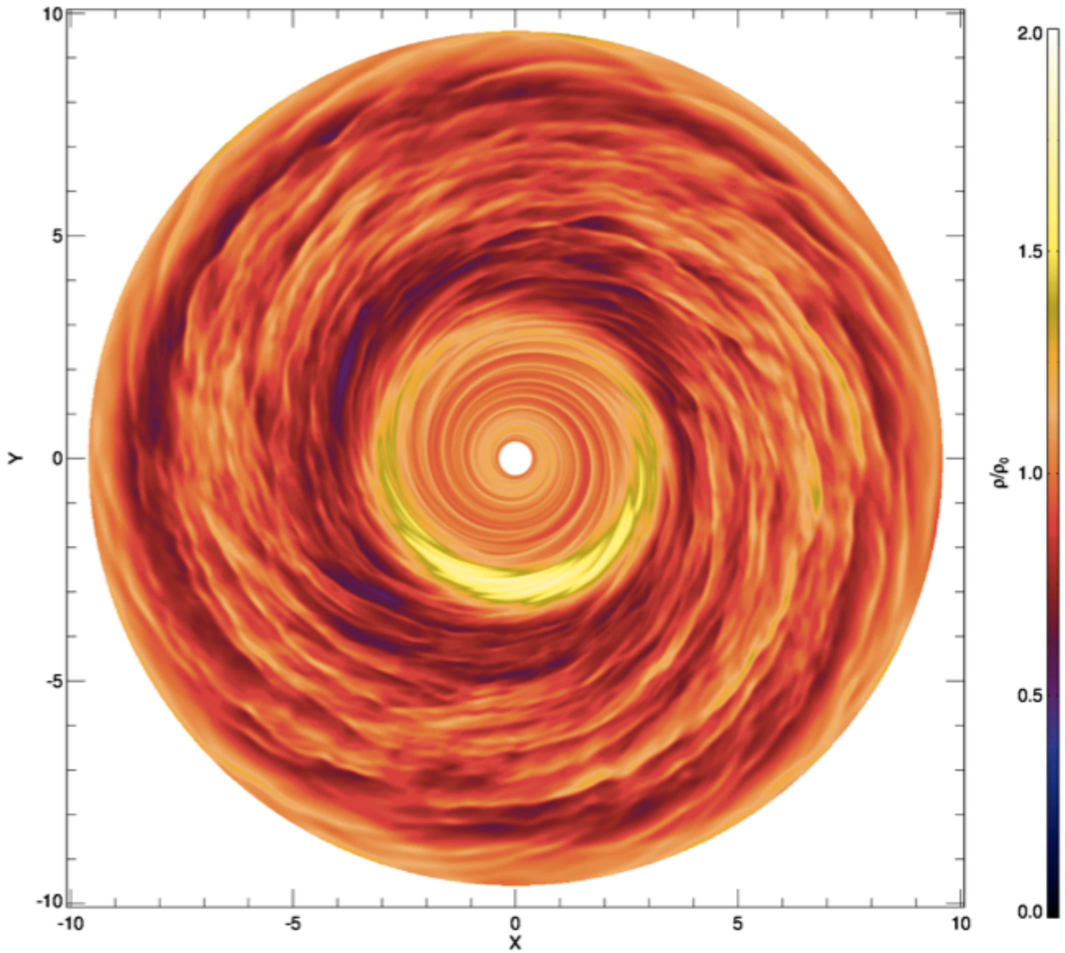

Resistive inner disk + magnetized outer disk

Lyra, Turner, & McNally (2015)

Outer Dead/Active zone transition RWI

MHD

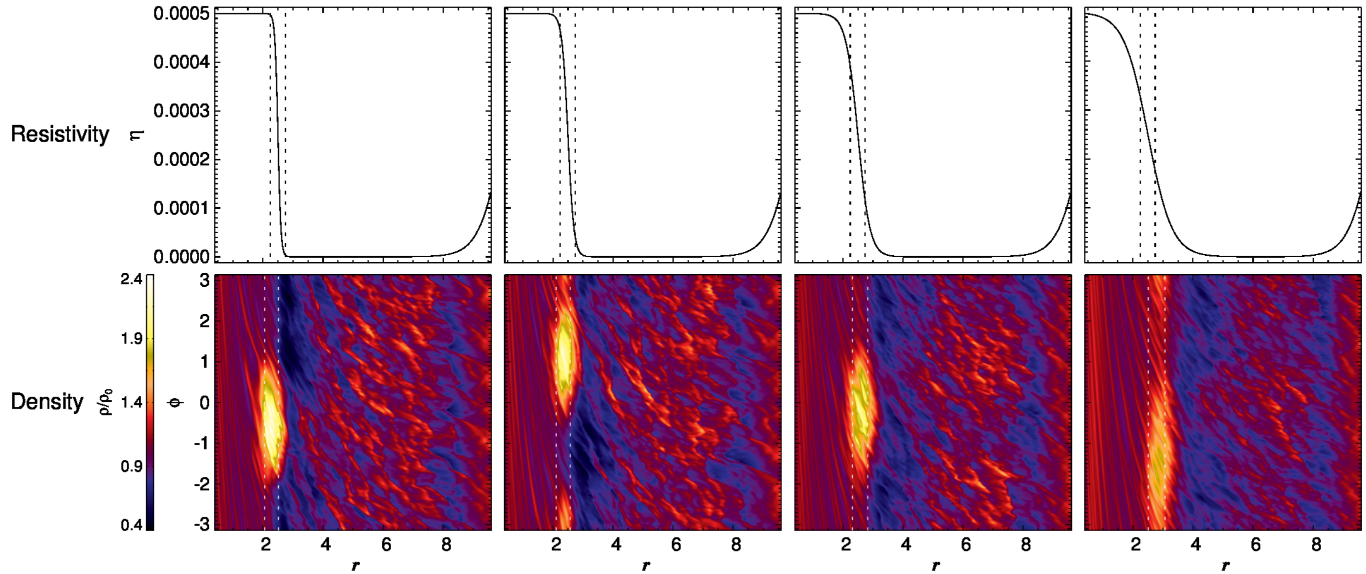

Hydro

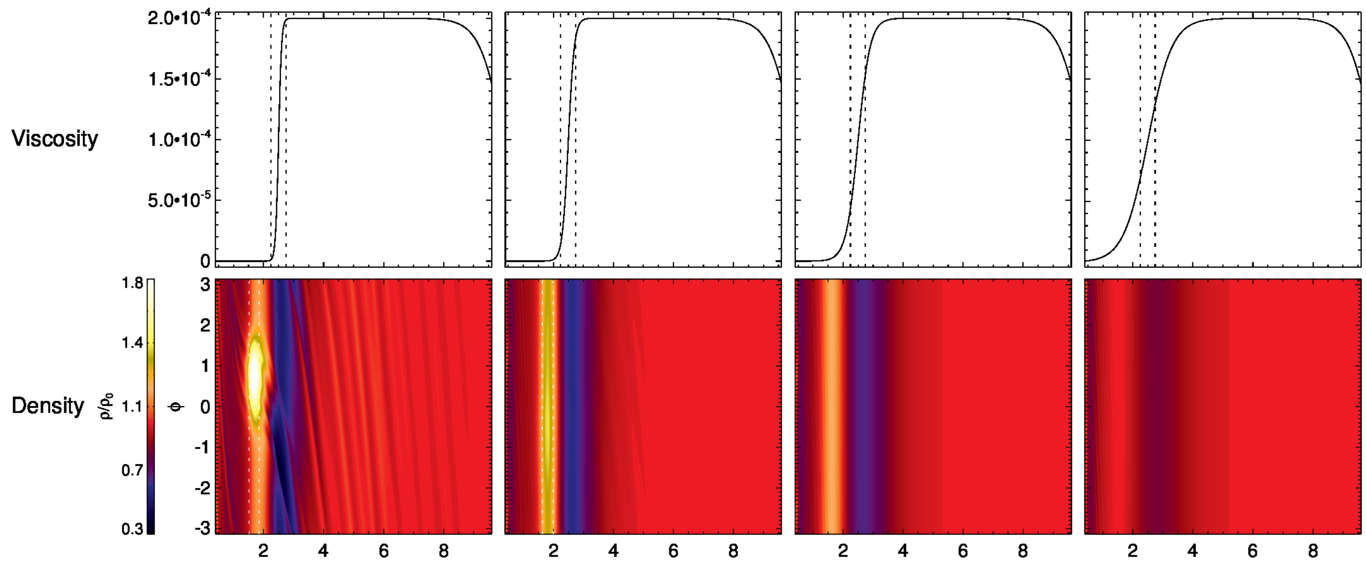

Lyra, Turner, & McNally (2015)

Outer Dead/Active zone transition RWI

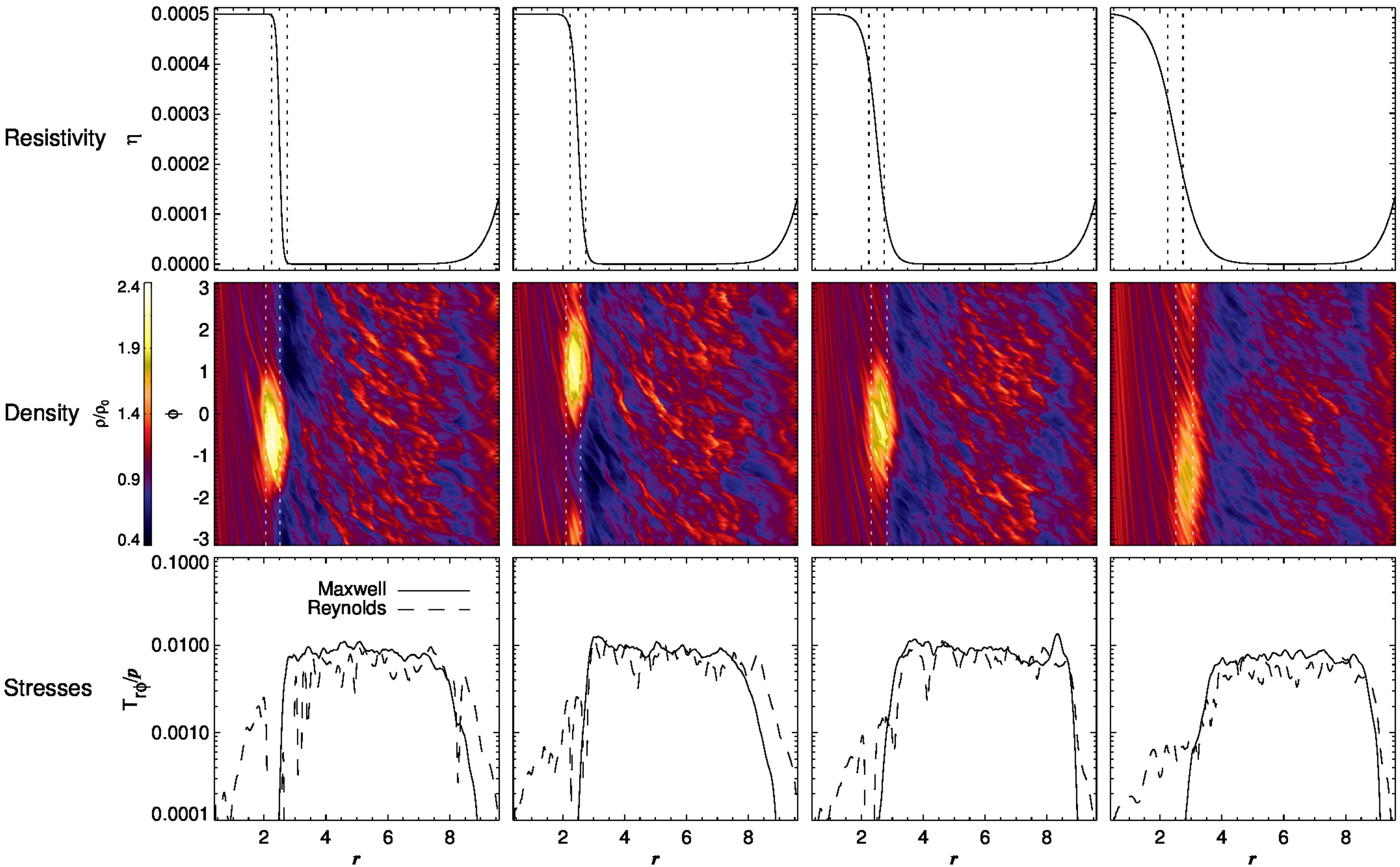

Lyra, Turner, & McNally (2015)

Outer Dead/Active zone transition RWI

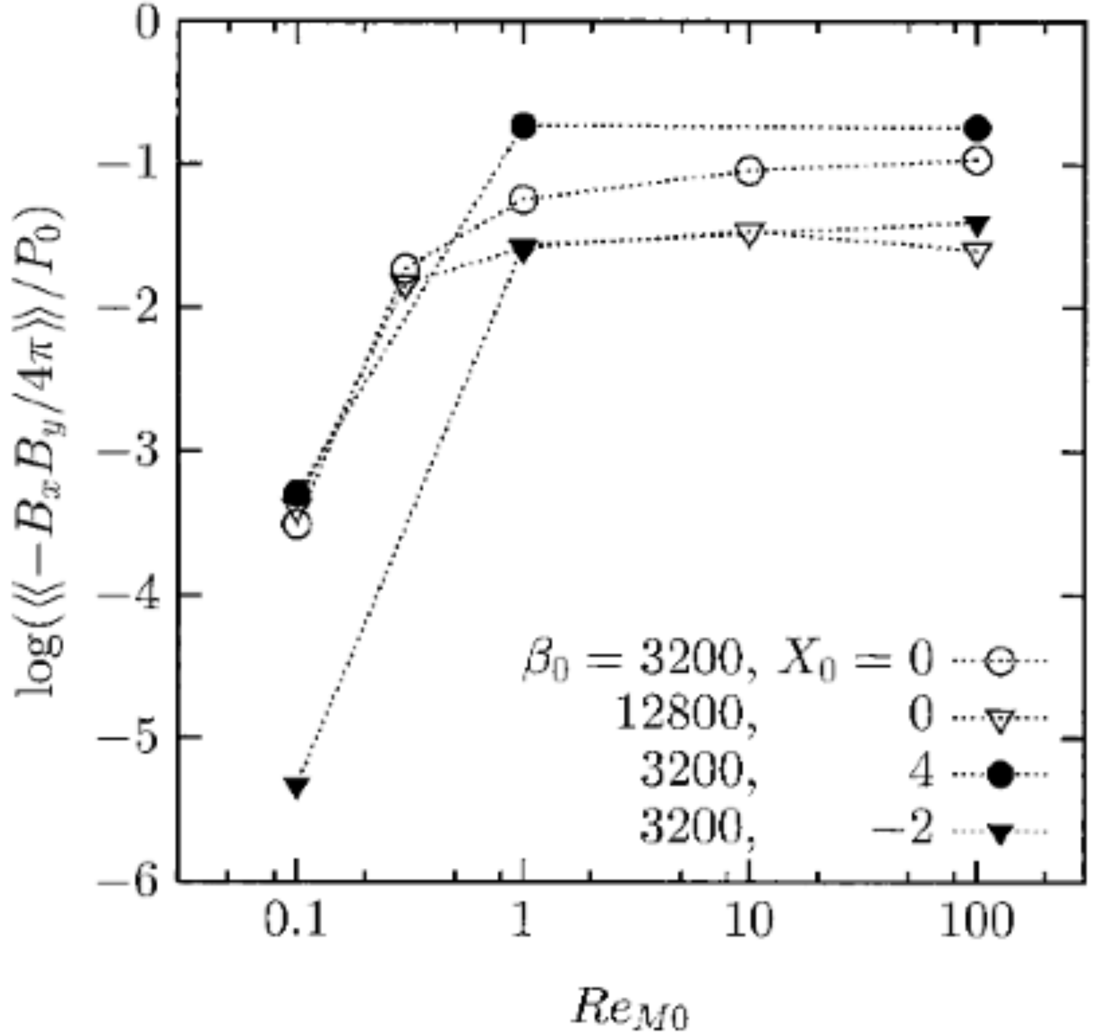

FIG. 9.—Saturation level of the Maxwell stress as a function of the magnetic Reynolds number Re_{M0}. Open circles and triangles denote the models without Hall term ($X_0 = 0$) for $\beta_0 = 3200$ and 12,800, respectively. The models including the Hall term are shown by filled circles ($X_0 = 4$) and triangles ($X_0 = -2$).

Sano & Stone (2002)

Too big to be vortices?

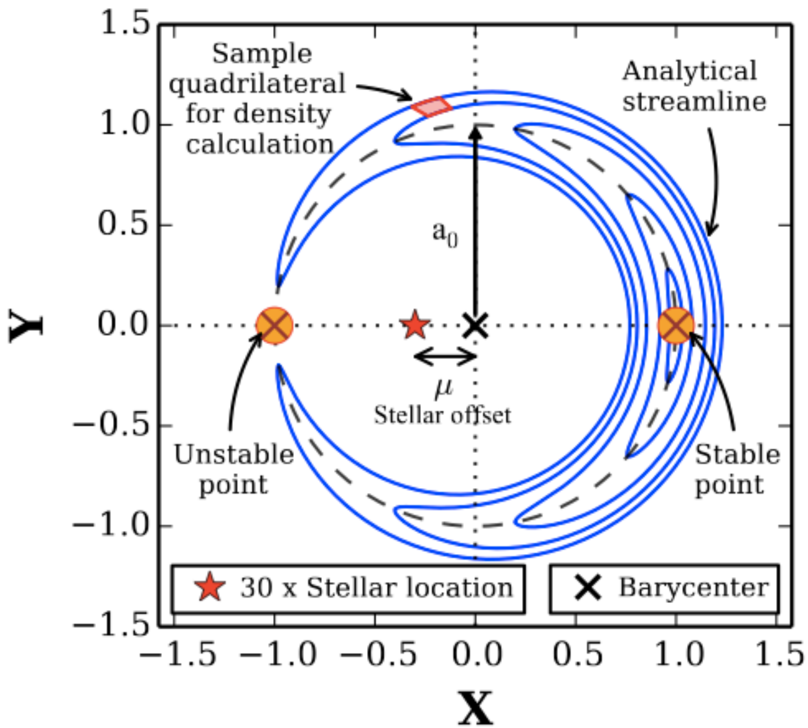

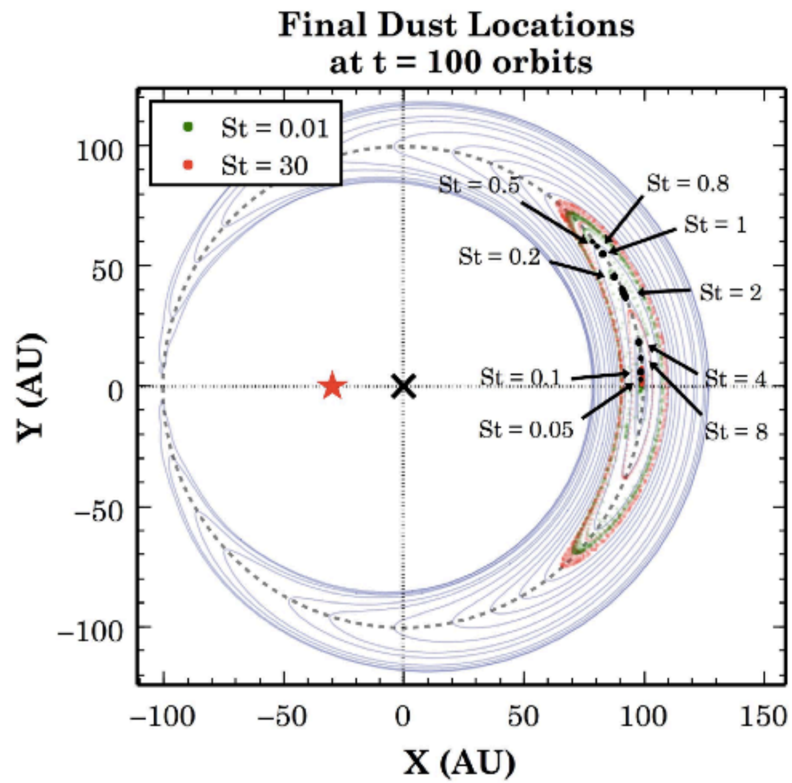

An offset stellar potential leads to horseshoe orbits

Mittal & Chiang (2015)

Tail trapping

The Lyra-Lin solution is for the core only.

But the logarithmic tail is significant for smaller particles.

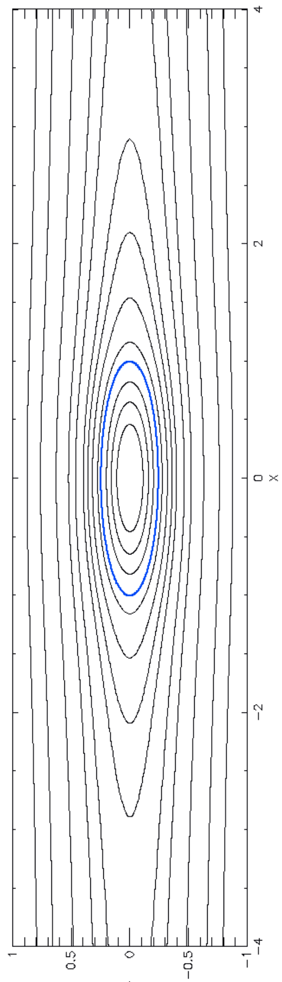

Lesur & Papaloizou (2009)

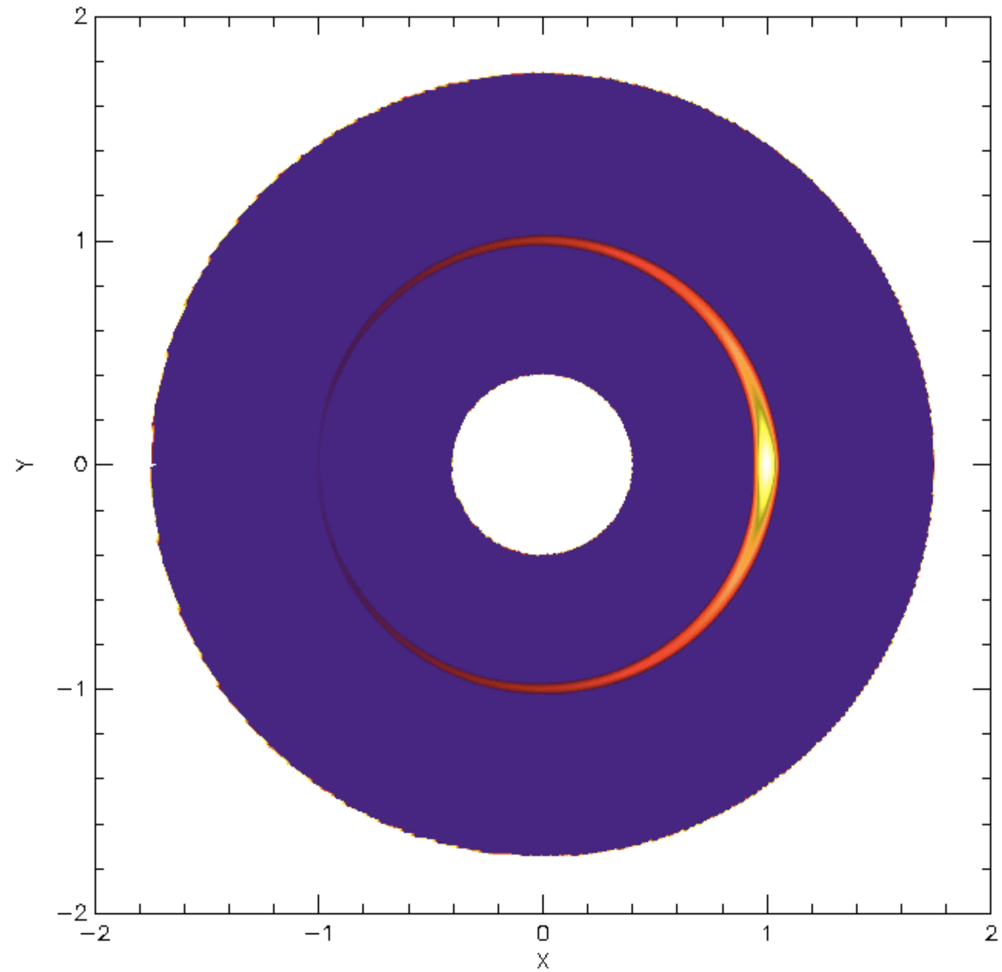

Global wrapping of tail

Lyra et al 2015 (in prep)

Waiting for ALMA cycle 3

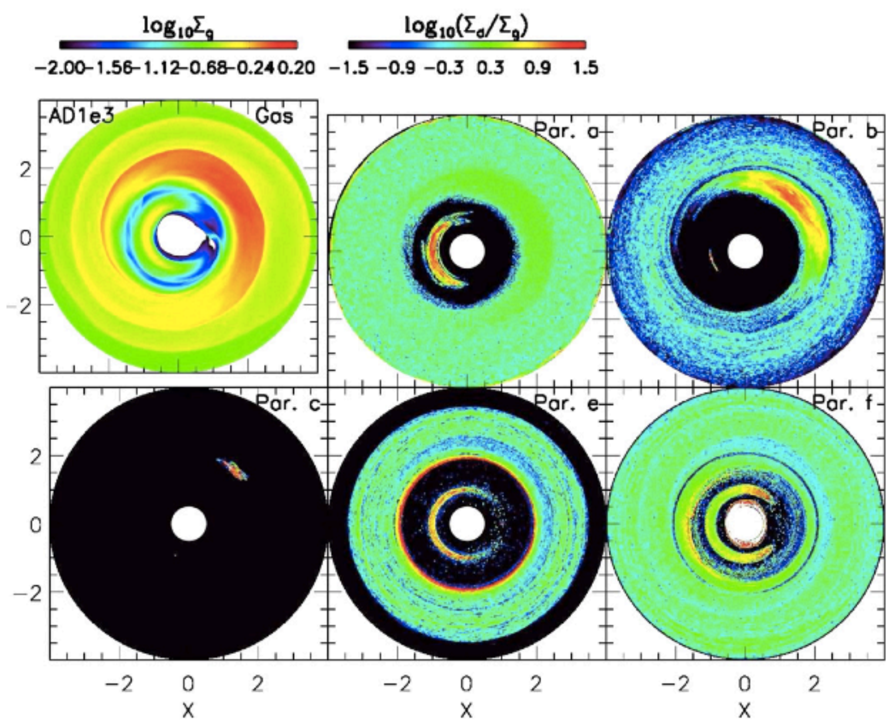

Zhu & Stone (2014)

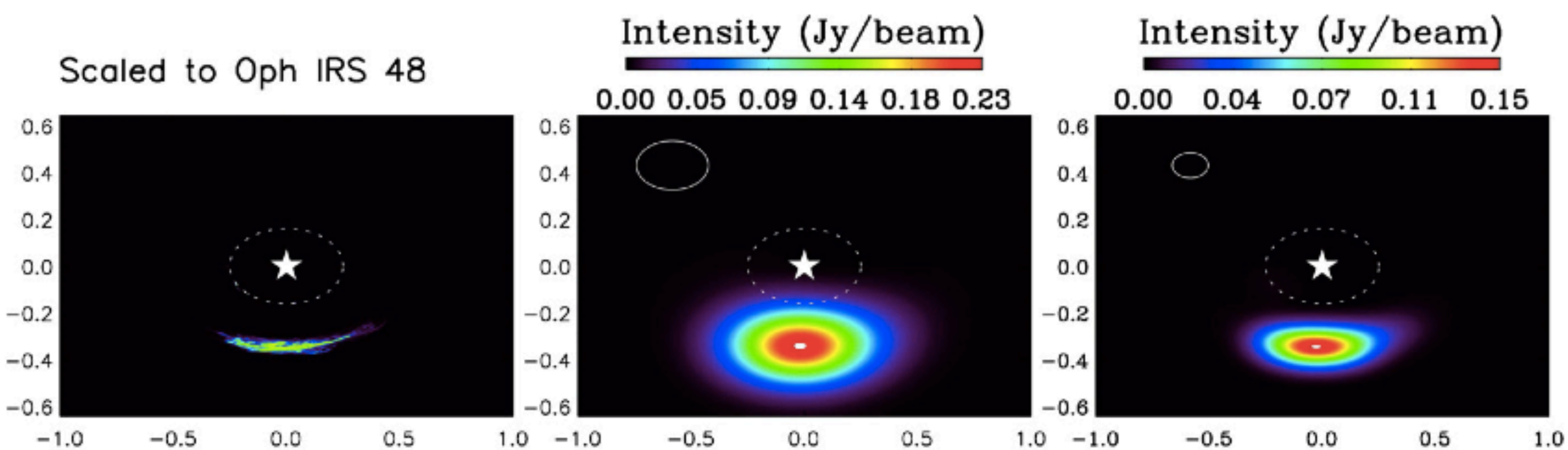

Outer Dead/Active zone transition: Spirals without planets

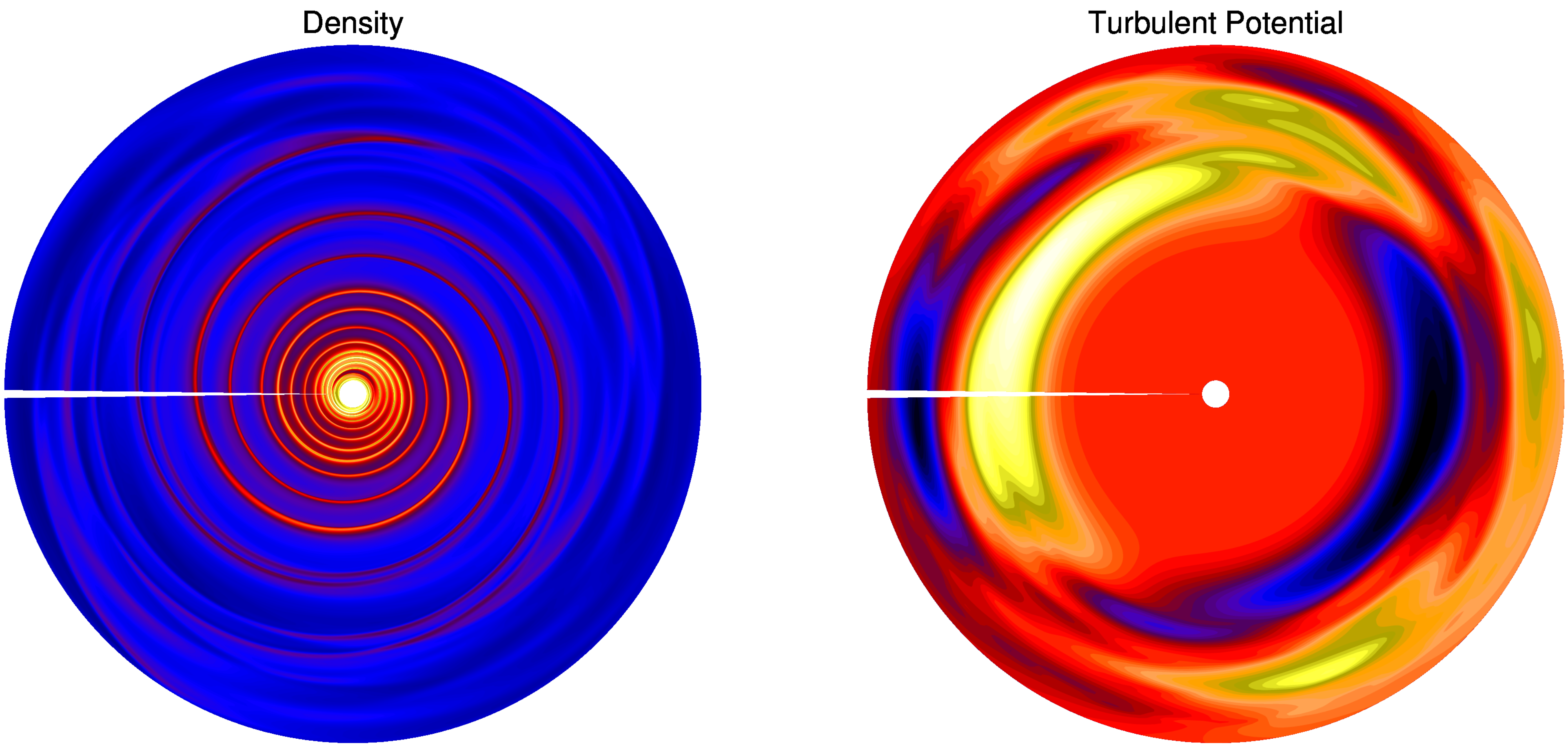

Waves launched at the active zone propagate into the dead zone as a coherent spiral.

Spirals in transition disks

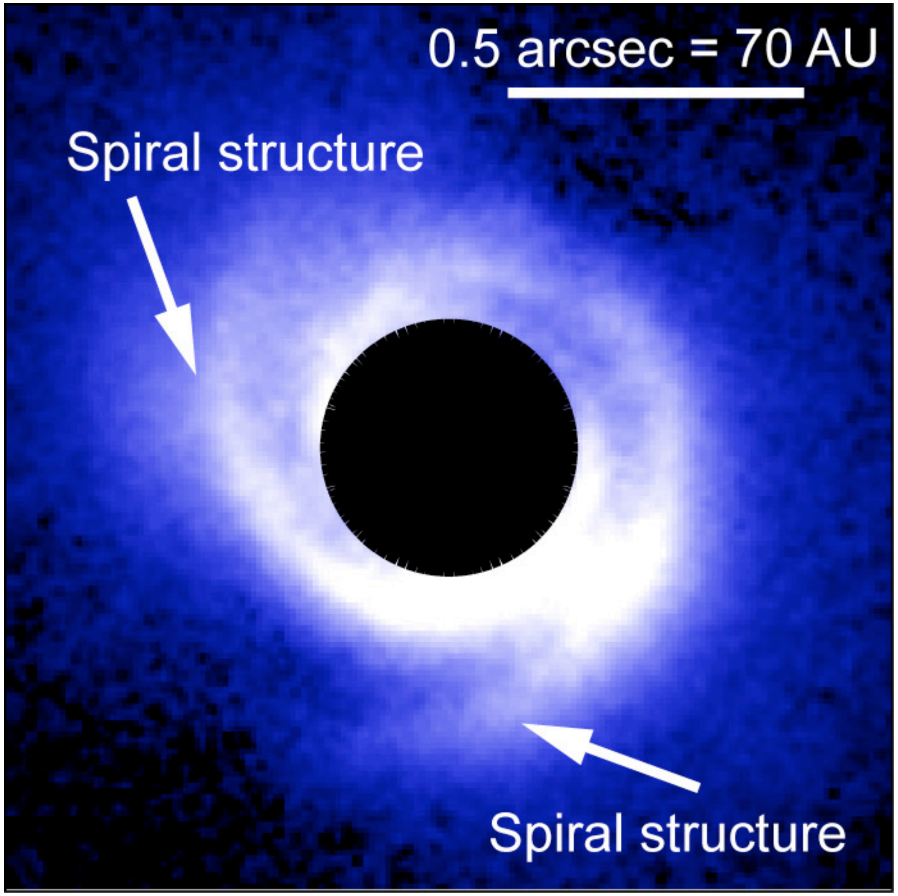

Muto et al. (2012)

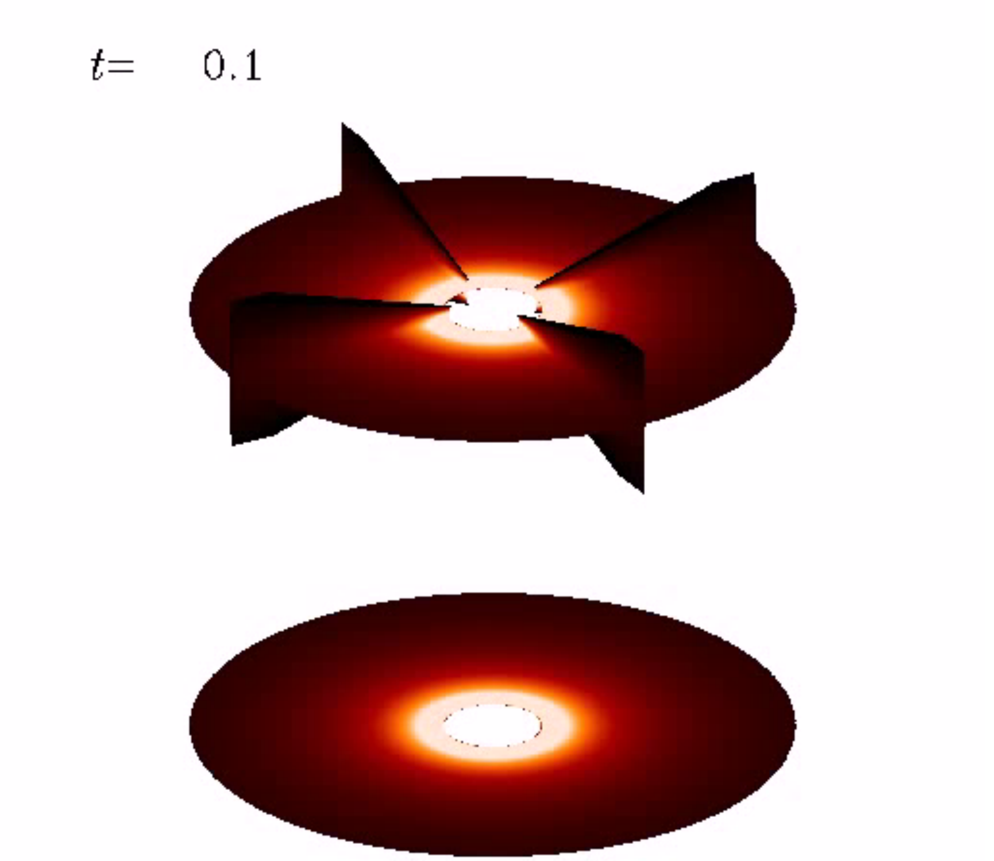

Lyra (2009)

SPHERE-ALMA-VLA overlay of MWC 758

SPHERE
ALMA
VLA

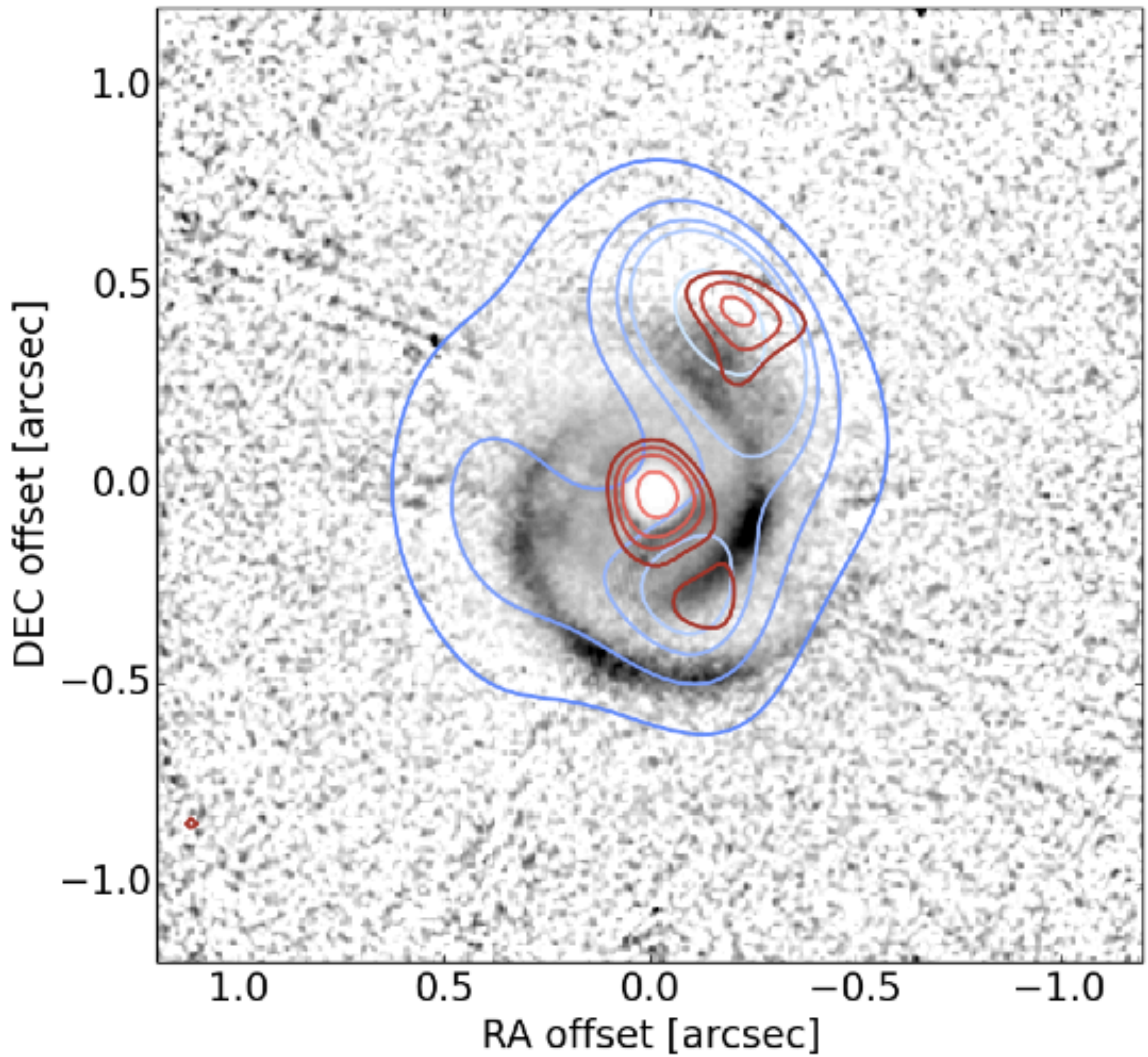

Marino et al. (2015)

Spiral arm fitting leads to problems

Analytical spiral fit

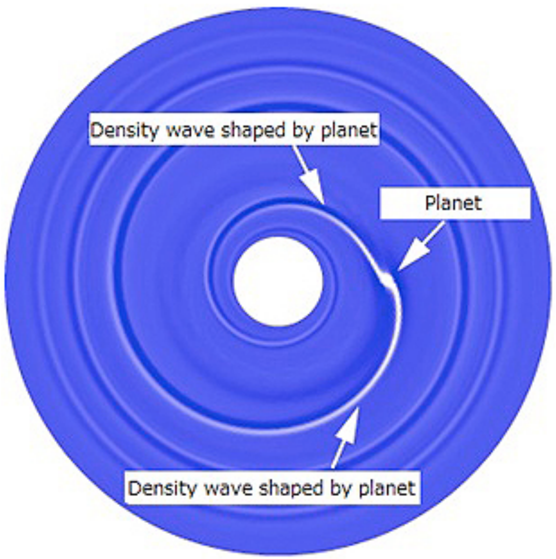

$$\theta(r) = \theta_c + \frac{\mathrm{sgn}(r - r_c)}{h_c} \times \left\{ \left(\frac{r}{r_c}\right)^{1+\beta} \left[\frac{1}{1+\beta} - \frac{1}{1-\alpha+\beta}\left(\frac{r}{r_c}\right)^{-\alpha}\right] - \left(\frac{1}{1+\beta} - \frac{1}{1-\alpha+\beta}\right) \right\},$$

Rafikov (2002)
Muto et al. (2012)

Spirals are too wide hotter (300K) than ambient gas (50K).

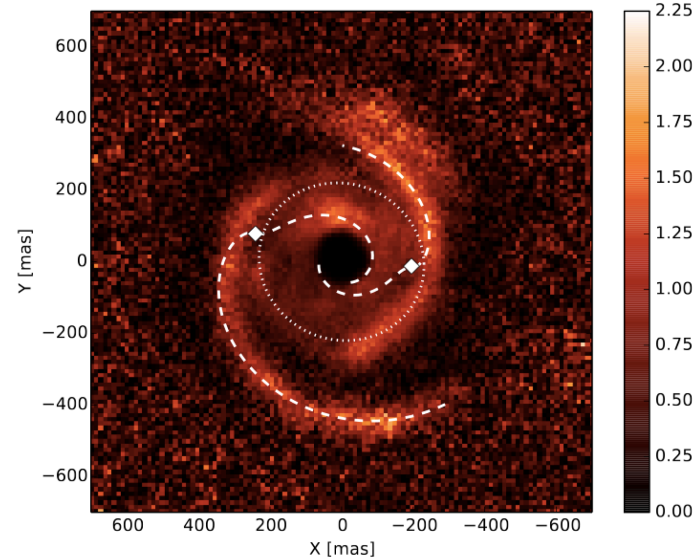

Benisty et al. (2015)

Spiral has little polarization. Must be thermal emission at 1000K.

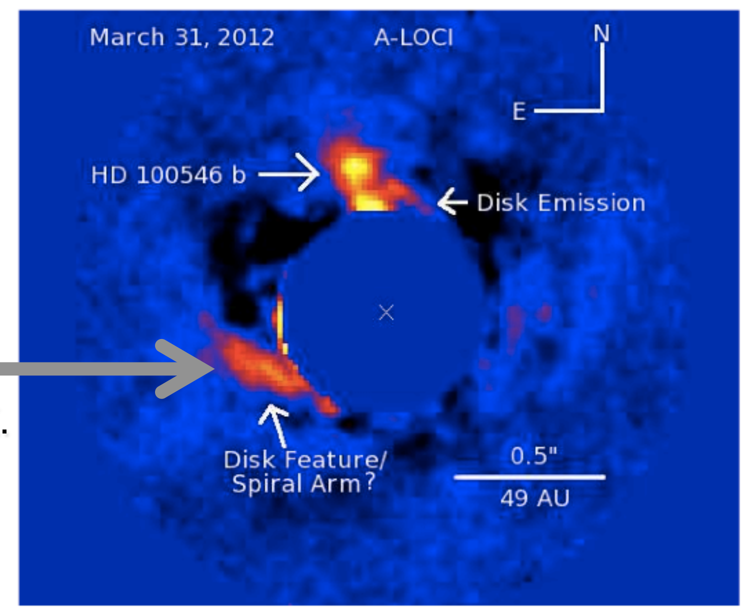

Currie et al. (2014)

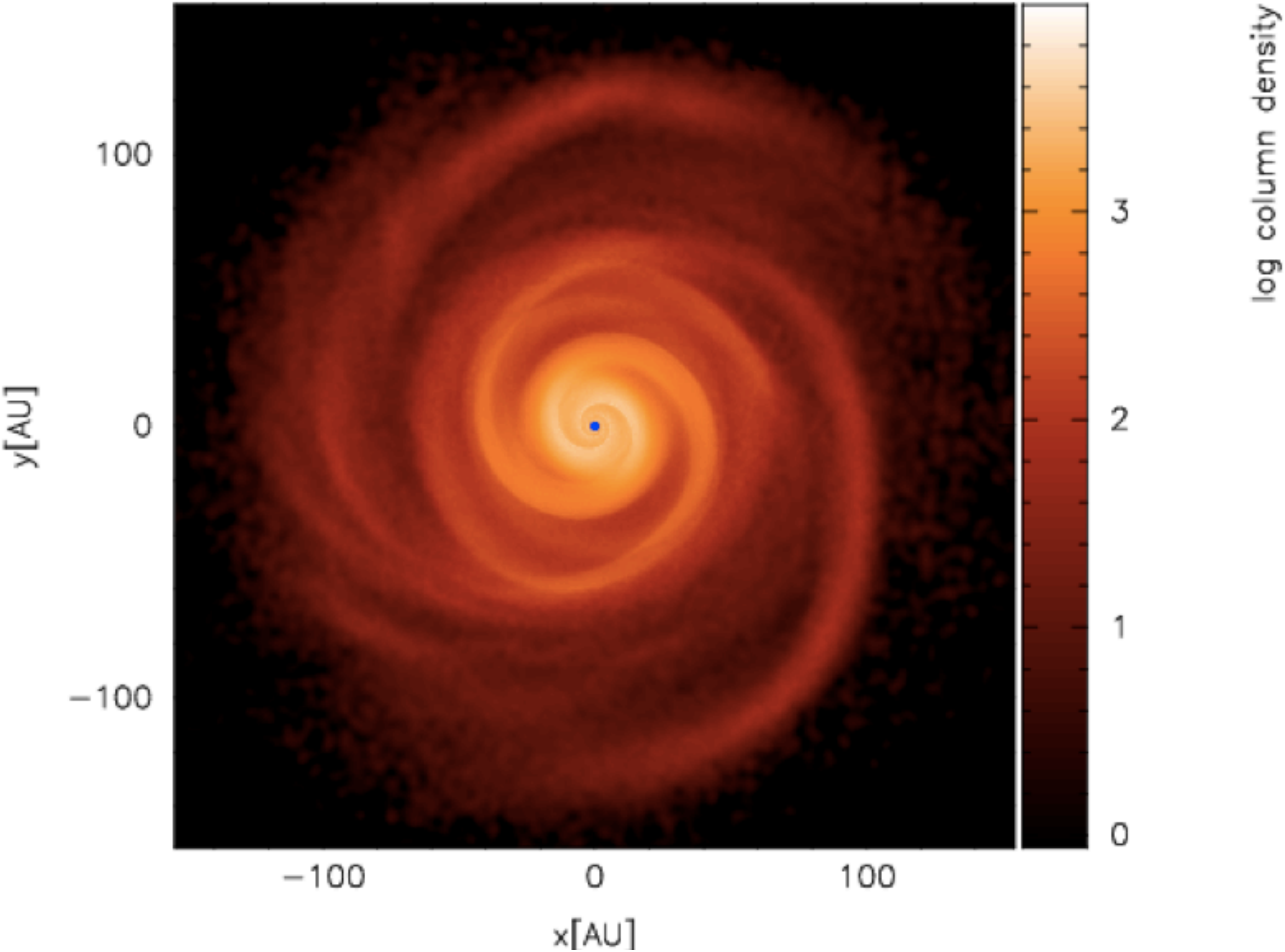
y[AU]
100
0
−100
−100
0
100
x[AU]
log column density
3
2
1
0

Hot spirals

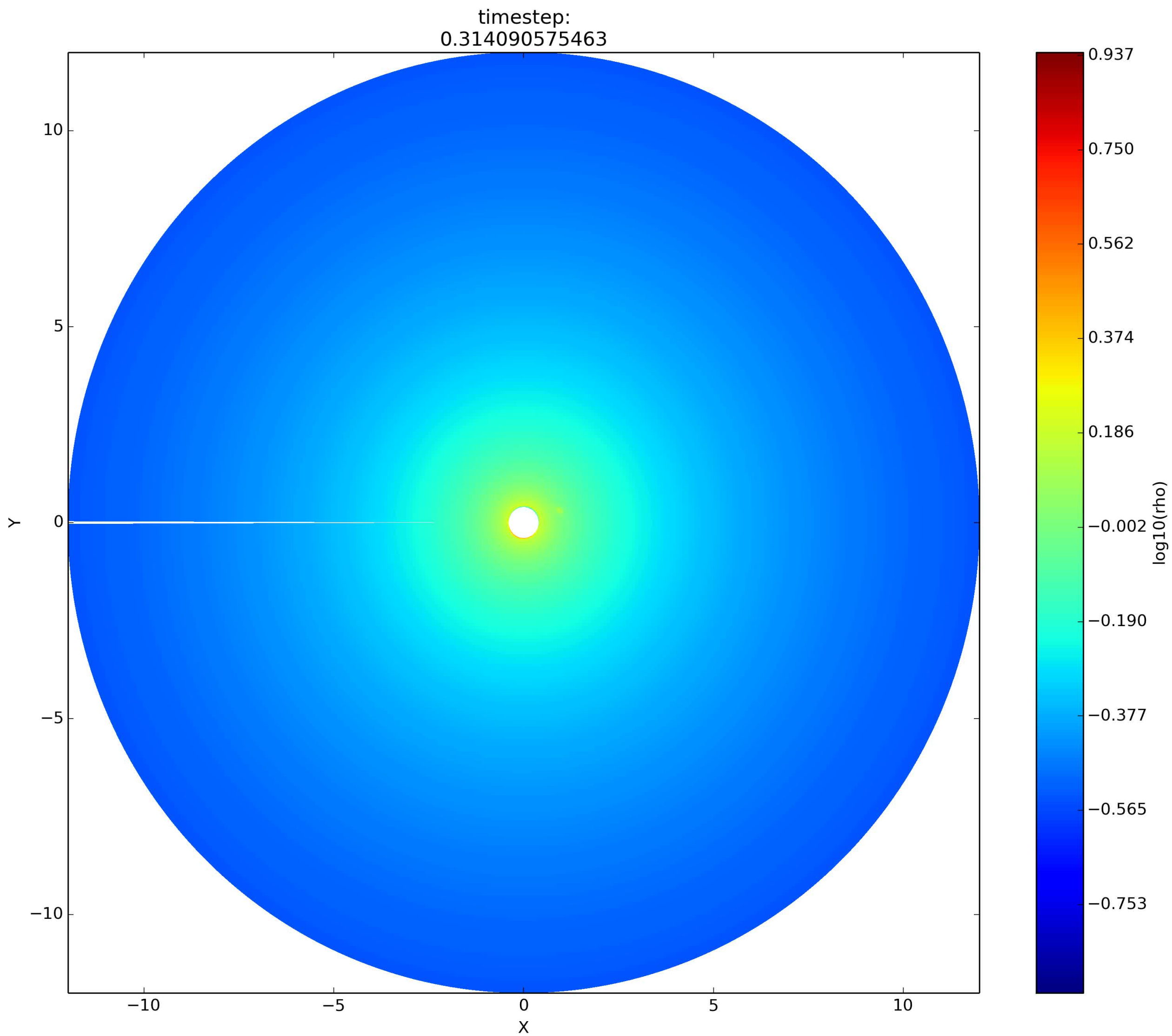

Richert et al. (2015)

Some crazy turbulence showing up at high planet mass….

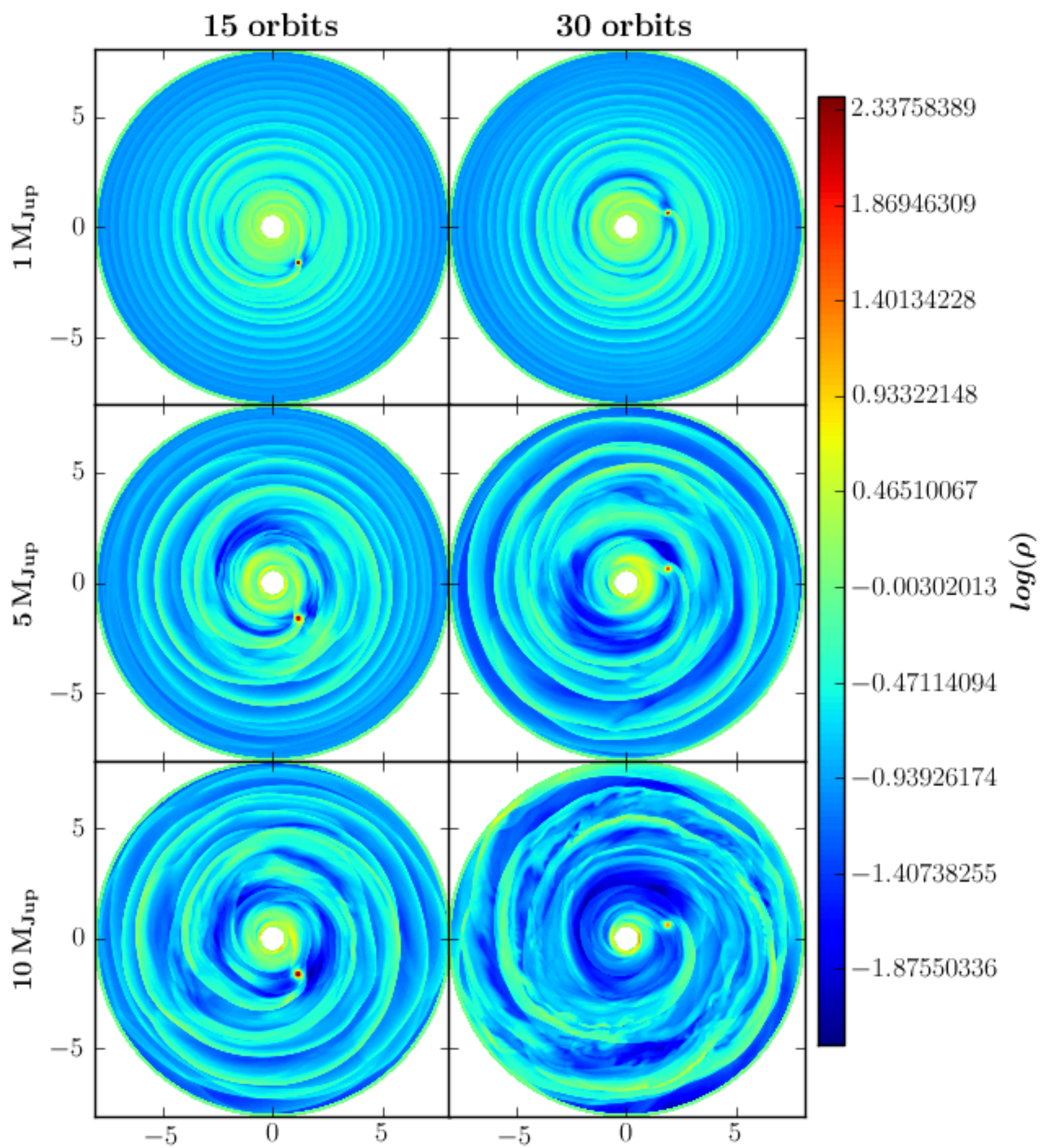

Isothermal vs Adiabatic

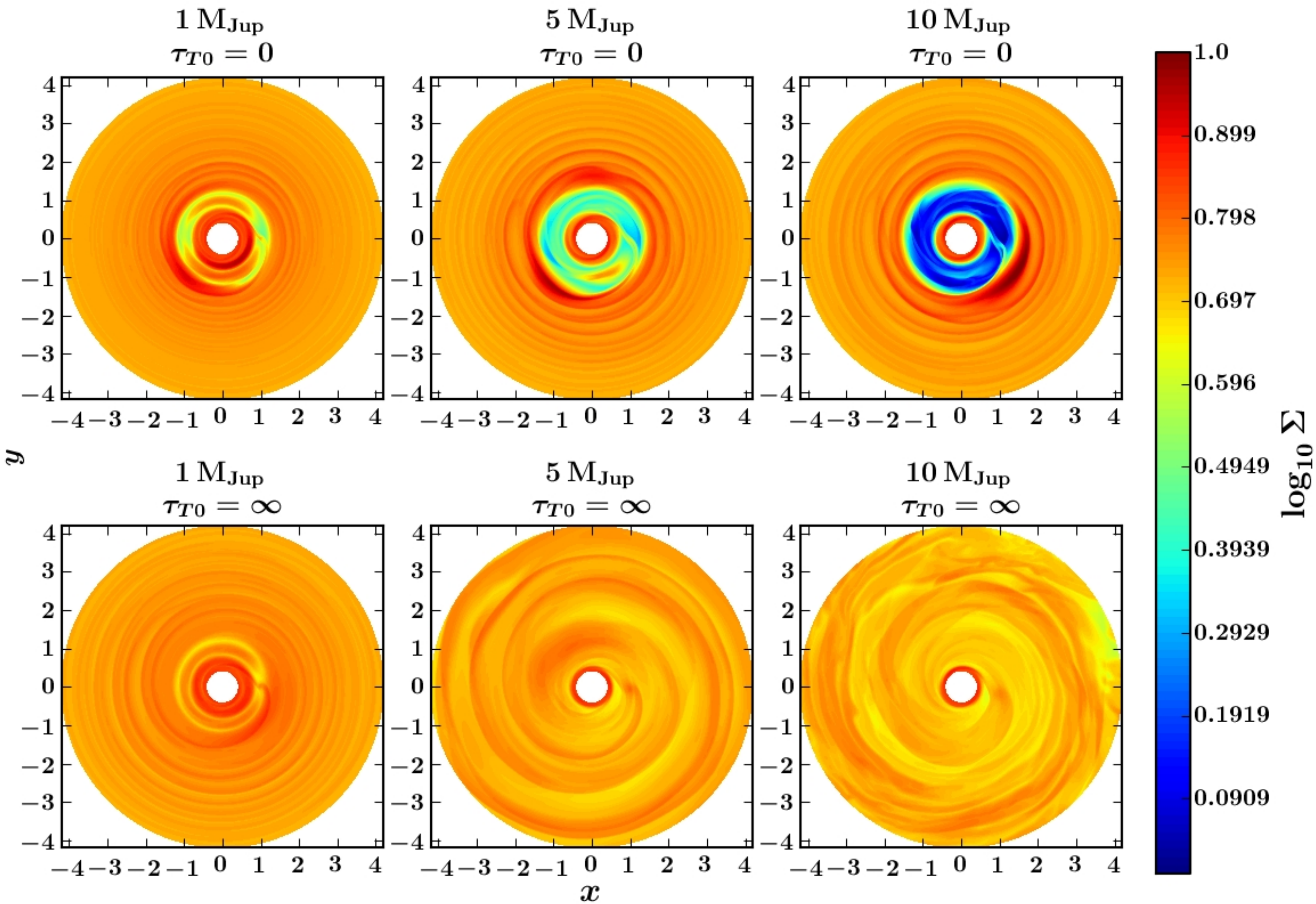

Richert et al. (2015)

Shows up for long cooling times….

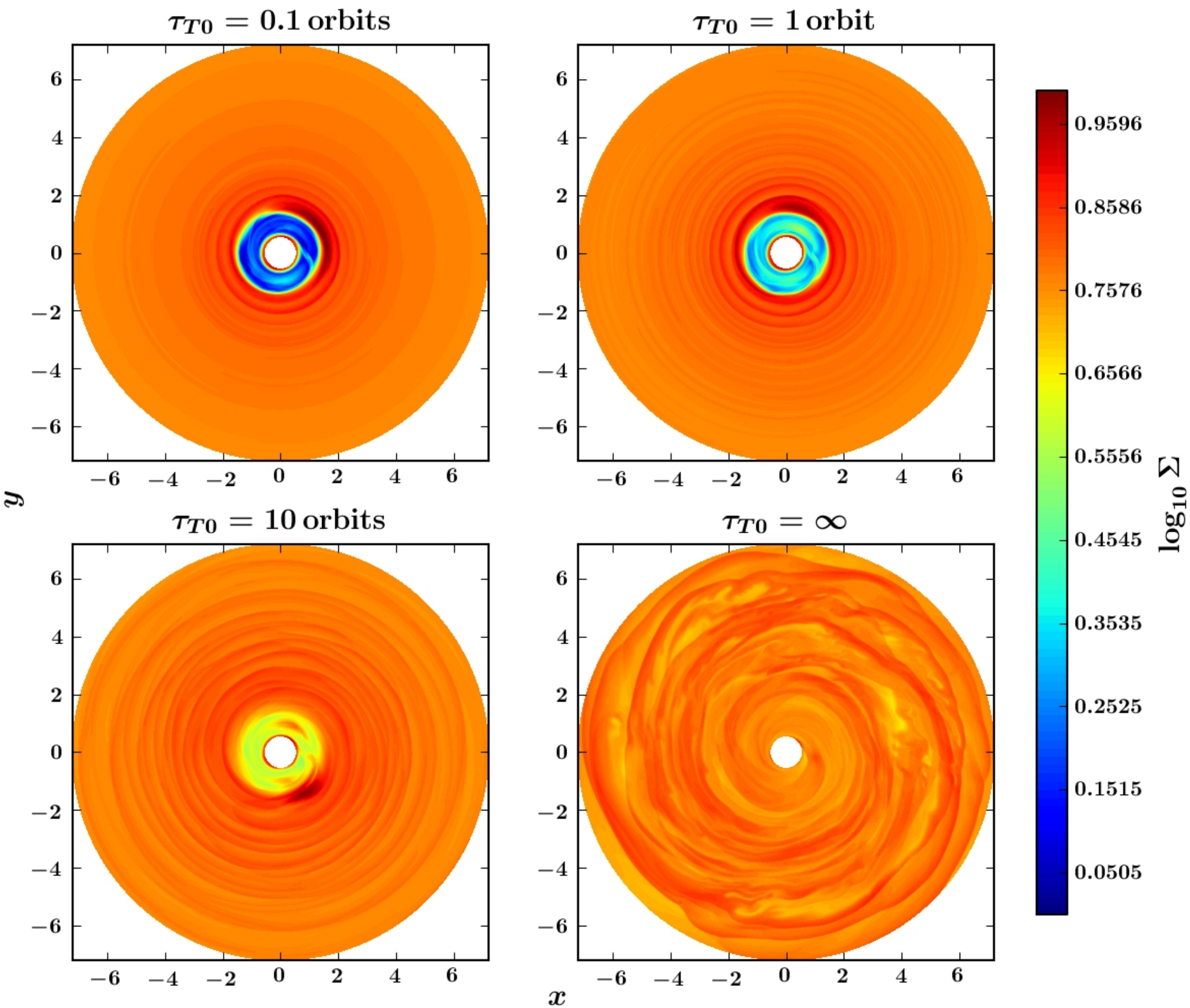

The energy source: shock heating!

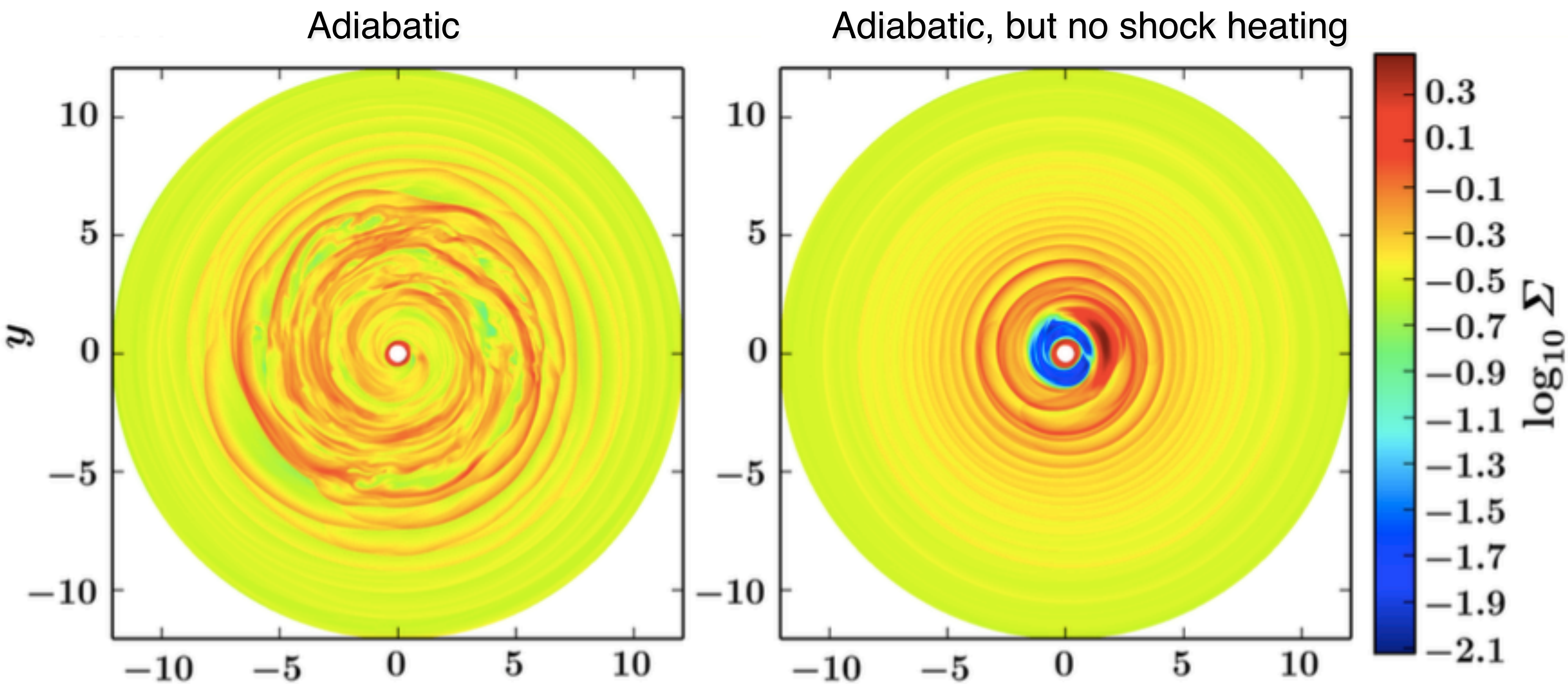

Richert et al. (2015)

The spiral is buoyantly unstable

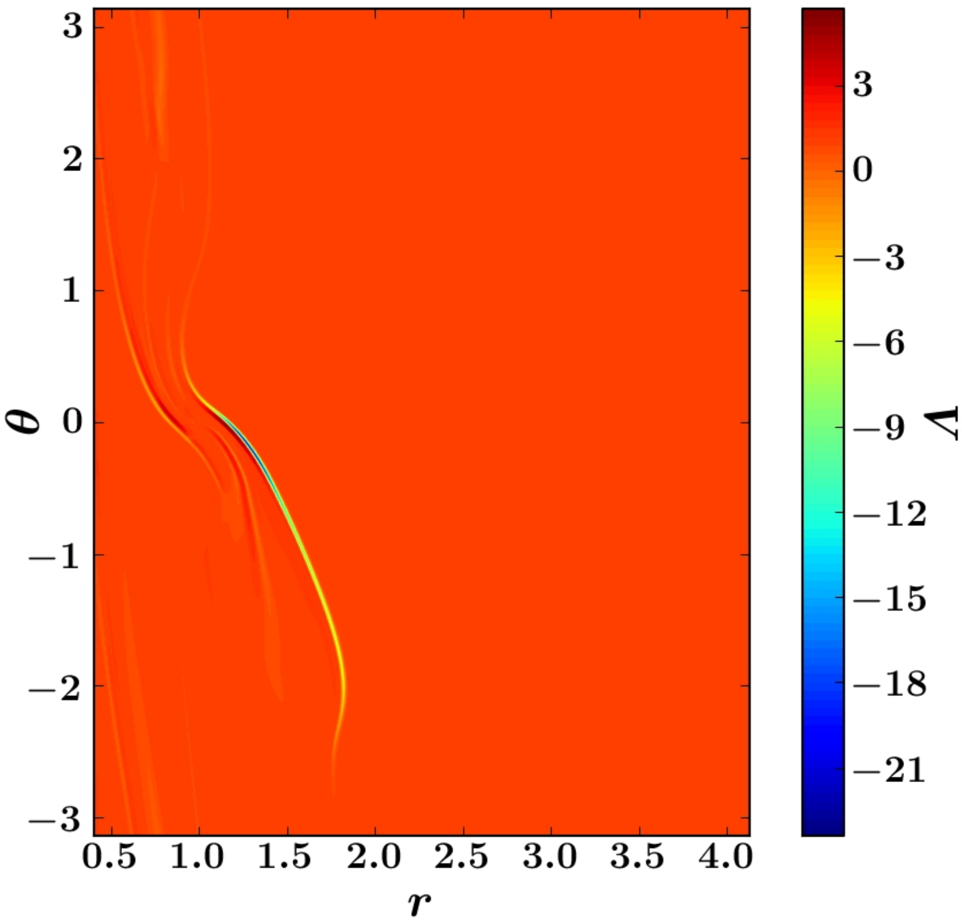

The spiral has Ma >~ 1

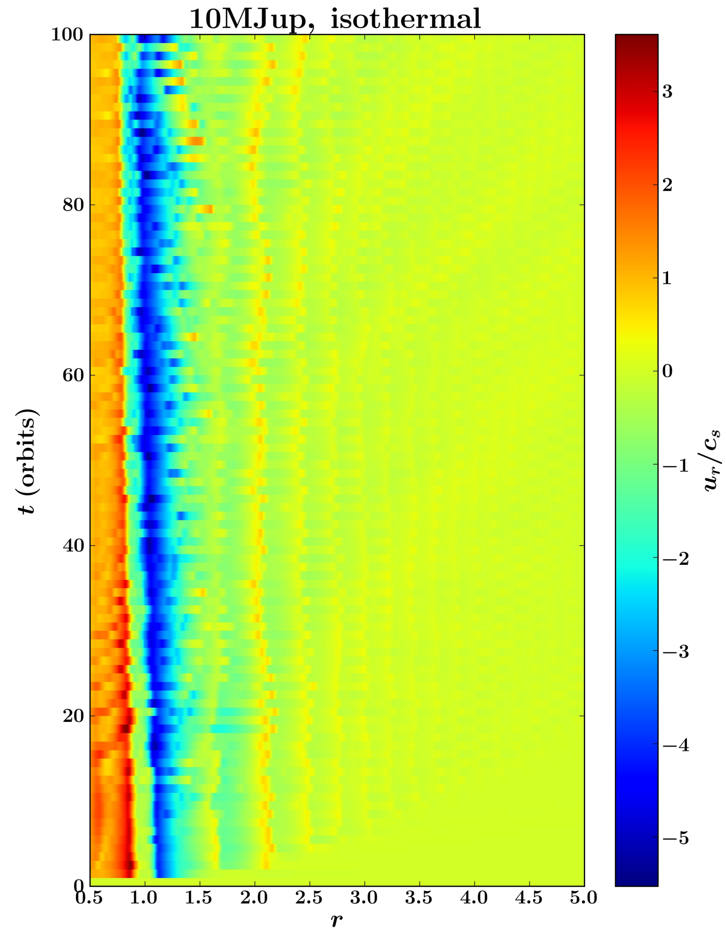

Richert et al. (2015)

3D shocks: ascending bores and breaking waves

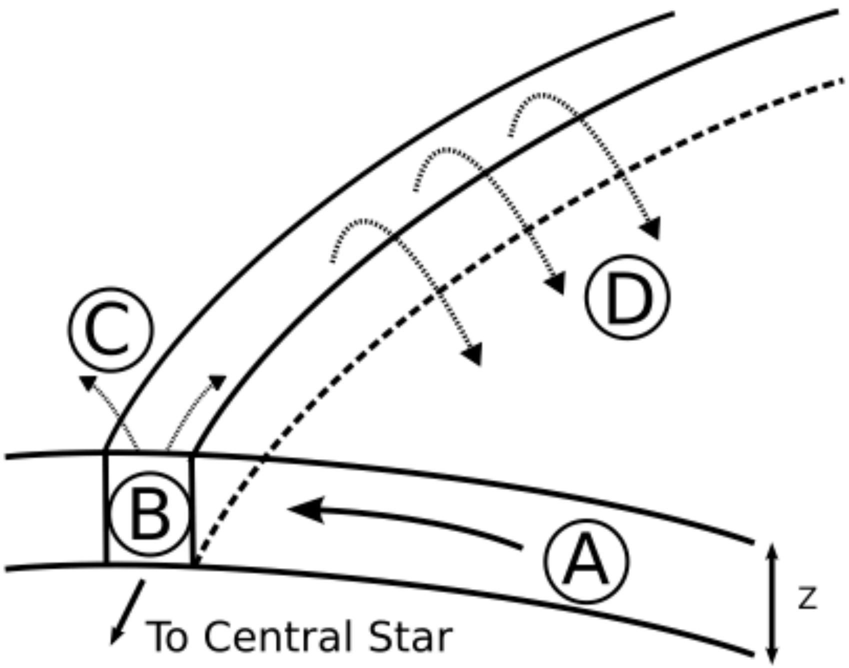

FIG. 2.—Cartoon depicting the gas flow in a shock bore in the frame of the spiral shock inside corotation. The gas in the preshock region flows into the spiral shock (A). The shock (B) causes the material to be out of vertical force balance and a rapid expansion results (C). Due to spiral streaming and the loss of pressure confinement, some of the gas will flow back over the spiral wave and break onto the disk in the preshock region at a radius inward from where it originated (D).

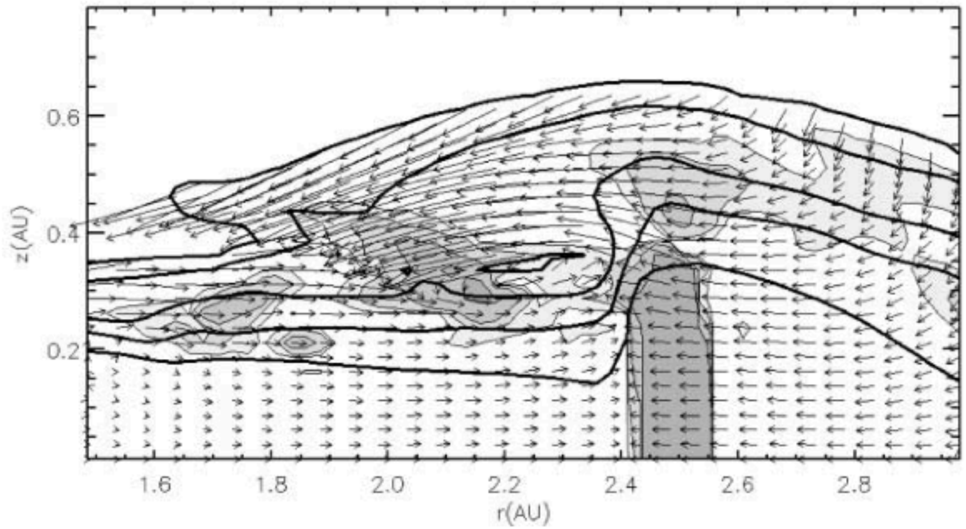

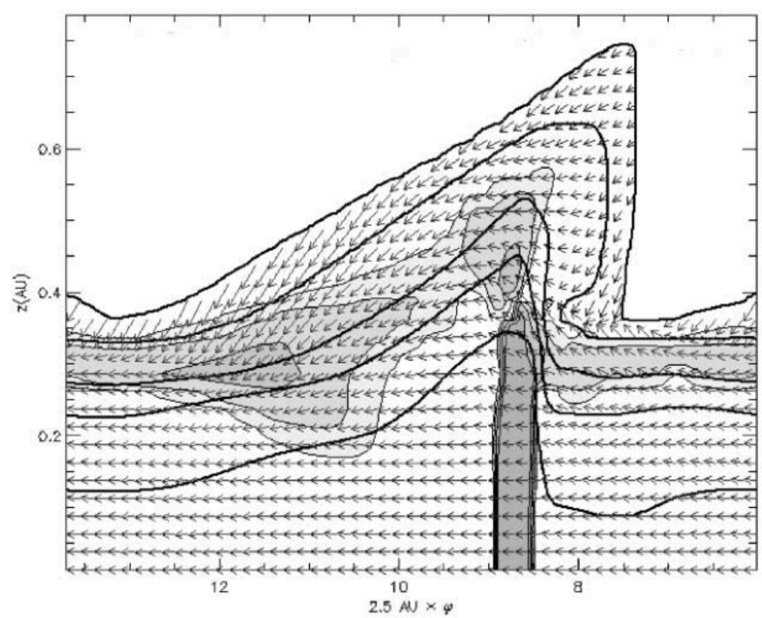

Boley & Durisen (2006)

3D shocks: ascending bores and breaking waves

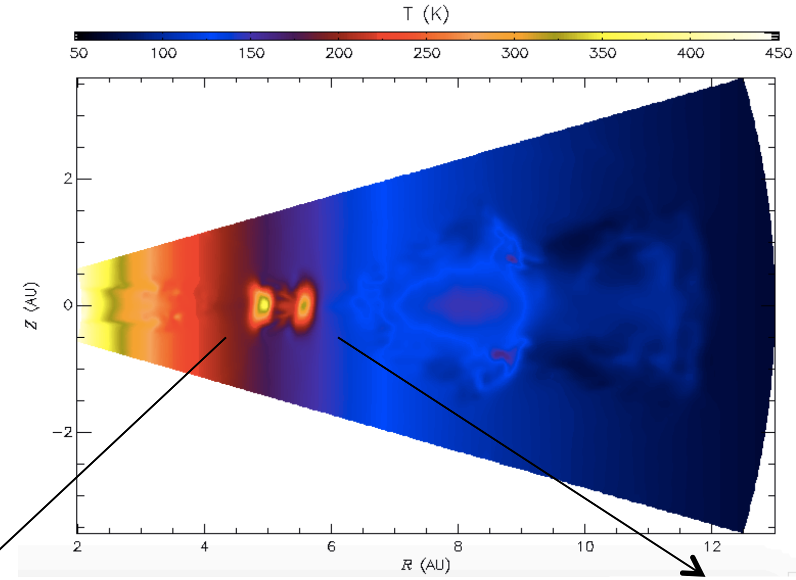

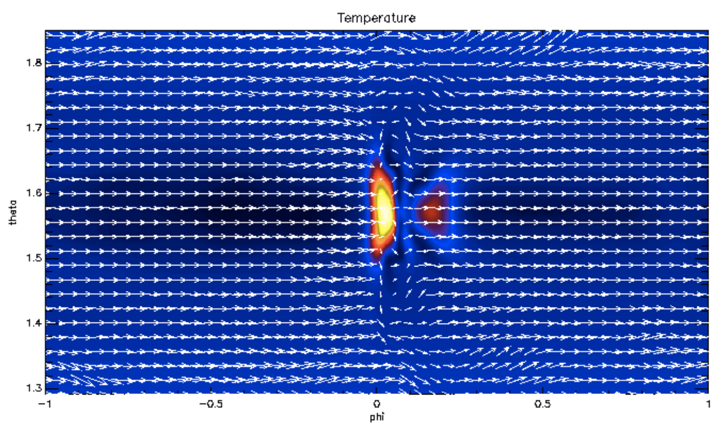

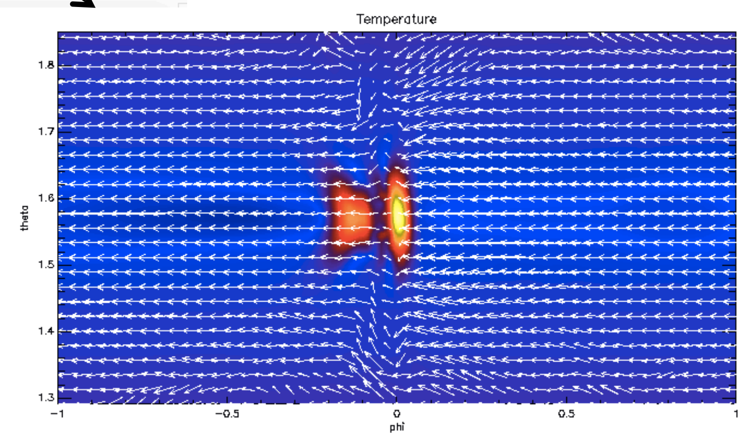

Temperature

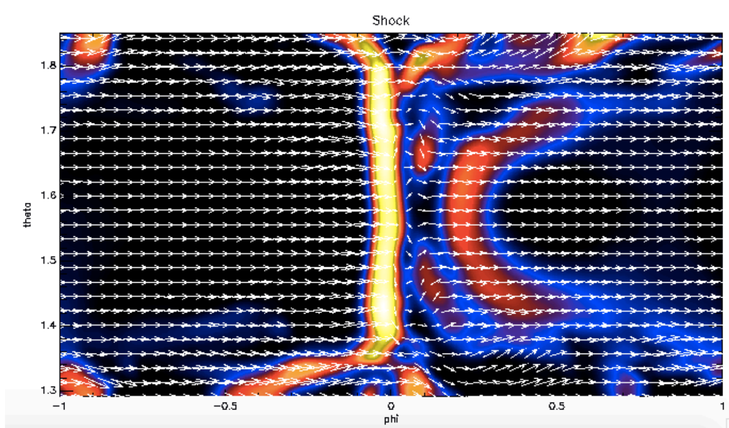

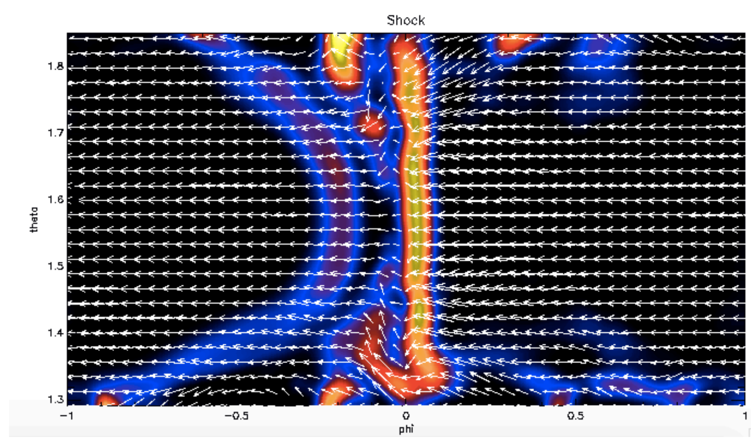

Div u (shock)

Lyra et al. (2015, in prep)

3D shocks: ascending bores and breaking waves

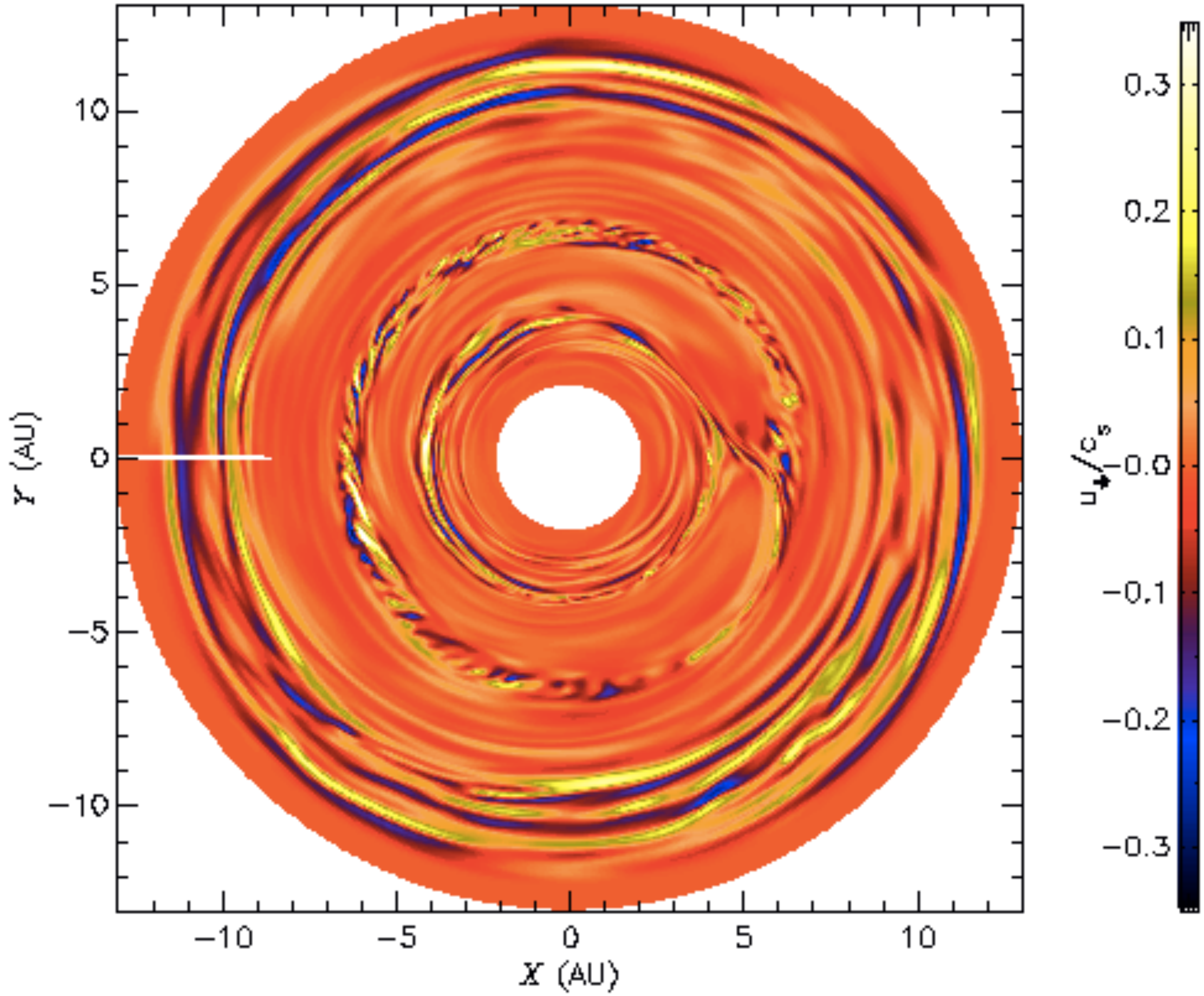

Lyra et al. (2015, in prep)

Observational evidence: Gaps

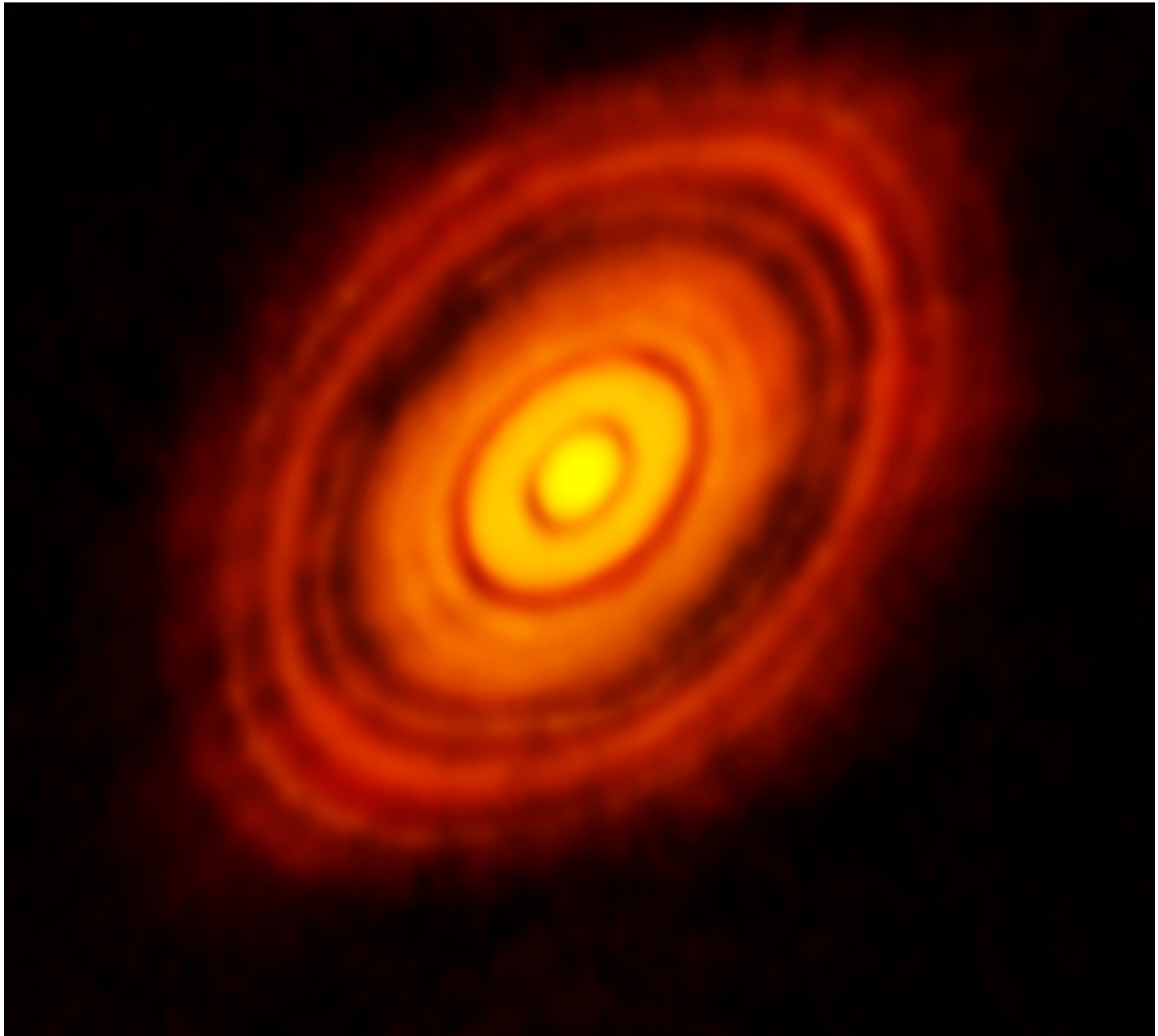

Possible Interpretation?

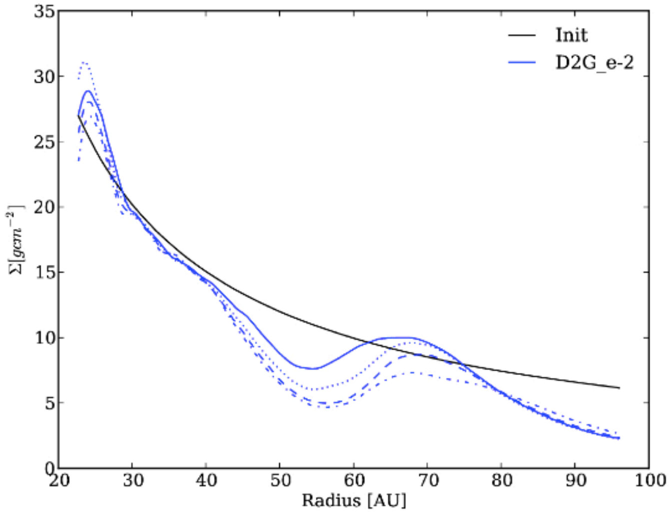

Dead zone boundary:
density enhancement

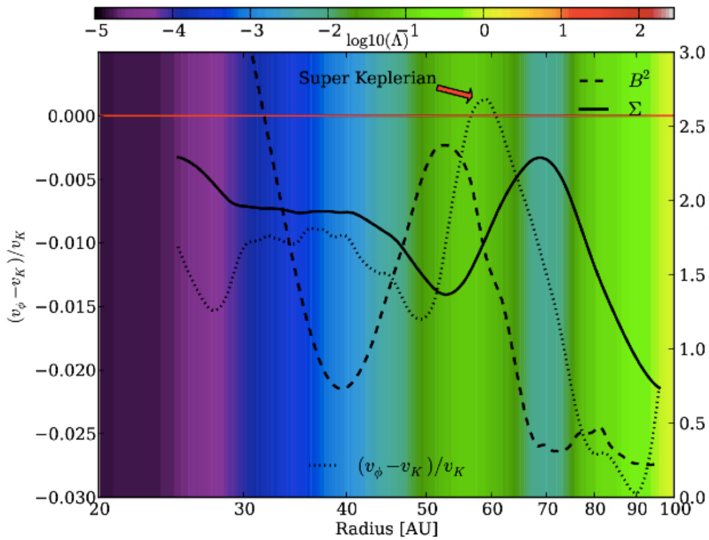

Super-Keplerian:
Magnetic pressure build-up

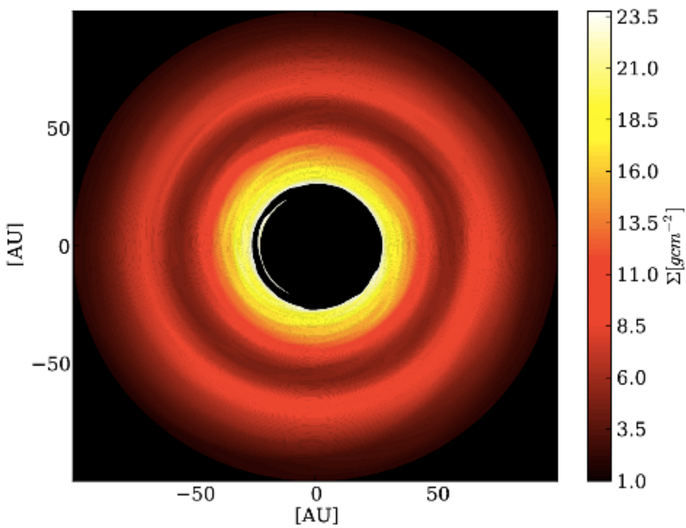

Magnetic pressure
expels gas

Flock et al. (2015)

Shallow gaps located at icelines of common volatiles.

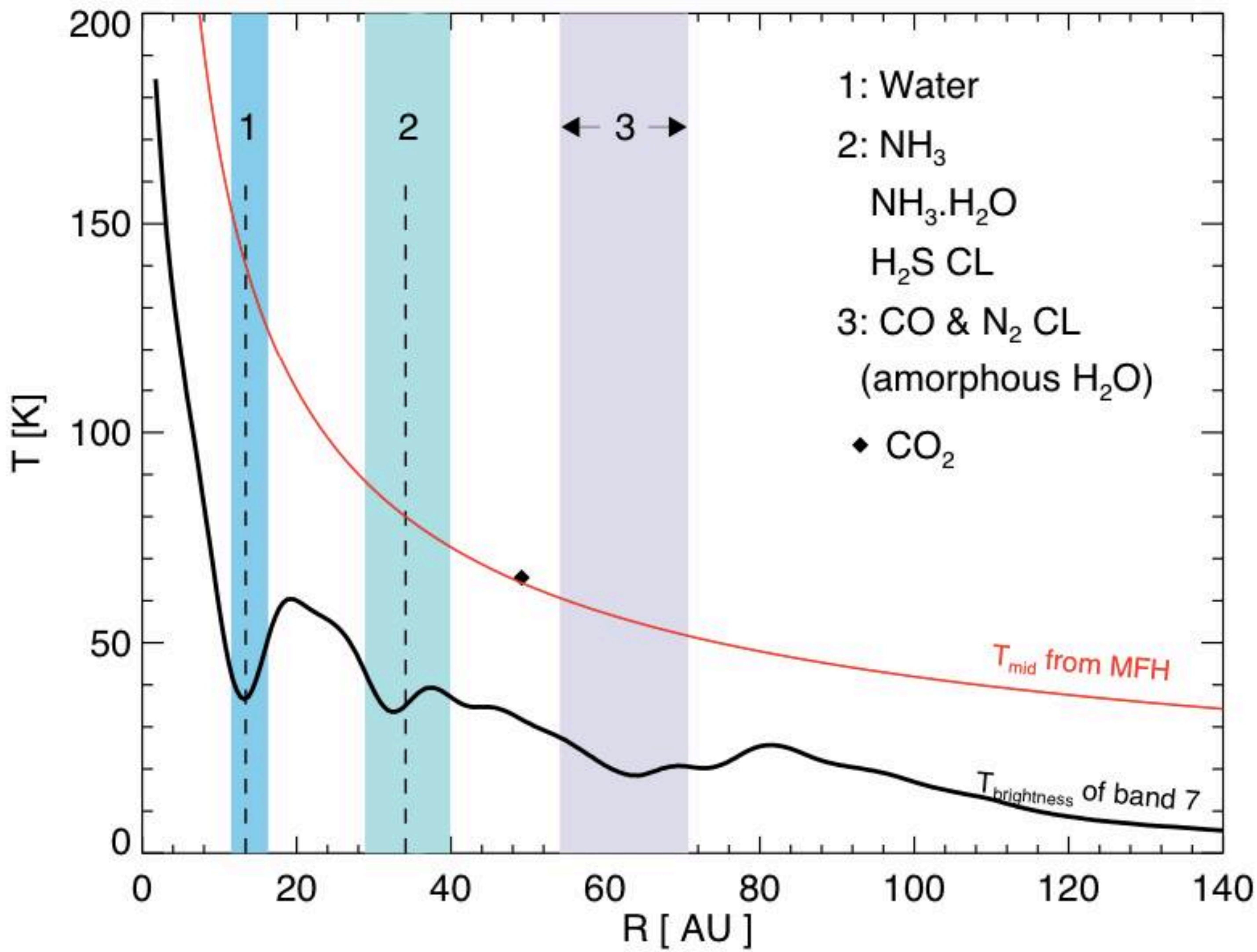

Zheng et al. (2015)

Summary and Conclusions

- Observational evidence: spirals, gaps, and vortices.

  Planet-disk interaction: spirals, gaps, and vortices.

  Disk dynamical instabilities: spirals, gaps, and vortices.

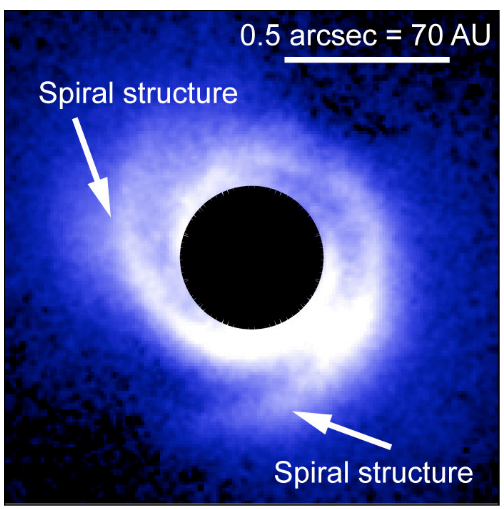

Muto et al. (2012)

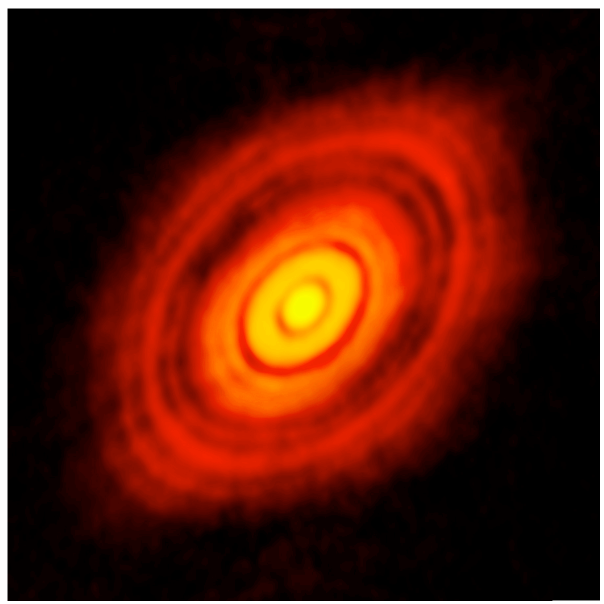

ALMA et al. (2015)

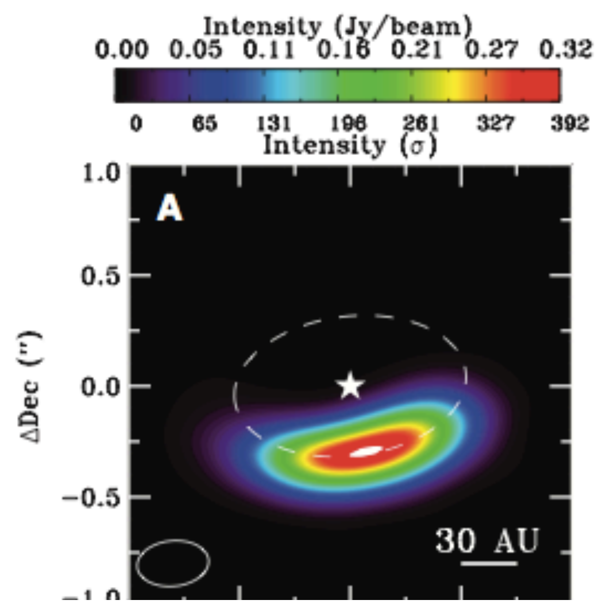

van der Marel et al. (2013)

Summary and Conclusions

Observational evidence: spirals, gaps, and vortices.

- Planet-disk interaction: spirals, gaps, and vortices.

Disk dynamical instabilities: spirals, gaps, and vortices.

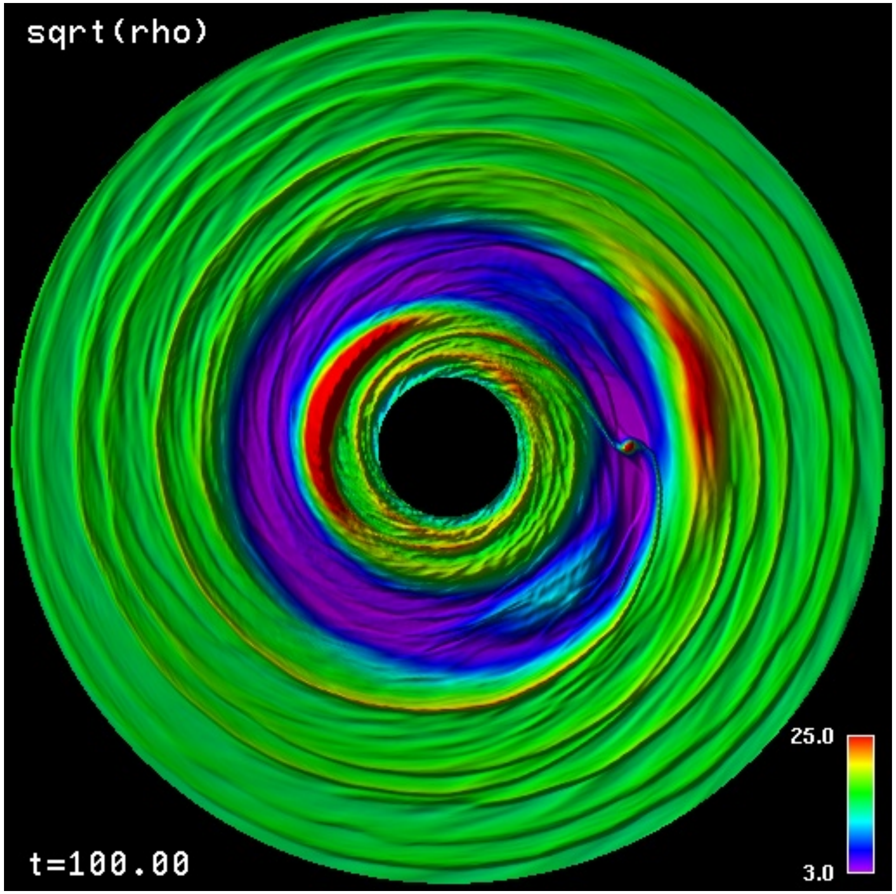

Summary and Conclusions

Observational evidence: spirals, gaps, and vortices.

Planet-disk interaction: spirals, gaps, and vortices.

- Disk dynamical instabilities: spirals, gaps, and vortices.

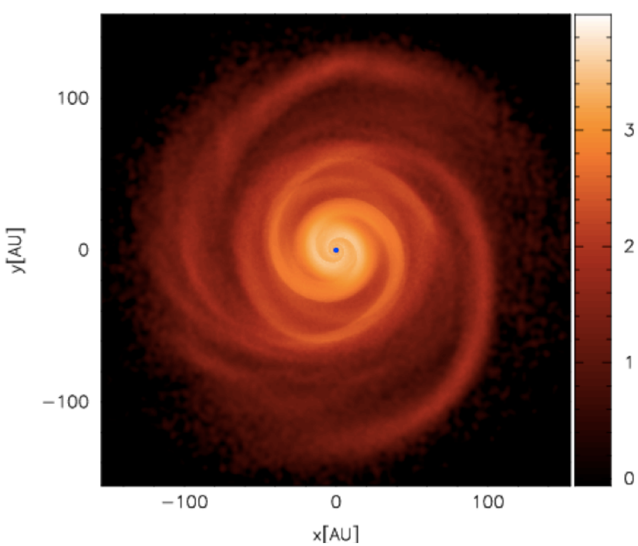

Dipierro et al. (2015)

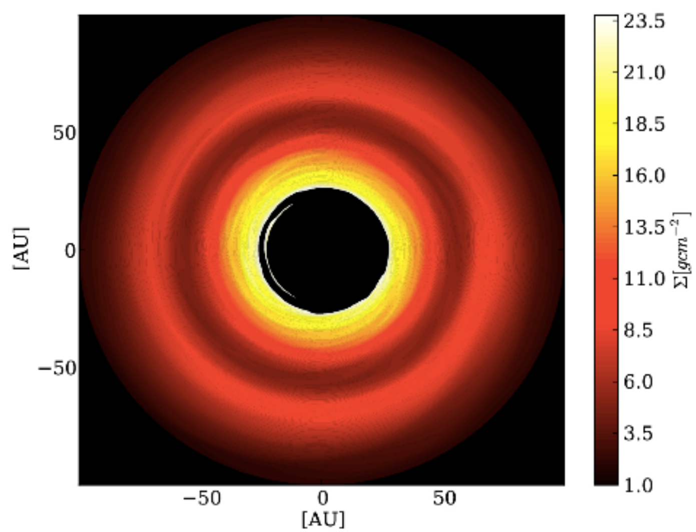

Flock et al. (2015)

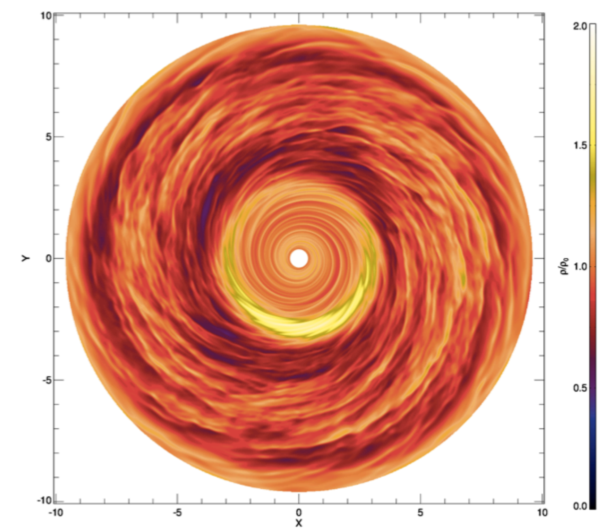

Lyra et al. (2015)